

Deltares

Developing a design criterion for the shoreline response to multiple submerged breakwaters

MSc Thesis



A.L. van der Baan

Developing a design criterion for the shoreline response to multiple submerged breakwaters

By

Aljosja Laurus van der Baan

1365835

A research thesis completed as part of the Master of Science degree in Coastal Engineering at the Delft University of Technology, The Netherlands



Graduation committee:

Prof. Dr. Ir. M.J.F. Stive

Assoc. Prof. Dr. R. Ranasinghe

Ir. A.P. Luijendijk

Dr. Ir. G.J. de Boer

Ir. J. van Overeem

TU Delft

TU Delft, UNESCO IHE, Deltares

TU Delft, Deltares

TU Delft, Deltares

TU Delft, Arcadis

Summary

Introduction

Shore-parallel submerged breakwaters (SBWs) appear as an attractive form of coastal protection. Compared to their emergent counterpart there is no impact on the beach amenity and aesthetics. In addition, there is a possibility for recreational purposes. However, the actual application of SBWs is often discouraged because the complexity of the hydrodynamics in the vicinity of SBWs makes the shoreline response hard to predict. This complexity further increases in the case of multiple SBWs. Added processes such as the distribution of the return flow and the (hydrodynamic) interaction between the separate SBWs induce a complex wave and flow pattern in the lee of the SBWs. The objective of this thesis is to develop a design criterion predicting the shoreline response to multiple SBWs.

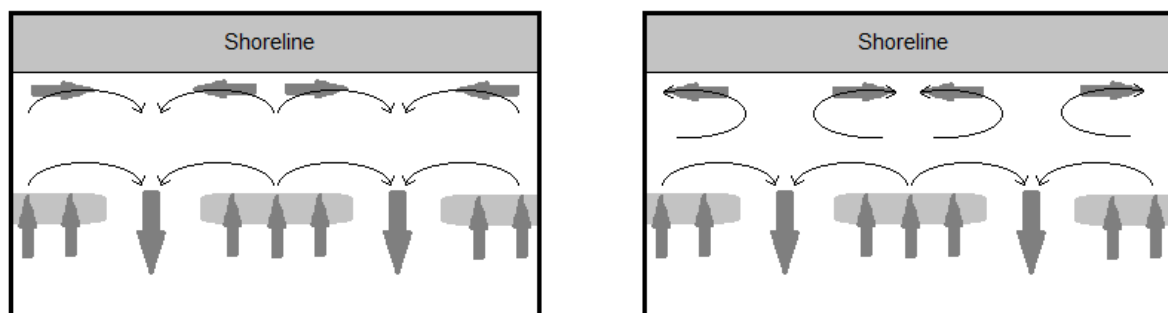


Figure 1 - 2-cell flow pattern with divergent flow at the shoreline (left) and 4-cell flow pattern with convergent flow at the shoreline (right)

Studies showed that the initial mode of the shoreline response can be linked to the flow pattern observed in the lee of the SBW. A 2-cell flow pattern causes a divergent flow at the shoreline and therefore local erosion, whereas a 4-cell flow pattern causes convergent flow at the shoreline with local accretion as a result (Figure 1). These patterns have comparable results in cases with a single SBW and cases with multiple SBWs. There are multiple methods to predict if a certain SBW system will cause a 2-cell or 4-cell flow pattern. One can use the cross-shore momentum balance to calculate the longshore differences in water level set-up at the shoreline and use that to predict the direction of the flow at the shoreline in the lee of the SBW (convergent or divergent). Another method of predicting the shoreline response is based on the relation of solely physical parameters of the system. The parameters included in this criterion at the time of writing are: wave height, water depth, length of the SBW, submergence level of the crest and a parameter dependent on the grain diameter of the sediment. Cases are plotted as a single data point in a graph with an erosive area and accretive area divided by a constant line. By means of numerical modelling the relation was found describing the mode of shoreline response. Whereas the cross-shore momentum based method is susceptible to errors in the formula for the wave transmission over the SBW crest and the wave breaker index is dependent on the rip current flow, the physical parameter based criterion only gains validity with a large amount of numerical model runs used for the data fit of the criterion. It is argued that, based on the availability of the used parameters, the second criterion is better as a rule of thumb for first assessment of the shoreline response. Use of the other criterion in combination with numerical modelling is still advisable in a later stage of the development process.

Numerical modelling

The physical parameter criterion in its current form is only valid for single SBW cases. To extend this criterion for multiple SBW cases the same method is used as was used to obtain the single SBW criterion. Evaluation of the relation of the new parameters and the possible change of the existing ones was done with a numerical model: Delft3D. This depth averaged model has been validated for cases with single SBWs and from that study the idealized and computational efficient model is used to map the morphological impact of a system of multiple SBWs. To overcome the uncertainties introduced by adding more SBWs to the model, it was first validated by reproducing models from previous studies and comparing the results. While conformity with the literature does not guaranty full validity, the model does gain value when its output is in the same order as the results of one or more of the equation and/or data from the literature. On this ground the model proved applicable.

The numerical modelling consisted of monitoring the morphological response of an idealized shoreline profile to multiple SBWs. Physical parameters of the existing criterion for a single SBW (wave height (H_0), water depth (h_b), submergence level (s_b), length of the breakwater (L_b) and a grain diameter parameter (A)) were varied as well as the new parameter introduced by multiple SBWs: the gap width over barrier length ratio. The shoreline development was analysed by comparison of the 0.5 m depth contours over time and the cumulative sediment displacement in the lee of an SBW. Subsequently, numerical modelling showed, conform literature, that the difference in impact on the shoreline of a multiple SBW system relative to a single SBW is governed by the ratio of gap width over barrier length; the lateral confinement ratio. Not only the availability of sediment is influenced, also the wave energy that penetrates the coastal defence is affected; a different degree of wave sheltering is observed. To describe these differences in parameters with a certain relation, the availability of sediment and wave sheltering are viewed as separate as possible. This is done by varying the lateral confinement ratio with a constant wave height to map the influence of the availability of sediment. The wave height is varied with a constant lateral confinement ratio to research the contribution of the different degree of wave sheltering (with respect to a single SBW case). Note that a complete separation of the contribution of these processes by numerical modelling is not possible since the processes are both governed by the lateral confinement ratio.

Developing the criterion

The contribution of the variation of the lateral confinement ratio (L_g/L_b) can be analysed using the cumulative sediment displacement values in the lee of the SBWs. The different degree in wave sheltering is shown to be dependent on the relative wave height (h_b/H_0 , with h_b being the depth at the location of the breakwater). Based on these relations and a fit through the data of 72 model runs, the following equation can be derived for the location of a data point on the x-axis (λ). The bracketed part is the added term for multiple SBWs.

$$\lambda = \left(\frac{s_b}{h_b}\right)^{\frac{3}{2}} \left(\frac{L_b}{h_b}\right)^2 \left(\frac{A^3}{h_b}\right)^{\frac{1}{2}} \left[1.22 \left(\frac{L_g}{L_b}\right)^2 - 3.67 \left(\frac{L_g}{L_b}\right) + 3.22 * 0.4 \left(\frac{h_b}{H_0}\right)^2 \right] \quad (1)$$

The value for the data point on the y-axis of a given case remains equal to that of the single SBW criterion; h_b/H_0 .

In order to explore the applicability of the criterion outside an idealized model set-up, a number of model runs were executed with a changed or added hydrodynamic process (e.g. obliquely incident waves, tidal amplitude or a longshore current). While the number of model runs was insufficient to draw any solid conclusions, a preliminary conclusion can be made. Added or changed processes that cause a change in the availability of sediment and/or sediment transport capacity independent of the parameters in the criterion, can cause an erroneous prediction if the mode of shoreline response is close to the transitional area between an erosive or accretive response.

Conclusions

The criterion to predict the mode of shoreline response (accretive versus erosive) to single SBWs is made applicable to multiple SBW cases by adding a term accounting for the added processes. The extra term is based on a theoretical analysis and numerical modelling of the impact of the lateral confinement ratio and the different degree in wave sheltering with respect to single SBW cases.

Although the criterion cannot be used for a quantitative prediction of the shoreline response, it can function as a tool for the first assessment of the mode of shoreline response in cases of designing a coastal protection system based on multiple SBWs. The criterion can be used for preliminary designing advice or as a basis for further research regarding the utilization of SBWs as a form of coastal protection.

Further research can include a continuation of the research of the applicability of the criterion outside of idealized models and the necessity of treating certain aspects separately (e.g. a large tidal amplitude). The criterion would benefit from validation with field measurements and physical modelling. Additionally, research is needed on the sensitivity to the barrier width and roughness as these parameters are, as of now, not included in the criterion.

Preface and acknowledgements

This MSc thesis is part of my graduation program of Civil Engineering in the field of Coastal Engineering at the TU Delft. The research has been entirely conducted at Deltares.

I would like to thank Deltares for this opportunity to graduate at one of the leading institutes on research and consultancy in coastal engineering. Being part of a community of researchers and experts added a lot to the overall experience of writing this thesis. A part of this was provided by my fellow graduation students at Deltares, thanks for on topic tips and off topic conversations during the coffee breaks.

Furthermore, thanks to the members of my graduation committee, Prof. Dr. Ir. M.J.F. Stive Assoc. Prof. Dr. R. Ranasinghe, Ir. G.J. de Boer, J. van Overeem and my daily supervisor in particular, Ir. A.P. Lujendijk. Their insight, suggestions and enthusiasm greatly benefited this thesis.

Finally, a special thanks goes to my fellow students and friends for the enjoyable times during the study years as well as my thesis period, to my family for their support and especially to my father for his interest and always making time to read everything I write.

Jos van der Baan

Delft, October 2013

Table of Contents

List of figures.....	v
List of Tables.....	ix
List of symbols.....	xi
1 Introduction	1
1.1 Background.....	1
1.2 Problem definition	1
1.3 Research objective.....	2
1.4 Methodology.....	2
1.5 Reader	3
2 Literature review.....	5
2.1 Introduction	5
2.2 Waves.....	5
2.2.1 Spectrum.....	5
2.2.2 Shoaling	6
2.2.3 Refraction.....	6
2.2.4 Diffraction.....	6
2.2.5 Reflection	7
2.2.6 Momentum flux.....	7
2.2.7 Wave set-up.....	8
2.2.8 Wave breaking	9
2.2.9 Wave transmission.....	10
2.2.10 Wave sheltering	12
2.2.11 Mass transport over the SBW.....	12
2.3 Extending the theory for the addition of gaps in the SBW	13
2.3.1 Rip-currents	13
2.3.2 Mass balance	14
2.3.2.1 Return flow distribution	14
2.3.2.2 Velocity in the gap	15
2.3.2.3 Water level set-up in the lee of the SBW.....	16
2.4 Morphodynamics.....	18
2.4.1 Scour patterns.....	18
2.4.2 Scour dimensions.....	18

2.4.3	Shore-line changes	20
2.4.3.1	Rule of thumb	20
2.4.3.2	Criterion based on physical parameters.....	20
2.4.3.3	Criterion based on analytical formulae	24
2.5	Previous modelling with Delft3D on the subject of SBWs	25
3	Modelling tool	29
3.1	Flow module.....	29
3.2	Wave module	30
3.3	Model setup.....	31
3.3.1	Grid	31
3.3.2	Bathymetry.....	31
3.3.3	SBW shape	31
3.3.4	Time frame	32
3.3.5	Boundary conditions.....	32
3.3.6	Model parameters	32
3.3.7	Additional settings and comments	33
4	Comparing output Delft3D to empirical, analytical and numerical data	35
4.1	Magnitude of the set-up in the lee of the SBW.....	35
4.1.1	Analytic approach.....	35
4.1.2	Numerical approach	37
4.1.3	Comparison.....	38
4.2	Breakwater length and gap width ratio.....	40
4.2.1	Empirical data	40
4.2.2	Numerical reproduction	40
4.2.3	Comparison.....	41
4.3	2-cell versus 4-cell pattern.....	42
4.3.1	Analytical basis for the criterion and numerical validation with SWASH.....	42
4.3.2	Numerical validation with Delft3D and validation with analytical approach.....	43
4.3.3	Flow pattern analysis in Delft3D	46
4.4	Conclusions.....	47
5	Shoreline response	49
5.1	Model set-up and results	49
5.2	Prediction when using single SBW criterion	51
5.3	Conclusion	52
6	Analysing the shoreline response to multiple SBWs by means of scenario's	55
6.1	Added processes relative to a single SBW system	55

6.2	Model set-up	57
6.3	Transition between multiple and single SBW system.....	58
6.3.1	Morphologic changes	58
6.3.2	Flow velocity profile over the gap transect.....	60
6.4	Varying the lateral confinement ratio	62
6.5	Varying the relative wave height.....	63
6.6	Developing the criterion.....	66
6.7	Conclusion	68
7	Expanding the model parameters.....	71
7.1	Model set-up	71
7.2	Obliquely incident waves	71
7.3	Tide.....	72
7.4	Longshore tidal current.....	73
7.5	Conclusion	74
8	Conclusions and recommendations.....	75
8.1	Conclusions.....	75
8.2	Recommendations	76
8.2.1	Recommendations on general future research.....	77
8.2.2	Recommendations on improving the criterion.....	77
9	References.....	79

Appendices

A.	Numerical model parameters Delft3D	A-1
B.	Delft3D output for comparison with literature.....	B-1
C.	Developing the criterion.....	C-1

List of figures

Figure 2.1 - Definition for the energy balance by wave set-up over a submerged breakwater (Vicinanza et al., 2008).....	9
Figure 2.2 - Energy coefficients of wave reflection (K_R), wave transmission (K_T) and wave dissipation (K_D) versus wave non-linearity (Wu et al., 2012)	10
Figure 2.3 - Redistribution of wave forcing due to a SBW (Vlijm, 2011)	12
Figure 2.4 - Forms of rip currents (Dalrymple et al., 2011).....	14
Figure 2.5 - Piling-up P for different confinement conditions (Burcharth et al., 2007).....	15
Figure 2.6 - Distribution between return flow over the SBW (overtopping) and return flow through the gaps based on the set-up (Burcharth et al., 2007)	16
Figure 2.7 - Schematized overview of the parameters (Bellotti, 2004).	16
Figure 2.8 - Definition sketch of scour patterns and parameters: (a) attached scour, (b) detached scour (Young et al., 2009).....	19
Figure 2.9 - Schematic depiction of expected nearshore circulation patterns that may lead to shoreline erosion (Ranasinghe et al., 2006)	21
Figure 2.10 - Schematic diagram showing key structural/design parameters governing shoreline response to an SBW (Ranasinghe et al., 2010).....	22
Figure 2.11 - Visualization of the 2-cell pattern (above) and the 4-cell pattern (below) (Ranasinghe et al., 2010).	24
Figure 2.12 - The dependence of the mode of shoreline response on the two non-dimensional parameters identified in (2.50 (Ranasinghe et al., 2010).....	23
Figure 2.13 - 2-cell and 4-cell patterns in case of multiple SBWs (Villani et al., 2012).	24
Figure 2.14 - Overview of literature used for validation (Vlijm, 2011)	26
Figure 3.1 - Processes regarding the transport of constituents	30
Figure 4.1 – Cross-section of a typical submerged barrier (Bellotti, 2007).	36
Figure 4.2 - (a) Plan view and (b) cross-section of the experimental basin used by (Haller, Dalrymple, et al., 2002).	38
Figure 4.3 - Trendline trough the measured points from the physical model	40
Figure 4.4 - Trendline through the computed points from the Delft3D model	42
Figure 4.5 - 2-cell and 4-cell patterns in case of multiple SBWs (Villani et al., 2012).	43
Figure 4.6 - Analytical (red) and numerical (blue) values for the ratio r and the percentage difference.	43
Figure 4.7 - Set-up at shoreline, with average over section (red lines), for test B.....	44
Figure 4.8 - Deviation in generated r value related to rip current velocity.....	46
Figure 5.1 - Plot of the bed level height for test B (top left), C (top right), D (bottom left) and G (bottom right) after 3 months with the -0.5m contour lines with SBWs (black) and without (white)	50
Figure 5.2 - Monitor area from the inshore trunk of the SBW to the 0 water depth contour line, in the lee of the central SBW	51
Figure 5.3 – Results of tests B, C, D and G plotted as data points in the graph for the prediction of shoreline response to a single SBW	52
Figure 6.1 - Cumulative sediment/erosion profile for a single SBW (left) and multiple SBW (right) system	56
Figure 6.2 - Results of tests 1 to 12, plotted as data points in the graph for the prediction of shoreline response to a single SBW	58

Figure 6.3 - Relative bottom level change for lateral confinement ratio 1:4	59
Figure 6.4 - Relative bottom level change for lateral confinement ratio 1:1	59
Figure 6.5 - Relative bottom level change for lateral confinement ratio 2:1	60
Figure 6.6 - Longshore profile of the cross-shore flow velocity for $H_i = 1.0$, at the cross-shore height of the SBW crest.....	60
Figure 6.7 - Longshore profile of the cross-shore flow velocity for $H_i = 1.5$, at the cross-shore height of the SBW crest.....	61
Figure 6.8 - Longshore profile of the cross-shore flow velocity for $H_i = 1.8$, at the cross-shore height of the SBW crest.....	61
Figure 6.9 - Contribution of the lateral confinement ratio to the shoreline response for $H_i = 1.0$ m.....	62
Figure 6.10 - Normalized, averaged, cumulative sediment displacement	63
Figure 6.11 - Difference in directional spreading for a single SBW and multiple SBWs with a lateral confinement ratio of 1:1	64
Figure 6.12 - Visualisation of the wave sheltering effect of a single SBW (left) and multiple SBWs (right).....	64
Figure 6.13 - Data points of the LC = 1:1 case without the added relative wave height term	65
Figure 6.14 - Data points of the LC = 1:1 case with the added relative wave height term	66
Figure 6.15 - Inverted, normalized, averaged, cumulative sediment displacement	67
Figure 6.16 - Data points of all the LC ratios with the added term G	68
Figure 7.1 - Cumulative sediment displacement comparison, obliquely and normal incident waves.....	72
Figure 7.2 - Cumulative sediment displacement comparison, 0.5m tidal amplitude and no tide	73
Figure 7.3 - Comparison sediment displacement comparison, a longshore tidal current and no current.....	74
Figure 8.1 - Data points of all the lateral confinement ratios with the added term G.....	76
Figure A.1 - WAVE and FLOW grid superimposed, with length scales.	A-1
Figure A.2 - 3D representation of the initial bathymetry with 4 SBWs.	A-2
Figure B.1 - Set-up in the lee of the SBW, test B.....	B-1
Figure B.2 - Set-up in the lee of the SBW, test C.....	B-2
Figure B.3 - Set-up in the lee of the SBW, test D.....	B-2
Figure B.4 - Set-up in the lee of the SBW, test G.....	B-3
Figure B.5 - Plot of the data by Burcharth (2007).....	B-3
Figure B.6 - Plot of the data from Deft3D with a Chézy value of $65 \text{ m}^{0.5}/\text{s}$	B-4
Figure B.7 - Plot of the data from Deft3D with a Chézy value of $45 \text{ m}^{0.5}/\text{s}$	B-4
Figure B.8 - Plot of the data from Deft3D with the varying Chézy value as uncertainty band	B-5
Figure B.9 - Set-up at the shoreline, with average over sections, test B	B-5
Figure B.10 - Set-up at the shoreline, with average over sections, test C	B-6
Figure B.11 - Set-up at the shoreline, with average over sections, test D	B-6
Figure B.12 - Set-up at the shoreline, with average over sections, test G	B-7
Figure B.13 - Plan view of the time-averaged velocity vectors and set-up (colour map) from (Villani et al., 2012).....	B-8
Figure B.14 - Flow pattern test B	B-9
Figure B.15 - Flow pattern test C	B-10
Figure B.16 - Flow pattern test D	B-11
Figure B.17 - Flow pattern test G	B-12

Figure C.1 - Contribution of the lateral confinement ratio to the shoreline response for $H_i = 1.0\text{m}$ C-1

Figure C.2 - Contribution of the lateral confinement ratio to the shoreline response for $H_i = 1.5\text{m}$ C-2

Figure C.3 - Contribution of the lateral confinement ratio to the shoreline response for $H_i = 1.8\text{m}$ C-2

Figure C.4 - Contribution of the lateral confinement ratio to the shoreline response for $H_i = 3.0\text{m}$ C-3

Figure C.5 - Contribution of the lateral confinement ratio to the shoreline response for $H_i = 3.0\text{m}$ and $s_b = 0.2$ with $\text{morfac} = 1$ C-3

Figure C.6 - Data points for the LC ratio of 1:4 with the added term G C-4

Figure C.7 - Data points for the LC ratio of 1:2 with the added term G C-4

Figure C.8 - Data points for the LC ratio of 1:1 with the added term G C-5

Figure C.9 - Data points for the LC ratio of 1.5:1 with the added term G C-5

Figure C.10 - Data points for the LC ratio of 2:1 with the added term G C-6

Figure C.11 - Data points of all the LC ratios with the added term G C-6

List of Tables

Table 2.1 - Input model values of varying parameters (Blouin, 2012)	27
Table 2.2 - Collection of the results from modelling in Delft3D	27
Table 4.1 - Physical parameters of the tests	38
Table 4.2 - Comparison of the output of Delft3D and the analytical approximation by (Bellotti, 2007) regarding the set-up.	39
Table 4.3 - Comparison of the output of Delft3D and the analytical approximation by (Bellotti, 2007) regarding the set-up, with adjusted roughness coefficient.	39
Table 4.4 - Calculation of the wave pump efficiency with the Delft3D output	40
Table 4.5 - Physical parameters used in the Delft3D model runs	41
Table 4.6 - Wave set-up at shoreline from Delft3D output.	44
Table 4.7 - Averaged wave set-up at shoreline from Delft3D output.	44
Table 4.8 - Wave set-up at shoreline computed analytically.	45
Table 4.9 - Rip current velocity in relation to the deviation in the ratio r	45
Table 5.1 - Cumulative volumetric change per test	50
Table 5.2 - Parameters used in the criterion for the shoreline response to a single SBW	52
Table 6.1 - Physical parameters for the tests per ratio of L_b over L_g	57
Table 6.2 - Parameters of the three reviewed cases	58
Table 6.3 - Longshore disturbance length per wave height	61
Table 7.1 - Physical parameters of the 'normal' case	71
Table A.1 - Physical parameters Delft3D-Flow	A-3
Table A.2 - Physical parameters Delft3D-Wave	A-3
Table A.3 - Numerical parameters Delft3D-Flow	A-3
Table A.4 - Numerical parameters Delft3D-Wave	A-4

List of symbols

Symbol	Unit	Description
A	[m ²]	SBW cross-sectional area
A	[-]	Equilibrium beach profile parameter
a	[m]	Wave amplitude
B	[m]	SBW crest width
B ₀	[-]	Wave shape factor
c	[ms ⁻¹]	Wave celerity
c _f	[-]	Bottom friction coefficient
c _g	[ms ⁻¹]	Wave group celerity
D	[m]	Grain diameter
E	[Jm ⁻²]	Wave energy
F	[Nm ⁻²]	Wave force
f	[s ⁻¹]	Wave frequency
f _p	[s ⁻¹]	Wave peak frequency
g	[ms ⁻²]	Gravitational acceleration
H	[m]	Wave height
h	[m]	Water depth
H ₀	[m]	Deep water wave height
h _b	[m]	Wave breaker depth
h _c	[m]	SBW height
H _i	[m]	Incoming significant wave height
H _s	[m]	Significant wave height
k	[-]	Wave number
K _D	[-]	Wave dissipation coefficient
K _d	[-]	Wave diffraction coefficient
K _r	[-]	Wave reflection coefficient
K _t	[-]	Wave transmission coefficient
L	[m]	Wave length
L ₀	[m]	Deep water wave length
L _b	[m]	SBW length in y-direction
L _g	[m]	Gap length in y-direction
L _s	[m]	SBW bottom width
m _i	[m ²]	i th order wave moment
n	[-]	Ratio between phase and group celerity
P	[Nm ⁻²]	Hydrostatic pressure
q	[m ² s ⁻¹]	Discharge per meter
R	[m]	Tidal range
R _c	[m]	Crest submergence level
S	[Nm ⁻¹]	Radiation stress
s _b	[m]	Crest submergence level
T	[s]	Wave period
t	[s]	Time
u	[ms ⁻¹]	Current in x-direction
U _r	[-]	Ursel number
v	[ms ⁻¹]	Current in y-direction
w	[ms ⁻¹]	Current in z-direction
x	[-]	x-direction
x _b	[m]	Cross-shore distance SBW to shoreline
y	[-]	y-direction

z	[-]	z-direction
-----	-----	-------------

Greek symbols

Symbol	Unit	Description
α	[-]	Wave spectrum energy scale
α	$^{\circ}$	Bottom level gradient
γ	[-]	Wave height to water depth ratio
δ	[m]	Water level set-up
η	[m]	Surface elevation
θ	$^{\circ}$	Incoming wave angle
θ	[-]	Shields mobility parameter
ξ	[-]	Irribarren number
ρ	[kgm ⁻³]	Density
τ	[Nm ⁻²]	Bottom friction
ψ	[-]	Shields parameter

1 Introduction

1.1 Background

A relatively high percentage of human activities is located at the coastline or in the coastline area. This is due to the fact that the coastline area offers possibilities for tourism, recreation, trade and transport. As of late it is predominantly the residential and commercial sectors that influence the coastal development. This increase demands more and more a stable coastline or at least no prevailing coastal erosion.

To get a grip on the phenomenon 'erosion' one needs to look at the causes. Some of the more important causes of erosion are as follows (Silvester et al., 1997):

- A (man-made) change in the transport capacity of sediment,
- Tides, currents, (obliquely incident) waves, storms, sea level rise,
- Loss of sediment material due to transport by wind,
- Reduction of natural bottom protection by pollution.

As to be expected, many methods to prevent these events have been developed, with a wide variety of forms of impact on the coastline. One of these methods is the construction of shore parallel breakwaters. These structures can be designed to reduce erosion on an existing beach, support sedimentation, protect against storm damage, or help to prolong the results of beach nourishment (Pilarczyk et al., 1996). The primary cause for these results is a dissipation of wave energy and a modification of the wave and current fields in the lee of the breakwater. While all these results can support a stable or accreting coastline, popularity is reduced by the negative impact on the beach amenity and aesthetics (Ranasinghe et al., 2006). These forms of impacts can be reduced and maybe even removed by making use of a submerged breakwater (SBW). In fact, by maintaining more contact with the open water compared to an emergent breakwater, not only the benefits of an emergent breakwater prevail, a SBW also provides new functions. Besides coastal protection there is also an improvement for the marine biodiversity since an open connection to the open water remains. Recreational functions include the possibility of surfing and the safety for swimmers and divers. This makes an SBW a tempting alternative.

1.2 Problem definition

While the processes around an emergent breakwater and the impact on the shoreline of it are well known and researched, for the SBW that level of familiarity has not yet been reached. So before the concept 'submerged breakwater' can safely be implemented as a solution or controlling element at the coastline, more research is needed to be able to quantify the impact of such an element. From a construction point of view there are differences in stability, strength and the forces generated on the structure when comparing submerged to emergent breakwaters. In addition, since there is a constant mass transport over the SBW, there are also major differences in the hydrodynamic aspect and with that, the morphological aspect. In this report it is this aspect and its impact on the coastline that is being looked at.

As defined earlier, a breakwater protects the coastline by dissipation of wave energy and modification of the wave and current fields in the lee of the breakwater. When this protection

is only partial, in the case of an SBW, the efficiency of the breakwater is still largely unknown. In fact, in most cases the use of an SBW resulted in erosion of the coastline (Ranasinghe et al., 2006). To predict this efficiency one needs to include multiple environmental parameters (e.g. SBW length, submergence level, distance from the shoreline, wave height) in a criterion. These parameters influence the hydrodynamic processes such as wave set-up and set down, onshore mass flux and longshore currents which in turn govern the shoreline response. These processes will be elaborated more extensively in section 2.

1.3 Research objective

The objective of this MSc Thesis is to develop a generally applicable design criterion for the shoreline response to multiple SBWs by extending the research by (Blouin, 2012) regarding the sensitivity of the parameters in the design criterion for a single shore parallel SBWs.

This objective will be reached by way of the following points:

- A literature study on (the impact on the coastline of) submerged breakwaters,
- Short explanation of the modelling tool that will be used (Delft3D),
- Analytic prediction of the change in the total hydrodynamic conditions caused by adding (a) gap(s) in the SBW,
- Extending the existing models with the addition of multiple SBWs, and a validation with Delft3D of the hydrodynamic processes caused by the added gap(s) in the SBW,
- Including morphodynamics and linking them to the hydrodynamic processes,
- Development of a (or addition to an existing) criterion that is based on structural parameters to predict the shoreline response when placing an SBW with certain dimensions,
- Expanding the hydrodynamic parameters in an attempt to solidify the criterion.

1.4 Methodology

The general methodology to achieve the objective is using the same framework that was used by (Blouin, 2012). Additionally a series of Delft3D simulations will be undertaken for the modelling of the morphological impact of multiple SBWs. The result will be analysed to develop a generally applicable design criterion for the shoreline response to SBWs.

This can be divided into multiple steps by treating the steps mentioned in the previous paragraph:

- *A literature study on (the impact on the coastline) of submerged breakwaters.* The literature study will provide insight in the parameters and processes that control the morphological impact of the SBW. It will also include previous researches on SBWs with the MSc Thesis of (Vlijm, 2011) in particular, since this thesis is an indirect continuation on the subject.
- *Short explanation of the modelling tool that will be used (Delft3D).* A quick look into the way Delft3D operates as a process based, two-dimensional, depth averaged model, with a side-step to the tools used in this case in particular.
- *Analytic prediction of the change in the total hydrodynamic conditions caused by adding (a) gap(s) in the SBW.* What does the literature predict when looking at the hydrodynamic conditions at the location of the gap in the SBW?
- *Extending the existing models with the addition of multiple SBWs, and a validation with Delft3D of the hydrodynamic processes caused by the added gap(s) in the SBW.*

When familiar with the current standing of the Delft3D models, it can be extended in a way to serve the objective of this thesis. In this case, the addition of multiple SBWs with gaps in between. Following the previous point it is checked if Delft3D shows correlation with this prediction.

- *Including morphodynamics and linking them to the hydrodynamic processes.* When the consequences of adding (a) gap(s) to the SBW, expressed in changes in hydrodynamic processes, are known, the impact on the morphodynamics in the vicinity of the SBW system can be analysed.
- *Development of a (or addition to an existing) criterion to predict the shoreline response when placing an SBW with certain dimensions.* From these relations it is then possible to develop a criterion to predict the magnitude of the shoreline response when constructing a SBW with certain dimension and in that way, use that criterion as a guideline when designing SBWs.
- *Expanding the hydrodynamic parameters in an attempt to solidify the criterion.* The criterion is developed using simplified models. It is important to research the validity of the criterion in more common cases (e.g. the addition of obliquely incident waves and/or tide).

1.5 Reader

Section 2 will give a summary of the findings of relevant studies and the theoretical background of the hydrodynamic and morphodynamic processes regarding SBWs. Additionally, an overview of the previous modelling on the shoreline response to SBWs is given. In section 3 the conversion of these processes to a numerical model is looked at and how this model is going to be set up to be used in this thesis. In section 4 the results are presented from the comparison between a collection of empirical, analytical and numerical models and their reproduction in Delft3D. Section 5 relates the described hydrodynamic processes to the observed morphologic changes. From these results a range of model will be set up with predetermined physical parameters to develop a design criterion for the shoreline response to multiple SBWs, this is described in section 6. To increase the robustness of this criterion, section 7 includes the testing of the developed criterion when certain non-idealized hydrodynamic processes are added to the model. Finally, section 8 will give the conclusions of this thesis and recommendations for further research.

2 Literature review

2.1 Introduction

In this section relevant studies are reviewed. This includes published works regarding the hydrodynamics and morphodynamics in the vicinity of submerged breakwaters. Where data is scarce for SBWs, comparisons can be made with studies concerning low crested breakwaters (i.e. breakwaters with a crest at or around the still water level) or even emergent breakwaters instead, while keeping in mind the differences.

Aspects included are: the offshore conditions (waves), the interaction between the waves and the structure, ponding in the lee of the breakwater, the currents that present sediment transport, morphological changes and finally previous modelling with Delft3D and other modelling tools.

Since this thesis works from cases with the focus on 2D processes (longshore uniform assumption) and then extends to treat cases with 3D aspects, this review includes studies focussing on 2D formulae but also the formulae needed to describe 3D phenomena, where available.

2.2 Waves

Waves form an important part of the hydrodynamics around an SBW. It is important to review the different aspects (e.g. spectrum and interaction with the SBW and bottom profile). The simplest way to describe a wave, propagating along the x-direction is:

$$\eta(x, t) = a \cos(kx - \omega t) \quad (2.1)$$

For clarity some basic concepts used in the following paragraphs are explained here.

In linear wave theory, wave length $L = 2\pi/k$ is related to the local water depth, h , and period, $T = 2\pi/\omega$, by the dispersion relationship:

$$\omega^2 = gk \tanh kh = gk_0 \quad (2.2)$$

Wave length decreases as the wave propagates from deep to shallow water, assuming $L_0 = gT^2/2\omega$ for deep water and $L = \sqrt{gh}T$ in shallow water. Wave celerity is defined as $c = L/T$. Wave energy is proportional to the square of the wave amplitude and travels in wave direction at group velocity c_g which is related to the wave celerity c :

$$c_g = nc = \frac{1}{2} \left(1 + \frac{2kh}{\sinh 2kh} \right) c \quad (2.3)$$

The significant wave height, H_s , is defined as the average of the highest third of the waves.

2.2.1 Spectrum

One of the boundary conditions is the wave input at the offshore boundary. The spectrum of these waves will be of a JONSWAP spectrum. The JONSWAP spectrum has been shown to be rather universal. This spectrum is originally a Pierson-Moskovitz spectrum with the addition of a peak enhancement function (Holthuijsen, 2007). With the addition of this peak enhancement, this spectrum represents a young sea state with wind generated waves. Since

a lot of the following theories use the spectrum and a significant wave height for the incoming wave, it is important to note that the H_s can be obtained by use of a Rayleigh distribution for the probability density function.

2.2.2 Shoaling

When looking at a harmonic wave at a simplified longshore uniform coast with gentle slopes and no currents, a relation can be described regarding the increase in wave height experienced (Holthuijsen, 2007). The wave retains its frequency, but, since the dispersion relationship is still valid, its wave length will decrease and with that the phase speed. Initially the group velocity increases but then it also decreases. Nearing zero at the waterline, this decrease in velocity will cause an increase in wave amplitude to comply with the energy balance (2.4).

$$[Ec_g]_1 = [Ec_g]_2 \rightarrow \frac{1}{2} \rho g a_1^2 c_{g,1} = \frac{1}{2} \rho g a_2^2 c_{g,2} \quad (2.4)$$

Theoretically this would give infinite wave heights at the waterline but then other mechanisms come into play, such as wave breaking. However, before that point the increase in wave height can cause water level gradients and from that point of view, be relevant for rip-currents (paragraph 2.3.1).

2.2.3 Refraction

When the same longshore uniform situation is used, but now the waves have an oblique nature, another phenomenon is observed; the waves will change direction as they approach the coast. The depth variation of the length of the crest gives a variation in phase speed of this crest. The part in the deeper area will experience a higher phase velocity and will therefore move faster until the depth is equal over the length of the crest. In this simplified case that would mean a crest parallel to the coastline. In a more general situation this means that waves turn to be parallel with the depth contours.

2.2.4 Diffraction

Diffraction accounts for the wave disturbance in a shadow zone behind a headland or breakwater. Since there is no direct access for waves in that zone, there will be an area where there is a great difference in wave energy (the shadow line). Waves turn over this line into the shadow area, increasing wave height in the shadow area and reducing it on the other side of the shadow line (Holthuijsen, 2007). This effect is noticeable up to two wave lengths inward of the shadow zone (rule of thumb) and gives a relatively smaller change in wave climate behind the breakwater when it is submerged, since the shadow line is less well defined (waves can still cross over the structure giving a smaller difference in wave height). However, given the short nature of the crest length of the SBW with respect to the wave length, diffraction can still have a noticeable impact on the hydrodynamics in the lee and the gaps of the breakwaters. If the SBW is short enough, diffracted waves from multiple gaps can interact with each other directly in the lee of the SBW and have a noticeable influence on the wave properties. (Vicinanza et al., 2009) assumed an uncorrelated diffraction interaction from two different gaps to describe the diffraction coefficient in the lee of an SBW:

$$K_d = \sqrt{K_{d,A}^2 + K_{d,B}^2} \quad (2.5)$$

Further interaction with the wave over the SBW is discussed in paragraph 2.2.9.

2.2.5 Reflection

Just like a shoreline or emergent breakwater, an SBW is capable of wave reflection. In the case of an SBW the reflected wave also has a standing nature and is strongly dependent on crest submergence and wave height (Stamos et al., 2001). The study of (Van der Meer et al., 2005), related to the DELOS project, presented a formula for the wave reflection parameter. This formula indeed includes the submergence level and the wave height, in addition to the breakwater slope and wave slope. It does, however, not account for the permeability of the SBW. (Van der Meer et al., 2005) concludes that this formula needs more research before it can be used to accurately describe the phenomenon. The formula for the wave reflection parameter as well as the formula for the transmission parameter is discussed in paragraph 2.2.9. Additionally, the increasing wave reflection with an increasing wave non-linearity (Van der Meer et al., 2000) is addressed.

2.2.6 Momentum flux

Before looking at the water level set-up by wave hydrodynamics, it is important to understand the process behind it. For the previous processes the energy balance is mainly looked at. However, the momentum balance also influences the processes around and in the lee of the SBW. When waves encounter an SBW or shallower water in general, shoaling occurs and later wave breaking. This results in a change in wave forces expressed in radiation stress. Differences in radiation stress can lead to water level set-up/down and currents depending on local conditions.

To understand radiation stress, it is best to look at a longshore uniform coast with a wave propagating in the positive x-direction. The transport of momentum through the entire plane per unit crest length is obtained by integration over the depth from the bottom to the instantaneous water surface. It is transported by means of advection by horizontal particle velocity and pressure (Holthuijsen, 2007):

$$S_{xx} = S_{xx,pressure} + S_{xx,horizontal\ particle\ velocity} \\ = \left(n - \frac{1}{2}\right)E + nE \quad (2.6)$$

Differences in radiation stresses result in water level gradients obeying the first order momentum balance and can be described as follows:

$$F_x = -\frac{\partial S_{xx}}{\partial x} = \rho g h \frac{\partial \bar{\eta}}{\partial x} = \rho g (h_0 + \bar{\eta}) \frac{\partial \bar{\eta}}{\partial x} \quad (2.7)$$

In deep water ($n = 1/2$), the pressure term is 0, so the momentum flux is only expressed in the horizontal particle velocity. In shallow water ($n = 1$) the contribution of the pressure term is $1/2E$, giving $2/3E$ in total. Translating this in a water level gradient (normal incident waves on a longshore uniform coast):

$$S_{xx} = \frac{3}{2}E = \frac{3}{16}\rho g H^2 = \frac{3}{16}\rho g \gamma^2 h^2 \quad (2.8)$$

Substitution in (2.7) gives:

$$-\frac{\partial}{\partial x} \left(\frac{3}{16} \gamma^2 h^2 \right) = h \frac{\partial \bar{\eta}}{\partial x} \quad (2.9)$$

And thus:

$$\frac{\partial \bar{\eta}}{\partial x} = -\frac{3}{8} \gamma^2 \frac{\partial h}{\partial x} \quad (2.10)$$

When looking at non uniform longshore profile coastlines (which is the case with SBWs), differences in radiation stresses in the x-direction can be compensated by longshore transport as well. For the cross-shore direction the momentum balance then results in (Haller, Dalrymple, et al., 2002):

$$\rho \left[\frac{d}{dx} (U^2 h) + \frac{d}{dy} (UVh) \right] + \rho g h \frac{d\eta}{dx} \left(\frac{dS_{xx}}{dx} + \frac{dS_{xy}}{dx} \right) + \tau_x^b \quad (2.11)$$

And for the longshore-direction:

$$\rho \left[\frac{\partial}{\partial x} (UVh) + \frac{\partial}{\partial y} (V^2 h) \right] + \rho g h \frac{\partial \eta}{\partial y} \left(\frac{\partial S_{yy}}{\partial x} + \frac{\partial S_{xy}}{\partial x} \right) + \tau_y^b \quad (2.12)$$

Where the radiation stresses are given by:

$$S_{xx} = \frac{1}{8} \rho g H^2 \left[n(\cos^2 \theta + 1) - \frac{1}{2} \right] + \rho g H^2 \left(\frac{0.9H}{L} \right) \quad (2.13)$$

$$S_{yy} = \frac{1}{8} \rho g H^2 \left[n - \frac{1}{2} \right] \quad (2.14)$$

S_{xy} is neglected. Bottom shear stress for both x- and y-direction is given by:

$$\tau_{x,y}^b = \rho c_f \langle |u|u \rangle \quad (2.15)$$

With c_f being an empirical coefficient and u the flow velocity at the bottom.

Empirical relations describing wave induced water level set-up/down extracted from experimental data is reviewed in paragraph 2.2.7.

2.2.7 Wave set-up

The first mention of water level set-up behind a submerged breakwater appeared in (Homma et al., 1959). This mention provided only a qualitative view of the phenomenon. The solution developed by (Longuet-Higgins, 1967) included parameters to determine the magnitude of the set-up behind a SBW with non-breaking waves:

$$\delta' = \frac{H_i^2 (1 + K_r^2) k_I}{8 \sinh(2k_I h_I)} - \frac{H_i^2 K_t^2 k_{II}}{8 \sinh(2k_{II} h_{II})} \quad (2.16)$$

With the denotations I and II describing the locations offshore and inshore of the breakwater. (2.16) describes the difference in the mean water levels at the uniform depths at location I and II, using the second order Stokes wave theory. Regular wave test data (Dick et al., 1968) showed that (2.16) underestimated the magnitude of the set-up. (Diskin, 1970) performed a study on a 2-dimensional physical model of a trapezoidal breakwater. (Vicinanza et al., 2008) used the results to develop an empirical relationship between the set-up, the wave height and the submergence level:

$$\frac{\delta}{H_i} = 0.60 \exp \left[- \left(0.70 - \frac{R_c}{H_i} \right)^2 \right] \quad (2.17)$$

For:

$$-2 < -\frac{R_c}{H_i} < 1.5 \quad (2.18)$$

This would mean a maximum set-up when $R_c = 0.7 H_i$. Crest width and wave period are not included in this formula. Because of the simplifications in the then existing formulae (Vicinanza et al., 2008) developed an alternative method based on the momentum flux balance:

$$S_{xx} - S'_{xx} + \Pi_2 - \Pi_1 + P_1 - P_2 = 0 \quad (2.19)$$

Where Π is the force of the structure exerted on the body of fluid and P is the hydrostatic pressure (shown in Figure 2.1).

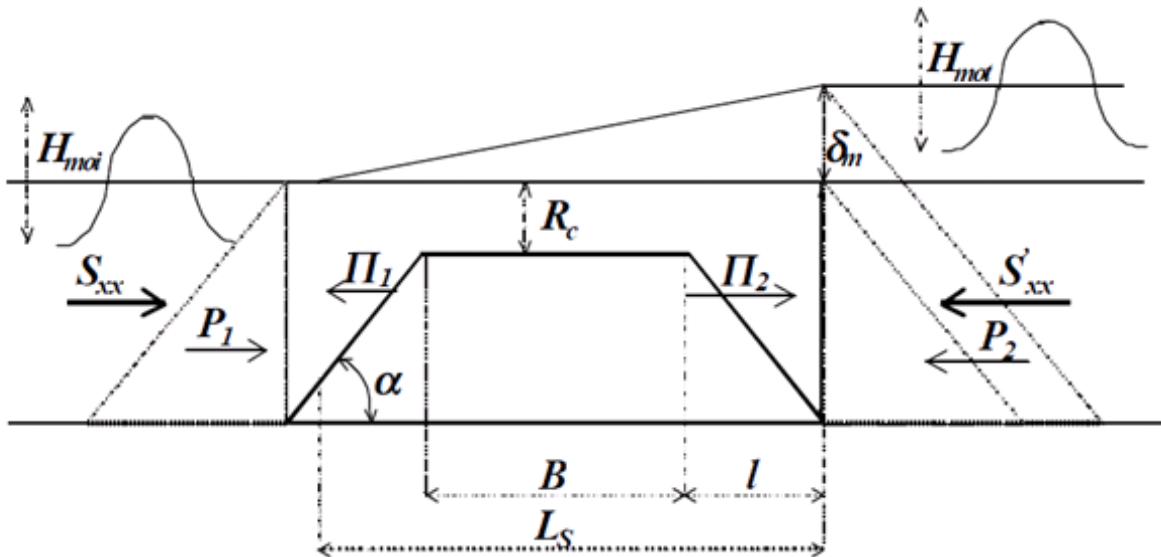


Figure 2.1 - Definition for the energy balance by wave set-up over a submerged breakwater (Vicinanza et al., 2008).

It is assumed that the SBW is impermeable and the waves are non-reflecting. Also the generation of higher harmonics, shoaling and initial water level set-up/down is neglected. The magnitude of the water level set-up, δ_m , can be solved using the momentum balance equation. This method of obtaining the water level set-up is comparable to the method used by (Bellotti, 2004). Because that study later included rip currents through gaps, that study is more extensively discussed in paragraph 2.3.2.

2.2.8 Wave breaking

Wave breaking can occur both in deep water (white-capping) and shallow water (bottom friction and depth induced). In this case only shallow water wave breaking is relevant when looking at wave breaking over the SBW and later in the surf zone.

The most wide known theory to describe this is the one from (Battjes et al., 1978). The same Rayleigh distribution is used to predict the wave height as for non-breaking waves, but

truncated at a certain depth dependent value. The maximum wave height is then proportional to a wave breaker index and the water depth, $H_{max} \cong \gamma h$, or more complete:

$$H_{max} = 0.88k^{-1} \tanh\left(\frac{\gamma kh}{0.88}\right) \quad (2.20)$$

The breaker parameter γ is tuneable. The default value for γ in SWAN is set to 0.73.

Since then a lot of research has been done to improve this theory to better fit the empirical data. For instance; replacing the clipped Rayleigh distribution with a Weibull distribution or a non-clipped Rayleigh distribution. It was also suggested that the breaker parameter γ was not only dependent on the water depth but also the slope (no slope would give a γ -value of 0.55 and a steep slope would yield higher values for γ then, for instance, 0.73).

When looking at depth induced breaking over an SBW, the slope of the SBW is now the bottom the wave will interact with and is much steeper than the average surf zone bottom slope. (Baldock et al., 1998) showed that for steeper bottom profiles the use of a non-clipped Rayleigh distribution yielded better results. Physically this is plausible: waves travel further up the slope, breaking relatively late, giving a higher breaker index.

Additionally, when looking at wave breaking, a mention needs to be made with regard to the roller model. When this is not accounted for, the start of the water level gradient caused by wave breaking is calculated too far seaward. (Nairn et al., 1990) showed that before dissipating the energy by breaking the wave energy is first converted to kinetic energy travelling as a bore at the phase velocity, effectively postponing the moment of dissipation and therefore the water level setup. When a roller term is added to the original model, the starting point corresponds better with field data.

2.2.9 Wave transmission

The effectiveness of an SBW can be measured in terms of the coefficients for wave reflection, wave dissipation and wave transmission. Or, when taking the process as a whole, the wave attenuation.

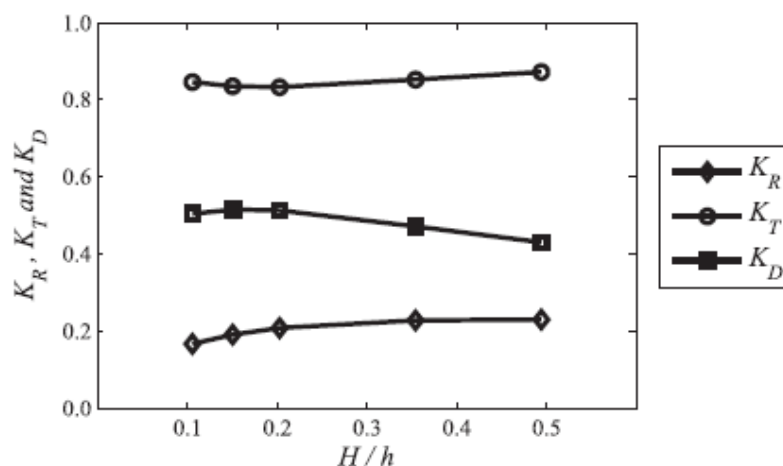


Figure 2.2 - Energy coefficients of wave reflection (K_R), wave transmission (K_T) and wave dissipation (K_D) versus wave non-linearity (Wu et al., 2012)

These parameters are usually based on linear wave theory, assuming the flow to be irrotational and only dependent on wave height. Since the interaction between wave and

structure includes vortex shedding and wave breaking it is better to use the integral of the energy flux to determine the characteristics (Van der Meer et al., 2000). Using numerical modelling it was concluded that the largest wave dissipation was found at $H/h = 0.15$ (Figure 2.2).

When describing the wave transmission as a visual process, 4 phases can be discerned; the first phase is the separation of the incoming wave in a transmitted and reflected part, the second phase consists of the crest-crest interaction, the third phase shows backward breaking just over the SBW and finally the fourth phase has multiple smaller breaking events caused by the backward breaking in phase 3. Regarding the wave shape in this process (Battjes et al., 1978) shows that the wave skewness is drastically increased when the wave crosses the SBW and decreases again over the onshore side. The wave asymmetry decreases over the SBW and increases again when the wave has passed the SBW.

To come to a formula for the K_t coefficient ($K_t = H_t/H_i$), data was acquired in multiple studies. Fitting the data led to 2 formulas:

From (Calabrese et al., 2007):

$$K_t = -0.4 \frac{R_c}{H_i} + 0.64 \left(\frac{B}{H_i} \right)^{-0.31} (1 - e^{-0.5\xi}) \quad (2.21)$$

for $\frac{B}{H_i} < 10$

From (Van der Meer et al., 2005):

$$K_t = -0.35 \frac{R_c}{H_i} + 0.51 \left(\frac{B}{H_i} \right)^{-0.65} (1 - e^{-0.41\xi}) \quad (2.22)$$

for $\frac{B}{H_i} < 10$

To overcome the discrepancy at $B/H_i = 10$ (Van der Meer et al., 2005) suggested to interpolate both formulae for $8 < B/H_i < 12$. In addition, for smooth structures, the crest width B can be neglected, leading to the following formula:

$$K_t = -0.3 \frac{R_c}{H_i} + 0.75(1 - e^{-0.5\xi}) \quad (2.23)$$

for $1 < \xi < 3$

Also the wave period is influenced by the interaction with the SBW. The wave spectrum change over the SBW results in a different wave energy distribution with more wave energy in higher frequencies. So a wave breaking over the structure may generate two or more transmitted waves in the lee of the breakwater. (Van der Meer et al., 2000) showed that the peak period remained the same, but the average period increases. In average 60 % of the wave energy is found in $< 1.5f_p$ and 40 % is distributed between $1.5f_p$ and the f_{max} of $3.5f_p$. However, when there is hardly wave breaking, there is also a frequency shift to higher harmonics. This is due to wave-wave interactions caused by the change in wave asymmetry over the offshore slope of the SBW.

The wave pattern behind the SBW consists then of the combination of two types of waves. The waves that pass over the SBW into the lee (K_t) and the waves that entered through the gaps and then started diffracting (K_d). This can be described by the following formula:

$$K_{t,d} = \sqrt{(K_t^2 + K_d^2)} \tag{2.24}$$

2.2.10 Wave sheltering

Wave sheltering is the more common term for the spatial distribution of wave forcing. The (partial) breaking of the waves over the SBW leads to directional spreading of the wave energy (Herbers et al., 1999). This results in a widened area of impact of the waves on the shoreline. Figure 2.3 visualizes this redistribution of wave forcing due to an SBW. For a single SBW this leads to a transitional zone (a fully protected zone if the SBW length is long enough and/or close enough to the shoreline). As a result, near the breakwater head, water levels decrease compared to the undisturbed coastline. In contrast, undisturbed waves will enter the lee of the SBW, reducing water level differences and increasing the total wave breaking over and in the lee of the SBW.

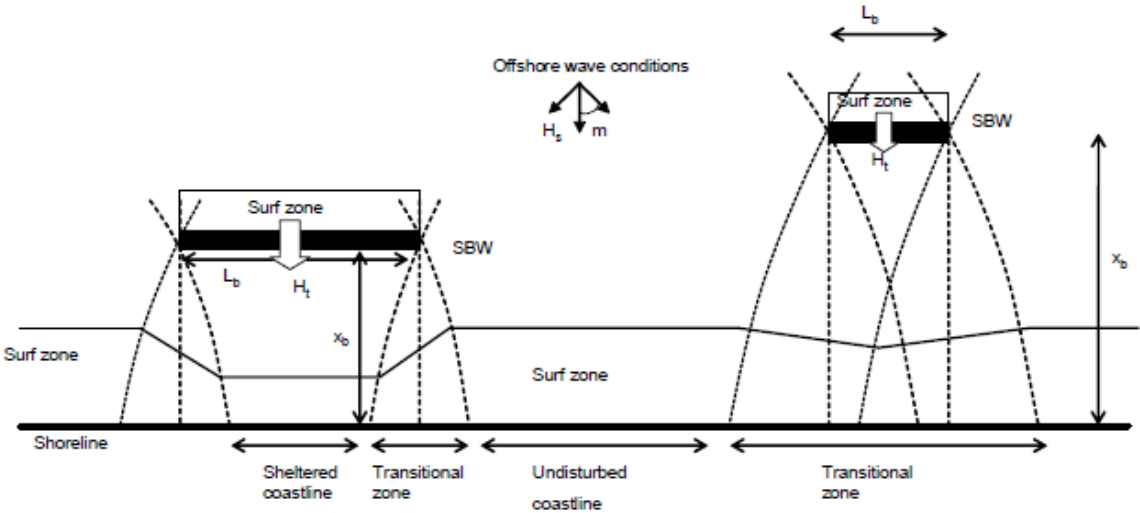


Figure 2.3 - Redistribution of wave forcing due to a SBW (Vlijm, 2011)

The wave spectrum in the lee of the SBW is influenced by diffraction from the waves next to the SBW and the directionally spread waves that crossed the barrier. Literature on the difference regarding this effect in the case of multiple SBWs is not available at the moment of writing. However, it is expected that the degree in wave sheltering is different with respect to single SBW when the SBWs are close enough to have cause interaction in or more of the aforementioned processes.

2.2.11 Mass transport over the SBW

While there is a variety of empirical formulae for the mass transport (overtopping) over low crested structures and emergent breakwaters, only recently (Calabrese et al., 2008) proposed a formula for the mass transport over SBWs:

$$q_{in} = \sqrt{gh}H \left(\frac{B_0H}{|R_c|} + 0.06 \right) \tag{2.25}$$

$$H = \frac{H_i(1 + K_t)}{2} \quad (2.26)$$

With shape factor B_0 :

$$B_0 = 0.125 \tanh\left(\frac{11.4}{\sqrt{U_r}}\right) \quad (2.27)$$

$$U_r = \frac{2\pi L_0}{H_i} \left(\frac{H_i}{|R_c|}\right)^2 \left(1 + \frac{H_i}{|R_c|}\right) \quad (2.28)$$

This formula accounts for the 2 main processes for mass transport: Stokes drift velocity and the addition by wave roller mass flow. The basis for this theory can be found in (Svendsen, 1986).

In the same sense, there is an outflow over the SBW, the offshore flow over the crest. The magnitude of this outflow is related to the outflow of the gap, since they both form a mass balance with the inflow (outflow through the SBW is negligible (Battjes et al., 1978)). This balance is discussed in paragraph 2.3.2.

2.3 Extending the theory for the addition of gaps in the SBW

A lot of the previously described processes are only valid for simplified cases like an infinitely long SBW or only one shore parallel breakwater. This section describes the additional processes or extends them for the hydrodynamics in the vicinity of multiple SBWs. The morphology for the complete region of interest is discussed in paragraph 2.4.

2.3.1 Rip-currents

A rip current is a strong channel of water flowing seaward from near the shore, typically through the surf-zone. There exist quite a range of theories to describe the generation and magnitude of rip-currents. The basis is given by the earlier studies. Some of these pertain only to rip-currents at a plane parallel beach (wave interaction induced); (Bowen et al., 1969), (Sasaki, 1975) and (Dalrymple, 1975). (Bowen, 1969) and (Noda, 1974) discuss bottom topography induced rip-currents and (Dalrymple et al., 1976) studied wave-induced currents on barred coastlines. More related to SBWs is (Liu et al., 1976), since it includes structural interaction with currents.

More recently (Dalrymple et al., 2011) studied rip currents in the vicinity of SBWs and compared them to other forms of rip currents. Figure 2.4 shows the forms of rip currents: a) Linear bar-through rip current. b) Semi-enclosed rip current. c) Rip current collocated with the pier. d) Mega rip-current associated with pocket beach. e) Swash rip currents. f) Obliquely incident wave angle. g) Near-normally incident wave angle. Rip currents caused by SBWs are best comparable with linear bar-through rip currents.

Rip-currents can be maintained on purpose (water circulation, getting surfers out of the surf zone), or circumstantial with a more unpredictable nature. What is certain is that rip-currents

have an impact on the morphology as such that they induce local scour. Since SBWs will induce rip-currents, it is important to determine a relation between the physical parameters of the SBW and the environment and the magnitude of the rip-current induced scour as well as the hydrodynamic aspects it influences, e.g. the steepening of the incoming waves at the location of the rip current.

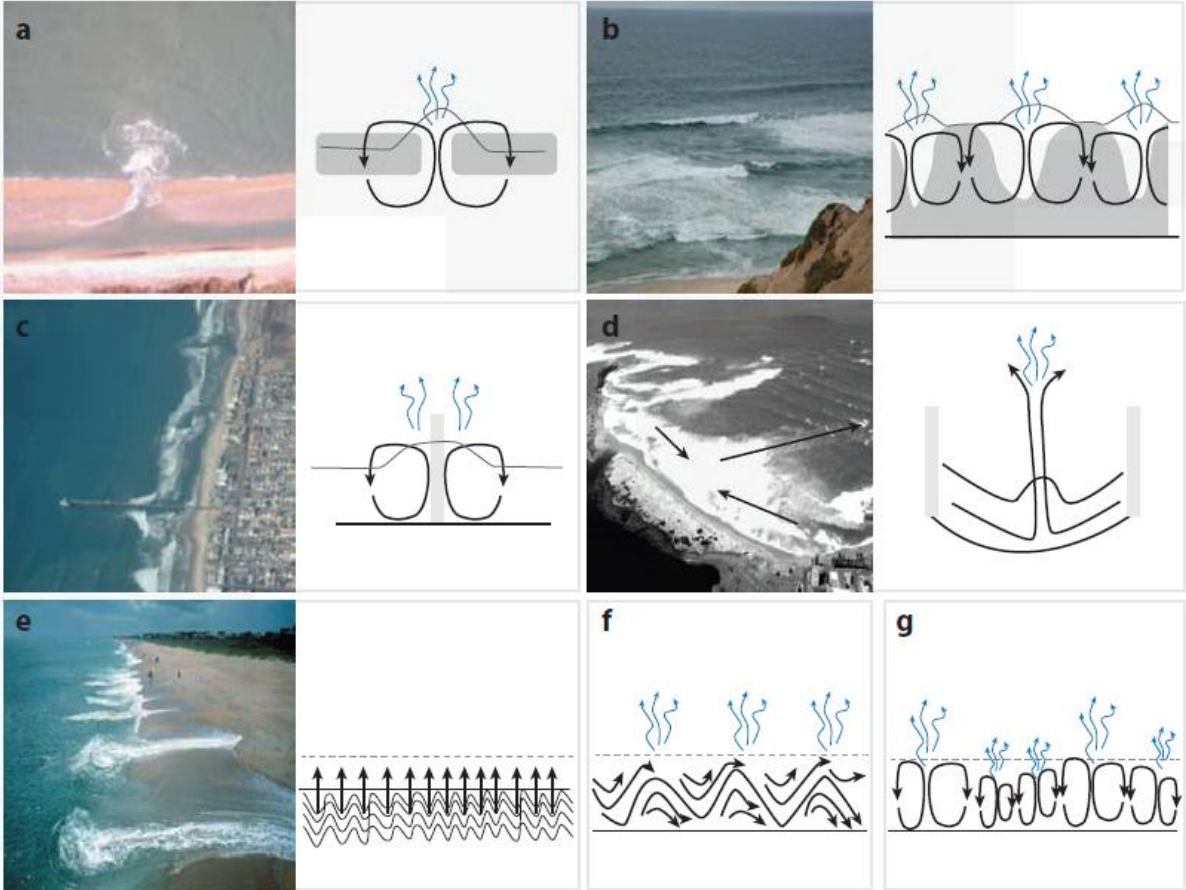


Figure 2.4 - Forms of rip currents (Dalrymple et al., 2011)

2.3.2 Mass balance

To determine the magnitude of the flow velocity in the gaps, one can use the mass balance. The mass balance can be proposed to consist of an inflow and a return flow over the SBW and a return flow through the gaps (Battjes et al., 1978). Using the mass balance a multitude of relations can be observed.

2.3.2.1 Return flow distribution

The return flow distribution is interrelated with the degree of lateral confinement; small gaps relative to the SBW length meaning a high degree of lateral confinement and vice versa. If the SBW is infinitely long, by mass balance, the inflow over the SBW would be equal to the outflow over the SBW. When there are relatively small gaps, the outflow part over the SBW would be relatively bigger than when there are relatively wide gaps. The flow subparts are interrelated and are all dependent on the piling up height in the lee of the breakwater (Figure 2.5). An empirical study by (Burcharth et al., 2007) showed that the piling-up height for a situation with no gaps ('Channel') is about 1.5 times as high as the piling-up height for narrow gaps ($L_g/L_b = 1/4$) and about 8 times as high compared to the piling up in case of wide gaps ($L_g/L_b = 1$) when looking at submerged conditions.

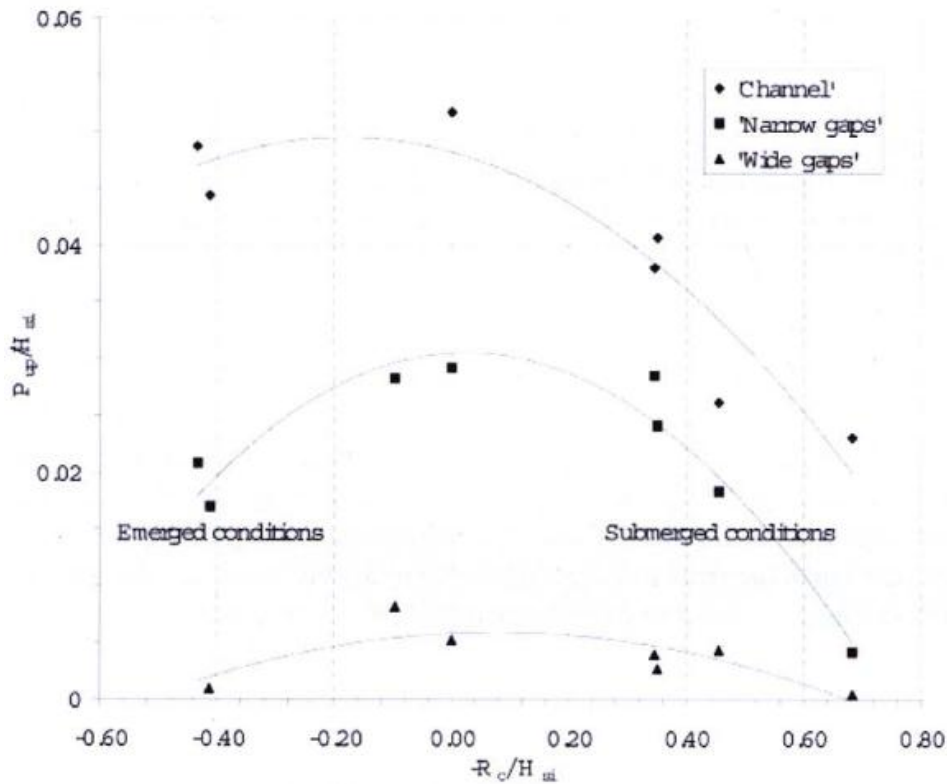


Figure 2.5 - Piling-up P for different confinement conditions (Burcharth et al., 2007)

Consequently, the piling-up can then be related to the distribution between the return flow over the SBW and through the gaps. When the piling-up is absent or negligible, the return flow consists almost entirely of return flow over the SBW. But with an increase in piling-up, the percentage of return flow through the gap with respect to the total return flow rises as well. When this is expressed in a graph, the balance for the system is found at the intersection (see Figure 2.6). The final distribution is of course dependent on the physical parameters of the system.

2.3.2.2 Velocity in the gap

When trying to compute the velocity at the gap one can use the generalised Bernoulli theorem, along with the return flow pattern (Burcharth et al., 2007). The first point (1) situated inshore at the centre of the SBW, where piling-up is assumed to be at its maximum and the velocity can be assumed to be zero due to symmetry. The second point (2) is in the centre of the gap, where piling-up can be assumed zero and the velocity unknown. Along this pattern exists a head loss due to friction (ΔH), giving the following equation:

$$H_1 - \Delta H = H_2 \quad (2.29)$$

Where H is given by the sum of the piling-up P , the energy head and the wave pressure excess height:

$$H = P + \frac{u^2}{2g} + \frac{\eta_{rms}^2 k_s}{\sinh(2k_s h)} \quad (2.30)$$

Computing values for H for both points and a value for the head loss by friction will give a value for the velocity in the gap. However this relation will not give information about the distribution of the velocity in the gap, both in horizontal and vertical direction. The relation is only for the order of magnitude of the flow velocity in the gap, the distribution needs to be computed by a physical or numerical model.

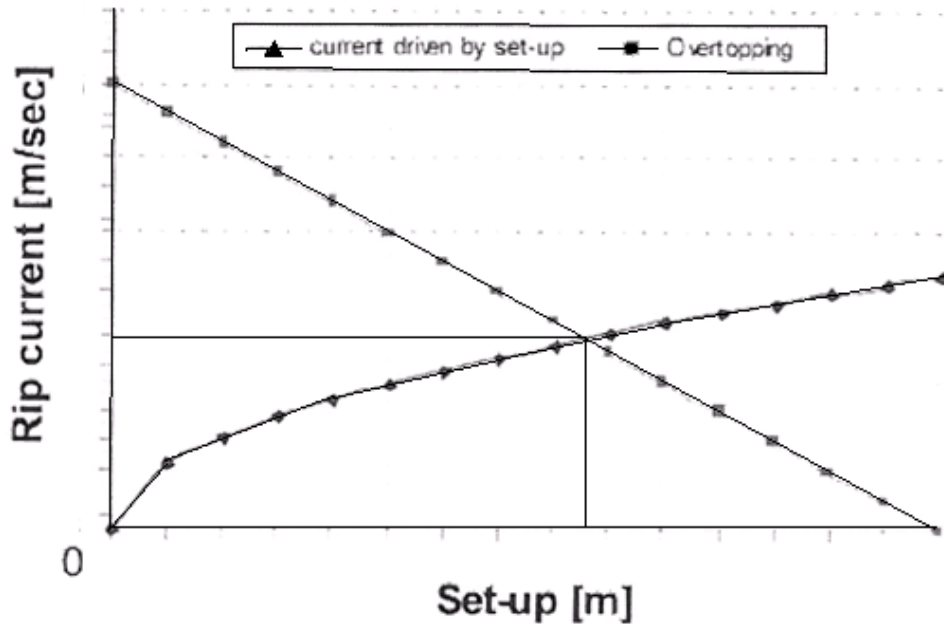


Figure 2.6 - Distribution between return flow over the SBW (overtopping) and return flow through the gaps based on the set-up (Burcharth et al., 2007)

2.3.2.3 Water level set-up in the lee of the SBW

(Bellotti, 2004) set up an approximation for the mass balance based on the continuity and momentum equations over a certain area.

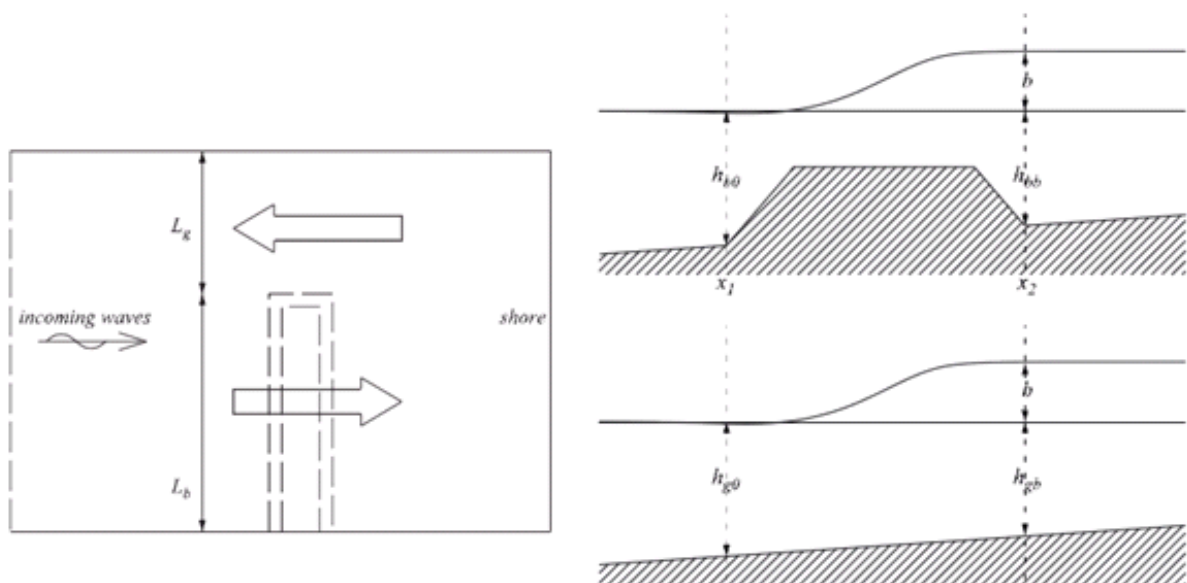


Figure 2.7 - Schematized overview (left) and cross-section (right) with the respective parameters (Bellotti, 2004).

Following the schematization as in Figure 2.7 the continuity equation (depth averaged) is as follows:

$$u_{b0} \cdot h_{b0} = u_{bb}(h_{bb} + b) \quad (2.31)$$

And the momentum equation:

$$\begin{aligned} \rho(h_{b0} \cdot u_{b0}^2) + \frac{1}{2} \rho g h_{b0}^2 + Z - \rho[(h_{bb} + b)u_{bb}^2] \\ - \frac{1}{2} \rho g (h_{bb} + b)^2 - \Delta S_{xx} - T_{xb} = 0 \end{aligned} \quad (2.32)$$

With Z being the hydrostatic force along the bottom between the offshore and onshore trunk of the breakwater. ΔS_{xx} is the difference in radiation stress caused by the wave transmission over the SBW and T_{xb} the bottom friction between points x_1 and x_2 . The SBW is assumed to be impermeable, which gives a negligible error (Van der Meer et al., 2005).

Z depends on the water depth which in turn depends on the bottom slope and the water level set-up.

$$Z = \int_{x_1}^{x_2} \rho g (h + \eta) \frac{\partial h}{\partial x} dx \quad (2.33)$$

Assuming both the bottom slope and the increase in water level set-up are linear between points x_1 and x_2 gives:

$$Z = g \int_{x_1}^{x_2} \left[h \frac{\partial h}{\partial x} + b \frac{(x - x_1)}{x_2 - x_1} \frac{\partial h}{\partial x} \right] dx \quad (2.34)$$

The water is shallow so ΔS_{xx} becomes:

$$\Delta S_{xx} = \frac{3}{16} \rho g (H_{s2}^2 - H_{s1}^2) \quad (2.35)$$

And the bottom friction:

$$T_{xb} = B c_f \left(\frac{u_{b1} + u_{b2}}{2} \right)^2 \quad (2.36)$$

Introducing the y -direction one can now relate the flow speed in the gap to the flow speed over the SBW with the help of the mass balance, for instance:

$$u_{bb} = \mu \sqrt{2gb} \frac{h_{g0}}{(h_{bb} + b)} \frac{L_g}{L_b} \quad (2.37)$$

An important remark for this approximation is that the average flow speed is positive in the x -direction and with that the bottom friction counters the set-up. However, the flow over the bottom profile is likely to be dominated by an undertow in the offshore direction, changing the sign for the force exerted on the system by the bottom stress, in that case increasing the set-up. In the study by (Zanuttigh et al., 2008) this phenomenon is looked at, but is not very relevant for this research since the numerical model used is of the 2DH type, effectively having 1 vertical layer and with that a depth averaged flow.

In a later study (Bellotti, 2007) extended this theory and this was used in the study by (Villani et al., 2012), discussed in paragraph 2.4.3.

2.4 Morphodynamics

Coastal changes occur in case of sediment transport gradients. A positive gradient (an increase in the sediment transport in the transport direction) leads to erosion. A negative gradient (a decrease in sediment transport in the transport direction) leads to accretion. If the gradient is zero, there are no changes in morphology (Bosboom et al., 2012). This means that if the net sediment flux over a certain area is negative, the bottom will supply the sediment deficit leading to erosion. The bottom lowers and so do the waves and tides, being dependent on the water depth. The change in hydrodynamics changes the sediment transport rates affecting, again, the morphology. This system of feedback is known as morphodynamics.

As discussed earlier, SBWs influence the hydrodynamics and with that the morphology. Since a stable or accreting coastline is preferred, it is important to understand the morphological patterns in the vicinity of an SBW. Some studies present predictions for the mode of shoreline response (accretion versus erosion) and some predict also the magnitude of the morphological changes.

2.4.1 Scour patterns

All the aforementioned hydrodynamic processes induce currents throughout the water column. If these currents present themselves at or near the bottom the bottom shear stress increases and when the shear stress caused by the hydrodynamic processes exceeds the critical sediment shear stress, grains will start to move. When persistent a scour hole occurs. (Sumer et al., 2005) showed that the scour at the offshore side of the SBW is in the same order of magnitude as is the case with an emergent breakwater. However it does not present the same scour/deposition pattern as emergent breakwaters where this pattern is correlated with the nodal and anti-nodal points of the standing wave in front of the breakwater. In addition, the erosion on the lee side of the SBW is in the same order of magnitude as the erosion on the offshore side whereas in the case of an emergent breakwater there is barely any scour. At the roundhead of an SBW severe scour is experienced both inshore and offshore. The offshore side scour is caused by unhindered waves and a steady offshore-directed current. Important parameters for the magnitude of this local scour are the wave height to submergence level ratio and the Keulegan-Carpenter number, KC. The scour at the inshore location is due to the wave breaking and wave overtopping over the SBW. Governing parameters here are the water depth to submergence level ratio and the dimensionless plunger parameter:

$$\frac{T\sqrt{gH}}{h} \quad (2.38)$$

2.4.2 Scour dimensions

The inshore scour parameters were studied by (Young et al., 2009). A clear difference was made between attached and detached scour, visible in Figure 2.8.

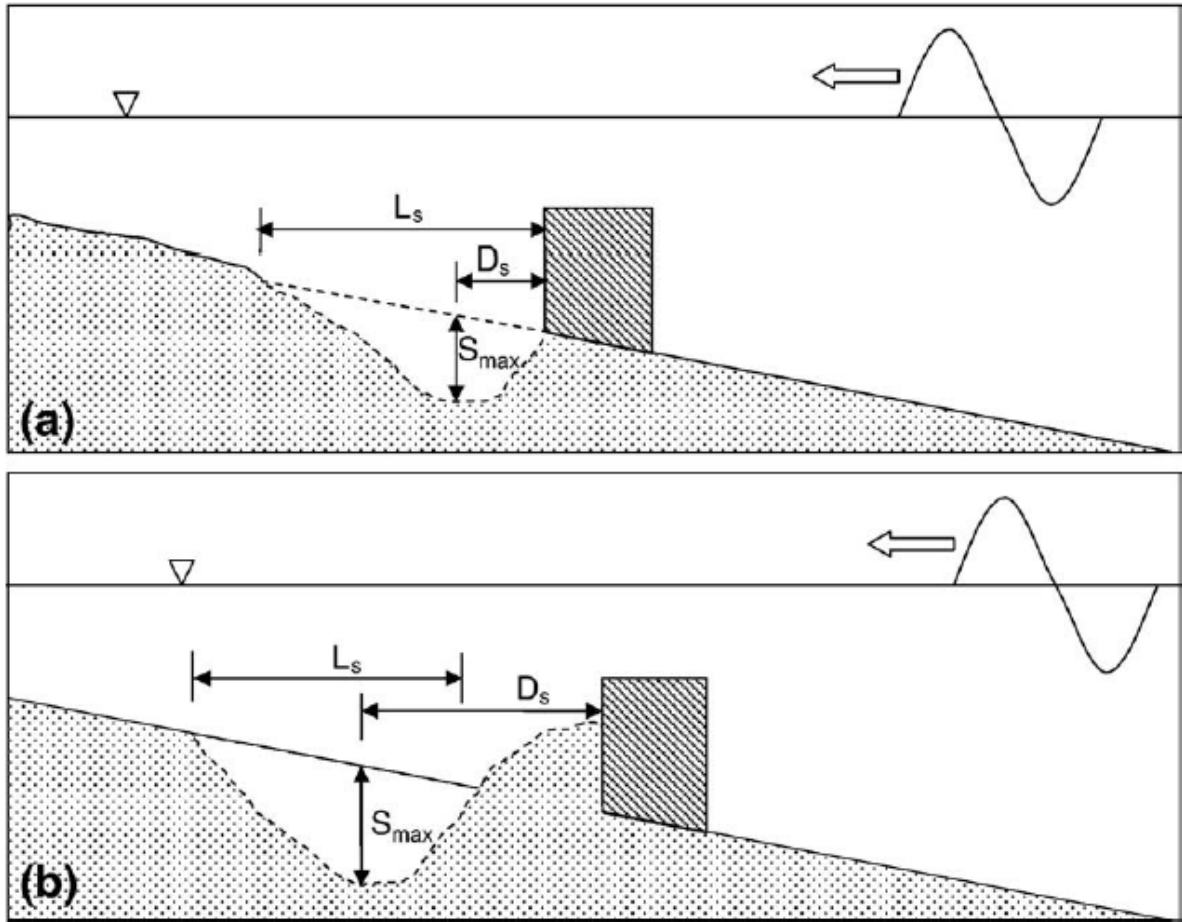


Figure 2.8 - Definition sketch of scour patterns and parameters: (a) attached scour, (b) detached scour (Young et al., 2009)

A criterion based on the KC-number determines if the scour is attached or detached. The scour is attached when:

$$KC = \left(\frac{H_i \pi}{B} \right) \leq \pi \quad (2.39)$$

And has a detached nature when:

$$KC = \left(\frac{H_i \pi}{B} \right) > \pi \quad (2.40)$$

This is due to the turbulent jet over the SBW created by the transmission of the waves. When the wave height is less than the width of the crest of the SBW, the turbulence impacts on and directly over the SBW, affecting the sediment at the inshore trunk. It is deposited over a greater stretch onshore. When the wave height exceeds the width of the SBW, the turbulent jet reaches over the crest forming a vortex inshore of the SBW. This vortex creates a detached scour hole and deposits the sediment offshore at the trunk of the SBW. However, this vortex formation is dependent on the form of the SBW and is less dominant when the SBW has a (milder) slope.

The other parameters; the maximum depth of the scour hole, S_{max} , the cross-shore length of the scour hole, L_s , and the distance from the inshore trunk of the SBW to the deepest point of the scour hole, D_s , are also dependent on the KC-number.

$$S_{max} = 0.0125\sqrt{\theta}KC \quad (2.41)$$

2.4.3 Shore-line changes

There are not many established guidelines to design a SBW to establish a certain shoreline response, hence the importance of this thesis. (Pilarczyk, 2003) extended the guidelines for emergent breakwaters by (Harris et al., 1986) to make them applicable to SBWs. These first guidelines can be seen as a rule of thumb. Later criteria for the mode of shoreline response followed, based on physical parameters and analytical formulae.

2.4.3.1 Rule of thumb

(Pilarczyk, 2003) proposed, as a first approximation, to add the factor $(1-K_t)$ to the existing guidelines for emergent breakwaters. With that the guidelines becomes:

Tombolo:

$$\begin{aligned} \frac{L_b}{x_b} > \frac{1.0 \text{ to } 1.5}{1 - K_t} \text{ or } \frac{x_b}{L_b} < \left(\frac{2}{3} \text{ to } 1\right) (1 - K_t) \\ \text{or } \frac{x_b}{1 - K_t} > \left(\frac{2}{3} \text{ to } 1\right) L_b \end{aligned} \quad (2.42)$$

Salient:

$$\frac{L_b}{x_b} < \frac{1.0}{1 - K_t} \text{ or } \frac{x_b}{L_b} < 1 - K_t \text{ or } \frac{x_b}{1 - K_t} > L_b \quad (2.43)$$

In the case of predicting the formation of salient in the lee of multiple SBWs, a parameter for the gap width is included:

$$\frac{L_g x_b}{L_b^2} > 0.5(1 - K_t) \quad (2.44)$$

A different criteria for salient formation is given by (Black et al., 2001). This study proposes the formation of a salient when $L_b/x_b < 2$. When this is the case it also gives a relation for the magnitude of the salient (Y):

$$\frac{(x_b - Y)}{L_b} = 0.498 \left(\frac{L_b}{x_b}\right)^{-1.268} \quad (2.45)$$

And the total length of the shoreline affected by the salient (D):

$$\frac{Y}{D} = 0.125 \pm 0.02 \quad (2.46)$$

2.4.3.2 Criterion based on physical parameters

As the main function of an SBW remains the same as that of an emergent breakwater the preferred shoreline change is accretion. Using the guidelines for emergent breakwaters, the guidelines shown in paragraph 2.4.3.1 only predict responses where there is accretion.

However, (Ranasinghe et al., 2006) pointed out that most field cases reported erosion despite the construction of SBWs. The study uses physical models to reproduce the flow patterns in the lee of the SBW that influences the shoreline response. One of the possible patterns (see Figure 2.9) indeed produces an erosive coastline.

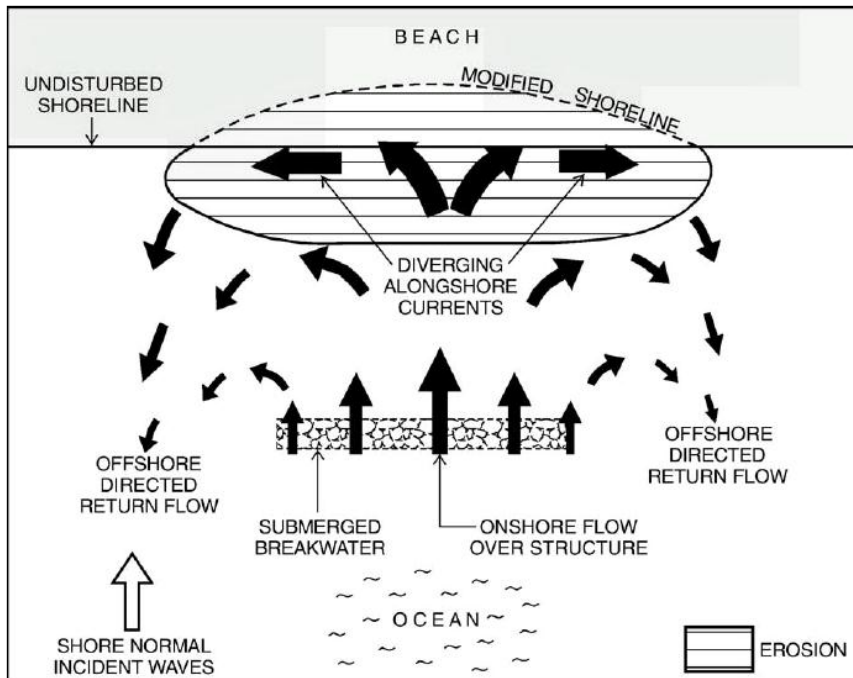


Figure 2.9 - Schematic depiction of expected nearshore circulation patterns that may lead to shoreline erosion (Ranasinghe et al., 2006)

To describe the phenomenon more accurately more parameters needed to be included. The parameters directly influencing the shoreline response can be divided into 3 categories (see also Figure 2.10) (Ranasinghe et al., 2010):

- Environmental and hydrodynamic properties of the SBW: wave height (H), wave period (T), wave direction (θ) and tidal range (R).
- Structural properties: submergence level (s_b), water depth at the location of the SBW (h_b), length of the SBW (L_b), SBW crest width (w_b) and the distance between the shoreline and the SBW (x_b).
- Physical properties: the gravitational acceleration (g) and the grain diameter (D_{50}).

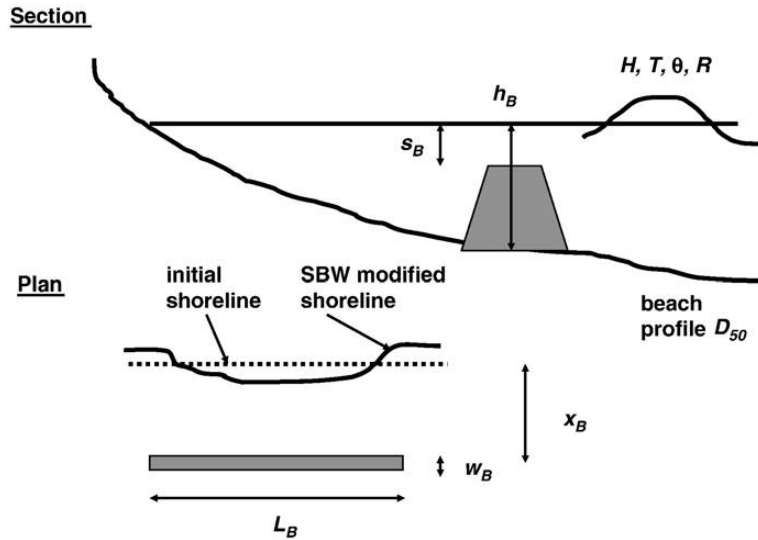


Figure 2.10 - Schematic diagram showing key structural/design parameters governing shoreline response to an SBW (Ranasinghe et al., 2010).

Using these parameters in a dimensional analysis it is shown that the shoreline response is governed by:

$$Response = function\left(\frac{H_0}{L_{w0}}, \frac{s_b}{H_0}, \frac{h_b}{H_0}, \frac{x_b}{L_{w0}}, \frac{L_b}{L_{w0}}\right) \quad (2.47)$$

With H_0 and L_{w0} describing respectively the wave height and wave length in deep water conditions.

However, including physical considerations, a response-function can also be developed based on the physics governing the problem. If the tendency of a shoreline to form a salient is expressed as the ratio λ between the onshore flow over the SBW (Q_C) and the longshore flow in the lee of the SBW (Q_L), the following criterion is obtained (Ranasinghe et al., 2010):

$$\lambda = \frac{Q_C}{Q_L} = function(\phi_1, \phi_2) \quad (2.48)$$

With:

$$\phi_1 = \left(\frac{s_b}{h_b}\right)^{\frac{3}{2}} \left(\frac{L_b}{h_b}\right)^2 \left(\frac{A^3}{h_b}\right)^{\frac{1}{2}} \quad (2.49)$$

$$\phi_2 = \left(\frac{h_b}{H_0}\right) \quad (2.50)$$

When plotting numerical and physical model data on a semi-logarithmic scale (see Figure 2.11), the line separating the erosive and accretive cases is found to be:

$$\frac{h_b}{H_0} = 2 \log_{10} \left[\left(\frac{s_b}{h_b}\right)^{\frac{3}{2}} \left(\frac{L_b}{h_b}\right)^2 \left(\frac{A^3}{h_b}\right)^{\frac{1}{2}} \right] + 0.65 \quad (2.51)$$

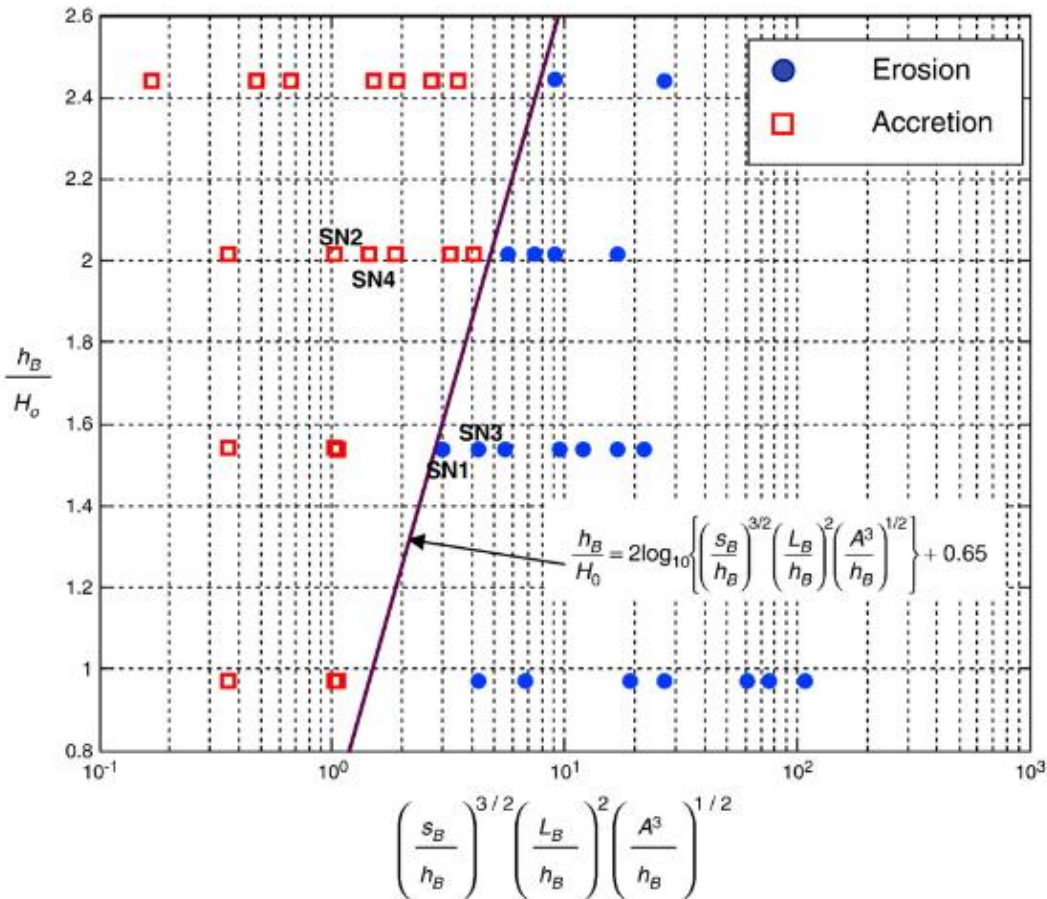


Figure 2.11 - The dependence of the mode of shoreline response on the two non-dimensional parameters identified in (2.48) (Ranasinghe et al., 2010).

Furthermore, it was discovered that multiple types of circulation patterns can be observed in the vicinity of SBWs and can be used to predict an erosive or accretive nature of the shoreline. This pattern occurs in two forms with vastly different impacts on the shoreline response; a 2-cell pattern resulting in shoreline erosion for both shore-normal and oblique waves and 4-cell pattern resulting in shoreline accretion for both shore-normal and oblique wave (see Figure 2.12).

Whether a 2-cell or a 4-cell pattern occurs is dependent on the distance between the shoreline and the SBW, where a relatively short distance results in a 2-cell pattern and a relatively large distance results in a 4-cell pattern.

However, certain cases did not obey to the criteria given above and experienced erosion where accretion was to be expected and vice-versa. It was concluded that the nearshore generated circulation pattern does not always reflect entirely the complexity of the SBW's hydrodynamics.

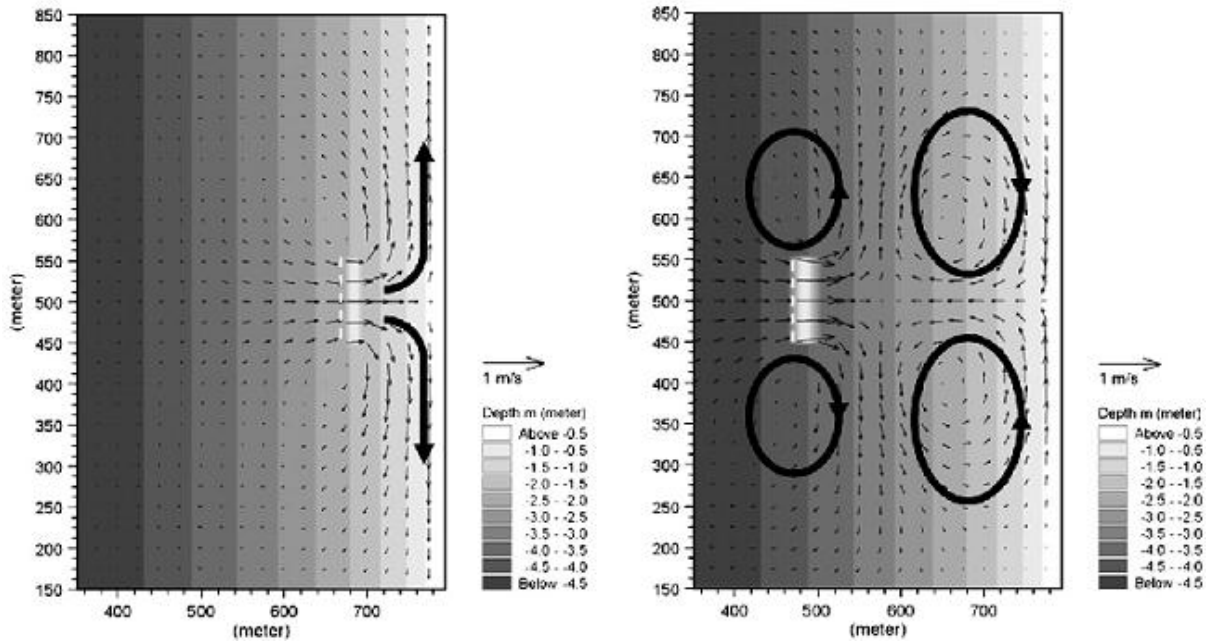


Figure 2.12 - Visualization of the 2-cell pattern (above) and the 4-cell pattern (below) (Ranasinghe et al., 2010).

2.4.3.3 Criterion based on analytical formulae

The study by (Villani et al., 2012) combines the 2-cell / 4-cell theory with the analytical models by (Bellotti, 2007) and (Zanuttigh et al., 2008). The aspect of multiple SBWs is also introduced:

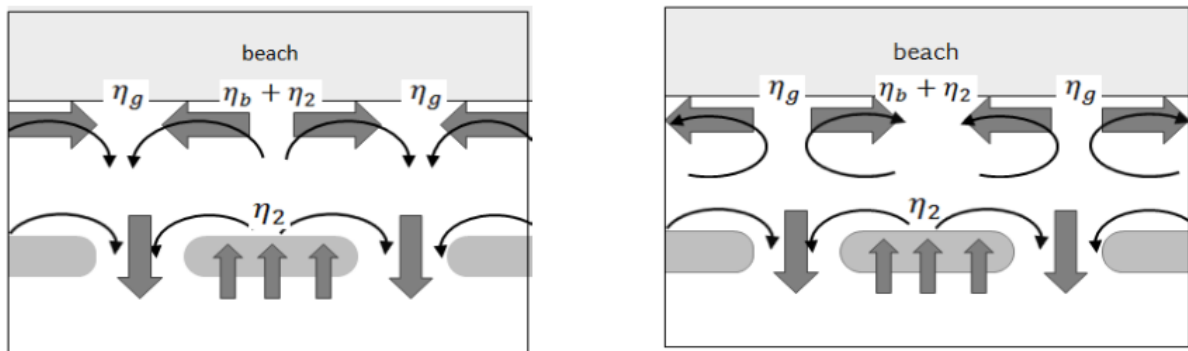


Figure 2.13 - 2-cell and 4-cell patterns in case of multiple SBWs (Villani et al., 2012).

Longshore variations in set-up, driving these patterns, are estimated using 1D cross-shore momentum balance equations in the middle of the gap and the middle of the breakwater length. From the combination of the patterns and the analytical approach, a criterion was proposed:

$$r = \frac{\eta_b + \eta_2}{\eta_g} \quad (2.52)$$

With $r > 1$ giving erosion and $r < 1$ giving accretion.

The proposed criterion is validated by applying it to the results of 4 cases performed by (Haller, Dalrymple, et al., 2002) as well as the numerical model SWASH. The second part

showed that the criterion could correctly identify the flow direction directly at the shore and could thus provide a rapid assessment of the potential shoreline response for the SBW design. For the first validation only the visually identified patterns could be compared and agreement was found in 3 of the 4 cases, the fourth case gave an erroneous erosive response ($r > 1$), which was likely due to being a transition between a 2-cell and 4-cell pattern.

2.5 Previous modelling with Delft3D on the subject of SBWs

A number of the previous theories have been used to validate Delft3D when modelling the hydrodynamic and morphodynamic response to an SBW in (Vlijm, 2011). Some of these validations are elaborated and an overview is given later in this paragraph.

Because the wave breaking and transmission is the dominant process that drives the shoreline change, it is paramount that this is modelled accurately by Delft3D for a realistic shoreline change. This is validated by comparing the empirical formula for dissipated wave heights by (Van der Meer et al., 2005) with the dissipated wave heights computed by Delft3D and assuming that if these results are in the same order, the energy dissipation is in the same order as well. The results are in agreement, however limitations on friction, permeability, diffraction and wave dissipation model make it difficult to quantify this judgment for every situation.

The computed water level set-up in the lee of the SBW is validated using the formula provided by (Longuet-Higgins, 1967). The general cross-shore water level fluctuations are in agreement with the theory; showing a small water level set-down on the offshore slope of the SBW by shoaling of the waves, a set-up over the crest and over the onshore slope of the SBW and a re-shoaling effect further in the lee of the SBW. The actual value for the set-up in the lee of the SBW is in agreement with the theory, mildly overestimating at a higher incoming wave height.

The magnitude of the mass-flux over the SBW is in agreement with the analytical mass-transport rates produced with the formula of (Svendsen, 1986). This is, however, limited to broad-crested SBWs, because of the theory's analogy to broad-crested weirs.

When looking at the cross-shore morphology one can validate the use of a depth-averaged model by comparing with the literature. The model is in agreement with the theory by (Young et al., 2009) computing the features described when a detached scour hole is produced, as well as the scour forms computed at the heads of the SBW.

An overview of literature used to validate a certain process is given in Figure 2.14.

<u>Process</u>	<u>Literature</u>	<u>Delft3D</u>	<u>Remarks</u>
Shoaling	[Deltares 2010b]	√	Calibrated/validated extensively by Deltares
Refraction	[Deltares 2010b]	√	Calibrated/validated extensively by Deltares
Diffraction	unknown	√	No literature for submerged breakwaters, but common sense suggest a small influence Not included, influence however small
Reflection	[Van der Meer et al. 2005]		Based on direct comparison to rubble mound sbw results
Wave transmission	[Van der Meer et al. 2005]	√	Influenced by mass-transport for higher values
Water level over breakwater	[Calabrese et al. 2008]	√	
Mass transport over breakwater	[Svendsen 1984] [Calabrese et al. 2008]	√	In general good, except 1 result
Spectral change	[Beji and Battjes 1993; Van der Meer et al. 2005]		Due to stability reasons of Delft3D neglected
Flow patterns	[Ranasinghe et al. 2006] [Sumer et al. 2005; Ranasinghe et al. 2006; Young and Testik 2009;	√	
Morphology	Ranasinghe et al. 2010]	√	Although relative large grid sizes, overall trend visible No changes accretive pattern, erosion included reasonable.
Shoreline changes	[Ranasinghe et al. 2010]		Take -0.5m contour

Figure 2.14 - Overview of literature used for validation (Vlijm, 2011)

Having Delft3D validated with the literature concerning the major processes, the model is used to research the influence of the physical parameters of the system. The results are in agreement with the paper by (Ranasinghe et al., 2010) with a note regarding the bottom roughness and the directional spreading of the waves. It is shown that these parameters can also (greatly) influence the shoreline response.

Following the thesis of (Vlijm, 2011), (Blouin, 2012) continued by studying additional physical parameters and attempting the validation with a field case, the findings and results are summarized below.

By making use of Delft3D, the influence of different physical parameters of the system could be researched. When changing these parameters separately and in certain combinations, the magnitude of the shoreline response (in salient width, negative for erosive cases) showed their power in the system as a whole. The parameters and their values can be seen in Table 2.1.

H_i [m]	x_b [m]	L_b [m]	R_c [m]	B [m]	R [m]
1.0	50	100	0.5	5	1.0
1.5	100	200	1.0	10	4.0
3.0	200	500			
	300				
	400				

Table 2.1 - Input model values of varying parameters (Blouin, 2012)

The model showed that the width (B) of the crest only affects the shoreline response when the submergence level is relatively small (< 0.5 m below MSL). In that case a wider crest would minimize the risk of shoreline erosion, because the dissipation of wave energy is larger.

Tides seem to have no impact on the net response of the shoreline (given there is an absence of strong tidal currents). Concerning the magnitude of the response, given an accretive case, where a small tidal range would still give accretion, this result may disappear when the tidal range is larger.

Other relations are summarized per parameter in Table 2.2:

Parameter	Shoreline response
x_b	Erosion if x_b generates a 2-cell current pattern, accretion if x_b generates a 4-cell current pattern
L_b	Proportional to the SBW length (erosive/accretive dependent on x_b)
H	Proportionally with the wave height
s_b	Inversely proportional to the submergence level

Table 2.2 - Collection of the results from modelling in Delft3D

These relations are all in accordance with the criterion by (Ranasinghe et al., 2010).

The thesis of (Blouin, 2012) proceeds with an attempt to validate Delft3D using these criteria as an expected result. A field case (a SBW project at the Sunny Isles, Florida) is used to further calibrate and validate the model. It is concluded that the case is far from optimal since there is minimal to no shoreline response to the SBW in addition to beach nourishment during the construction phase which only makes it harder to compare the results of the model to the field case. It is recommended to use another case to further calibrate the model and make the shoreline response quantifiable using Delft3D.

3 Modelling tool

With the increase in computational power and the continuing development of multiple modelling tools comes the possibility to evaluate more complex problems. The complexity of SBWs was already looked at with a 2D(V) model by (Groenewoud et al., 1996), but they concluded that 3D modelling is needed to model the complicated processes at the gaps of SBWs. 2DV models show only the (positive) effects regarding coastal accretion or erosion and the wave height reduction in the lee of the SBWs. 3D models can, however, include diffraction, complicated current patterns in the vicinity of the gaps and the influence of the ratio between the length of the gap and the length of the SBW. (Lesser et al., 2003) researched the optimisation and validity of a 3D morphological model. The results of this study are also relevant for the set-up of the models for this thesis.

In this thesis, as mentioned before, the modelling tool that is used is Delft3D. This process based modelling tool is developed by Deltares and has been proven to be robust and efficient in a range of previous studies. It can carry out simulations of flows, sediment transports, waves, water quality, morphological developments and ecology. To be able to do this, Delft3D is composed of several modules, grouped around a mutual interface, while being able to interact with one another. The main module is the Delft3D-Flow module, while using Delft3D-Wave for the wave properties. These two modules are discussed in more detail in the following paragraphs.

3.1 Flow module

Delft3D-Flow is a multi-dimensional (2D or 3D) hydrodynamic (and transport) simulation program which calculates non-steady flow and transport phenomena that result from tidal and meteorological forcing on a rectilinear or curvilinear, boundary fitted grid. In 3D simulations, the vertical grid is defined following the sigma co-ordinate approach (Deltares, 2011a). The model solves the Reynolds averaged Navier-Stokes equations for incompressible free surface flow numerically, with the assumption of shallow water and Boussinesq-type equations.

Instead of modelling turbulence on a particle scale, the viscosity of the fluid is increased to account for the effects of turbulence. This is done to prevent the need to model on extremely small time and spatial scales which play a role in the turbulent processes. There are different models in Delft3D available to include turbulence in the viscosity. These models differ in their prescription the mixing length, the turbulent energy and the dissipation rate of this turbulent energy.

In y-direction there is a momentum balance similar to the momentum balance in x-direction. In z-direction (or σ in this case), the vertical accelerations are neglected which leads to a hydrostatic pressure assumption to describe the momentum balance.

Since the transport of sediment is an important part in this thesis, it is relevant to look at the transport equation in Delft3D-Flow. Quantities, such as salinity, heat and sediment can be transported both by diffusion and by the fluid flow. To be able to calculate the spreading of these constituents this equation has to be approximated numerically as well. When the temperature, salinity and sediment concentration of each cell is calculated, this can be related to a density by an equation of state which relates all combinations of temperature,

salinity and sediment concentration to a density. The resulting density profiles are used in the mass and momentum equations.

$$\begin{aligned} \frac{\partial(hC)}{\partial t} + \frac{\partial(huC)}{\partial x} + \frac{\partial(hvC)}{\partial y} + \frac{\partial\omega C}{\partial\sigma} \\ = h \left[\frac{\partial}{\partial x} \left(D_H \frac{\partial C}{\partial x} \right) + \frac{\partial}{\partial y} \left(D_H \frac{\partial C}{\partial y} \right) \right] \\ + \frac{1}{h} \frac{\partial}{\partial\sigma} \left(D_V \frac{\partial C}{\partial\sigma} \right) - \lambda_d hC + S \end{aligned} \quad (3.1)$$

D_H and D_V represent the horizontal and vertical diffusion coefficient. λ_d is the first order decay process and S is again the source/sink term.

Several different sediment transport equations which relate sediment transport to flow velocities or shear stresses can be used (e.g. the Bijker or Van Rijn equation). The amount of sediment in a certain cell can only change if the inflow and outflow of these physical quantities are not equal (given S is equal to 0). Gradients in sediment transport cause changes in the bed level, which influence the hydrodynamics (see also paragraph 2.4). The complete process for transport of constituents is shown in Figure 3.1.

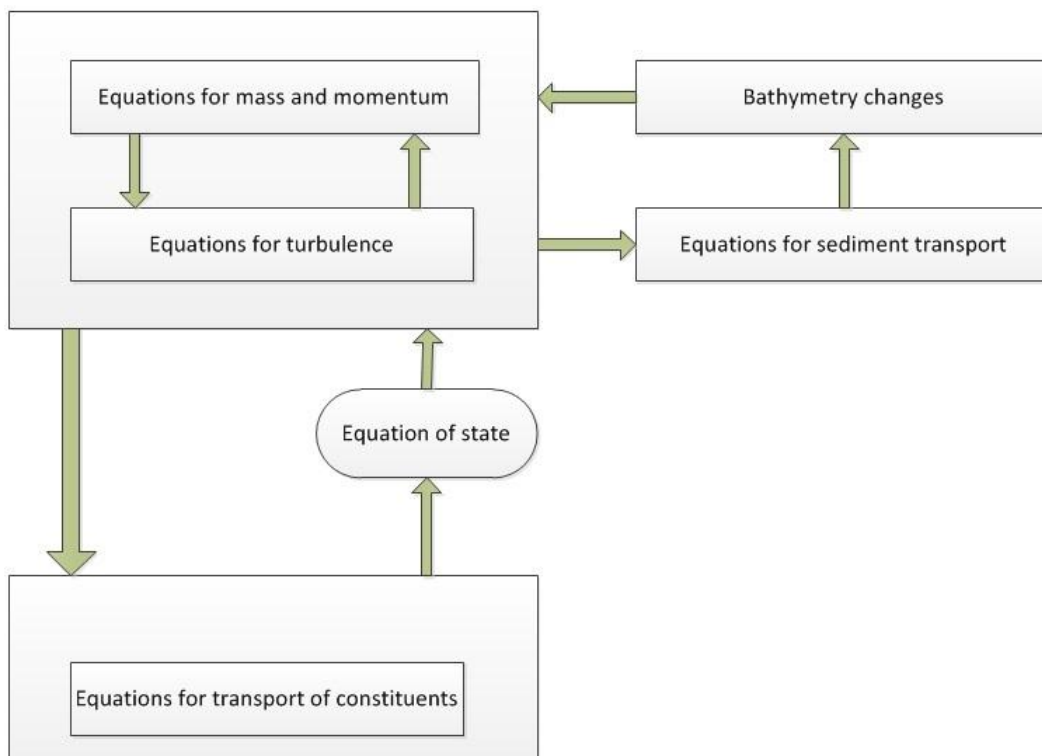


Figure 3.1 - Processes regarding the transport of constituents

3.2 Wave module

The Delft3D-Wave module consists of the SWAN (Simulating WAVes Nearshore) software, which is online coupled to the Delft3D-Flow module. SWAN is a third generation wave model, based on the discrete spectral balance equations, enabling it to handle waves from all directions (Deltares, 2011b). It computes wave propagation, wave generation by wind, wave-wave interactions and dissipation, for a given topography, wind field and defined water depth.

Propagation through and interaction with obstacles is also included, which is essential when studying the hydrodynamics around SBWs. Dissipation covers energy loss by whitecapping, bottom friction and depth induced wave breaking.

The online coupling provides the Delft3D-Flow module with the needed information for the effect on the flow by the wave-induced processes like added turbulence, wave-induced (shear) stresses, water level setup and bottom friction.

3.3 Model setup

Delft3D is a complex tool with a wide variety of options which are left for the user to choose from. These options can be set so that the efficiency and physical representation is optimal for a particular case. In this thesis multiple cases will be evaluated with an elaboration on the case specific physical and numerical parameters in the respective sections. However, given the close relation of the cases, there are also corresponding parameter values and settings for the cases. Those are discussed in this paragraph. For the values selected for a number of parameters, the studies of (Lesser et al., 2003), (Vlijm, 2011) and (Ranasinghe et al., 2011) are used.

3.3.1 Grid

The area of interest is represented by a staggered grid, used by Delft3D-FLOW to solve the discretised versions of the shallow water equations. This grid consists of 200x175 cells (longshore, cross-shore) with a 10x5m (longshore, cross-shore) cell resolution. An additional grid is used by the WAVE module. This grid consists of 89x289 cells with a constant longshore cell resolution of 10 meters and a varying cross-shore cell resolution from 40 meter offshore to 5 meter onshore, giving a more accurate computation in the area where the representation of the SBWs are (see Appendix A). For the computations the SBWs are represented in both the FLOW and WAVE grid.

3.3.2 Bathymetry

Despite imposing a great source of disturbance with the implementation of an SBW on the profile, the initial shore profile is shaped according to Dean's equilibrium shore profile.

$$d = Ax^{2/3} \quad (3.2)$$

With the sediment scale parameter A defined as:

$$A = \left(\frac{0.013gD_{50}T^2}{H_b^2} + 0.12 \right)^{2/3} \quad (3.3)$$

The water depth at the offshore (West) boundary is 8 m and leads up to a depth of -4.5 m at the East boundary. The initial longshore profile is constant in depth (apart from the depth differences caused by the representation of the SBW(s)).

3.3.3 SBW shape

The SBW is modelled as a submerged bar with a 1:5 slope. A mild slope is chosen to minimize the errors by sudden depth changes when using shallow water equations and with the current grid size. In addition, a milder slope yields better results when using the same wave breaker parameter for both wave breaking on the SBW and breaking on shore.

In addition to the definition of the slope in the x-direction, also the slope and shape of the SBW head is important in relation with the hydraulic resistance to the return flow and the

creation of turbulence with the resulting effect on the morphology. The crest width (in combination with the roughness of the SBW) affects the hydraulic resistance to the flow over the SBW.

3.3.4 Time frame

As mentioned before, Delft3D makes use of the ADI method, having multiple benefits. The results are at least second order accurate in space and being an implicit method, stability is guaranteed independent of the time step. However, for accuracy reasons, there is a limit on the maximum time step that can be used. This maximum time step can be calculated with a restriction based on the Courant number, in this case the accuracy need when using ADI for barotropic mode in complex geometries:

$$C_f = 2\Delta t \sqrt{gH \left(\frac{1}{\Delta x^2} + \frac{1}{\Delta y^2} \right)} < 4\sqrt{2} \quad (3.4)$$

Using the grid cell size, the maximum time step can be calculated. With Δx and Δy being 5 and 10 meter, a time step of 3 seconds will suffice.

For full morphological runs, the hydrodynamic run time is 6,5 days (including 12 hours spin-up interval) which translates to over 90 days for the morphological response with the morphological scale factor set to 15 (see paragraph 3.3.6).

3.3.5 Boundary conditions

For the numerical model to adequately represent a coastal system, certain types of boundary conditions should be imposed. Both the North and South boundaries are of the Neumann type. The West boundary is an open water level boundary and east represents the shoreline with a closed boundary.

3.3.6 Model parameters

An overview of the values or settings of the parameters in Delft3D-Flow is given in Appendix A. For both the bottom roughness and the initial sediment layer thickness at bed a data file will be used. This way a lower Chézy value can be defined at the location of the SBW to represent the more rough nature of the SBW relative to the sandy bottom. The SBW can also be defined non-erosive by setting the local initial sediment layer at that location at 0 in its respective data file. The morphological scale factor (as well as the online coupling interval) is limited by rate of the morphological changes. If this rate is high, the changes are easily overestimated with a larger morphological scale factor. A value of 15 is the highest achievable efficiency while still yielding accurate results. The Flow-Wave coupling is set on a 10 minute interval because rapid morphological changes are to be expected when imposing an SBW on a shore profile in an equilibrium state. Wave related suspended and bed load transport are switched off (0), since these transport types gave an unrealistic onshore net transport of sediment when switched on.

An overview of the values or settings of the physical parameters in Delft3D-Wave is given in Appendix A. Wave set-up is switched off to avoid it being accounted for twice; once in the flow module and then a second time in the wave module. For the depth-induced wave breaking the model of Battjes and Jansen is used. Although this implies a constant breaker depth for both breaking on the relatively steep SBW and less steep shore profile, this is the most reliable method and still gives satisfactory results (Vlijm, 2011). Non-linear triad

interactions, however important due to the creation of higher order wave harmonics over the SBW, are turned off due to stability reasons. In the wave module the bottom friction coefficient is set constant since the main source of energy dissipation for waves in this case is wave breaking. Despite the lack of literature in the area of diffraction by SBWs, diffraction is switched on since it has a dominant impact on the hydrodynamics in the lee of the SBW.

3.3.7 Additional settings and comments

There are a number of additional settings and comments, the most important ones are summarized below.

- To monitor the salient (changes), the -0.5 m depth contour is evaluated in Delft3D, since a phase-average model lacks accretive shoreline changes.
- Mass flux is disabled since the undertow is not accounted for in a depth averaged model, giving an imbalance for the morphology.
- Two-way coupling is enabled to account for the effect of local currents (flow module) on the wave propagation (wave module).
- The roller model is disabled since it gives spurious results, instead the wave dissipation model in the wave module will be used, using a constant wave breaker parameter.

4 Comparing output Delft3D to empirical, analytical and numerical data

Before using Delft3D to research the sensitivity of a multiple SBW system to its physical parameters with the analysis of multiple scenarios, it is useful to first compare the Delft3D output to what is known from literature regarding multiple SBW systems. While conformity with the literature does not guaranty full validity, the model does gain value when its output is in the same order as the results of 1 or more of the equations and/or data from the literature. This section will handle certain aspects of such a system in view of gaining confidence in the results computed by Delft3D with the settings and limitations discussed in section 3. Paragraph 4.1 will discuss the comparison of the water level set-up values caused by differences in radiation stress *directly in the lee of the SBW* calculated by the analytical approach by (Bellotti, 2007). Paragraph 4.2 describes the comparison with the empirical relation between the water level set-up value *directly in the lee of the SBW* and the lateral confinement of the system, from (Burcharth et al., 2007). Paragraph 4.3 concludes with the comparison of the values of the water level set-up *at the shoreline* behind the SBW, behind the gap and the resulting flow patterns with the study conducted by (Villani et al., 2012) which includes both an analytic and a numerical approach.

4.1 Magnitude of the set-up in the lee of the SBW

When overviewing a coastal defence system with SBWs there are many hydrodynamic processes present. Relative to this subject one of the important ones is the (partial) wave breaking on the crest of the SBW. There is a net transport of water over the barrier and an increase in water level in the lee of the SBW. The water level set-up forces return flows at the location with the lowest hydraulic resistance. This can be the crest of the SBW itself, through the gap in the form of a rip current, lateral currents or any combination of those. While the distribution of this return flow is mostly determined by the degree of lateral confinement (paragraph 4.2), one can determine the magnitude by making use of the mass balance and the cross-shore momentum balance (Bellotti, 2004).

4.1.1 Analytic approach

As discussed in paragraph 2.3.2 an analytic approximation can be developed from the equations describing these balances and (Bellotti, 2007) continues on this subject. Repeating:

The continuity equation (depth averaged):

$$u_{b0} \cdot h_{b0} = u_{bb}(h_{bb} + b) \quad (4.1)$$

Momentum equation:

$$\begin{aligned} \rho(h_{b0} \cdot u_{b0}^2) + \frac{1}{2} \rho g h_{b0}^2 + Z - \rho[(h_{bb} + b)u_{bb}^2] \\ - \frac{1}{2} \rho g (h_{bb} + b)^2 - \Delta S_{xx} - T_{xb} = 0 \end{aligned} \quad (4.2)$$

The subscripts describe the location of the values taken for the parameters following Figure 4.1.

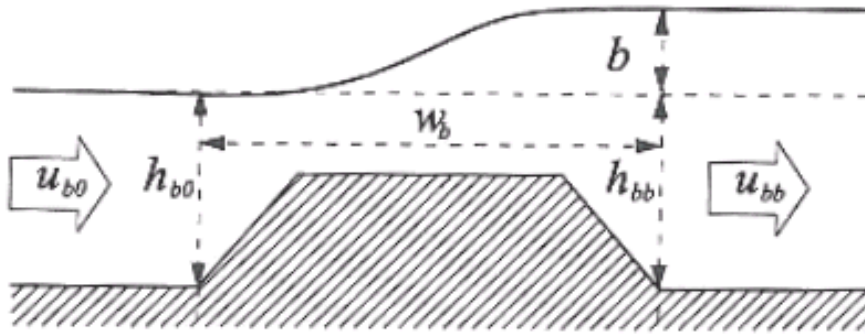


Figure 4.1 – Cross-section of a typical submerged barrier (Bellotti, 2007).

The difference in the cross-shore short wave forcing, ΔS_{xx} , is obtained when subtracting the radiation stress at the inshore location of the barrier from the radiation stress at the offshore point. With $S_{xx} = \beta \rho g H^2$, where:

$$\beta = \frac{1}{8} \left(\frac{1}{2} + \frac{2kh}{\sinh(2kh)} \right) + \left(\frac{0.9}{2\pi} kh \right) \quad (4.3)$$

The second right hand term describes the wave roller contribution, but since that process is switched off in the Delft3D model (see paragraph 3.3.7) it is neglected in the analytical approach as well. ΔS_{xx} can now be described by the following equation (using the same subscripts):

$$S = \rho g (\beta_{bb} H_{bb}^2 - \beta_{b0} H_{b0}^2) \quad (4.4)$$

The reaction of the bottom profile, Z , can be expressed in terms of local water depth and set-up (Bellotti, 2007):

$$Z = \rho g \left(\frac{h_{bb}^2}{2} - \frac{h_{b0}^2}{2} \right) + \rho g b (h_{bb} - \bar{h}) \quad (4.5)$$

Where \bar{h} is the average water depth over the barrier.

The addition of the bottom friction, T_{xb} , is chosen negative (offshore directed) since the dominant flow direction is assumed onshore when making use of a 2DH model. However, in reality this force might be positive since the flow at the barrier crest is likely dominated by the offshore directed undertow. When expressing this term in a friction term, a length term, local flow velocity and local water depth, one obtains (Bellotti, 2007):

$$T_{xb} = \rho \mu B u_{b0} h_{b0} \quad (4.6)$$

With:

$$\mu = f_w \frac{\gamma \sqrt{g}}{\pi} \quad (4.7)$$

$$B = \int_0^{w_b} \frac{1}{\sqrt{h(x)}} dx \quad (4.8)$$

Values for f_w are typically provided as functions of the non-dimensional bottom roughness a/D_{90} ($a = \frac{\bar{u}T}{2\pi}$ is the wave orbital amplitude just outside the boundary layer) and the Reynolds number. For submerged barriers consisting of rocks the value for f_w is between 0.1 and 1. This agrees with the data of (Kamphuis, 1975). For 'smooth' physical models with a concrete bottom profile it can be as small as 0.01. As an estimate f_w can be expressed as $\frac{0.2 T \sqrt{h}}{D_{90}}$.

Solving the continuity equation for the velocity at the inshore toe of the barrier and by inserting the resulting expression into the momentum equation and dividing by ρ , the following balance is obtained:

$$u_{b0}^2 \left(\frac{h_{b0}^2}{g(h_{bb} + b)} - \frac{h_{b0}}{g} \right) + u_{b0} \left(\mu B \frac{h_{b0}}{g} \right) + b\bar{h} + \frac{b^2}{2} \quad (4.9)$$

$$+ \beta_{bb} H_{bb}^2 - \beta_{b0} H_{b0}^2 = 0$$

This equation will be used to calculate the set-up (b) in the lee of the SBW.

4.1.2 Numerical approach

To compare this with the output of Delft3D a model has been set up. In general the settings are according to what is discussed in paragraph 3.3. However, both the FLOW grid cell size and the WAVE grid cell size have been made smaller to better display the processes in the gaps (a minimum of 10 cells for the gap width). This resulted in a FLOW grid of 185x140 cells of 2x2m (cross-shore, longshore) and a WAVE grid of 195x200 cells of 2x2m (cross-shore, longshore), again slightly overlapping the FLOW grid.

For the physical representation of a barred beach the scale models used by (Haller, Dalrymple, et al., 2002) are used as an example. This model consisted of a basin with one full SBW and two partial SBWs to represent a multiple SBW system (Figure 4.2) and study the nearshore dynamics on a barred beach with rip channels.

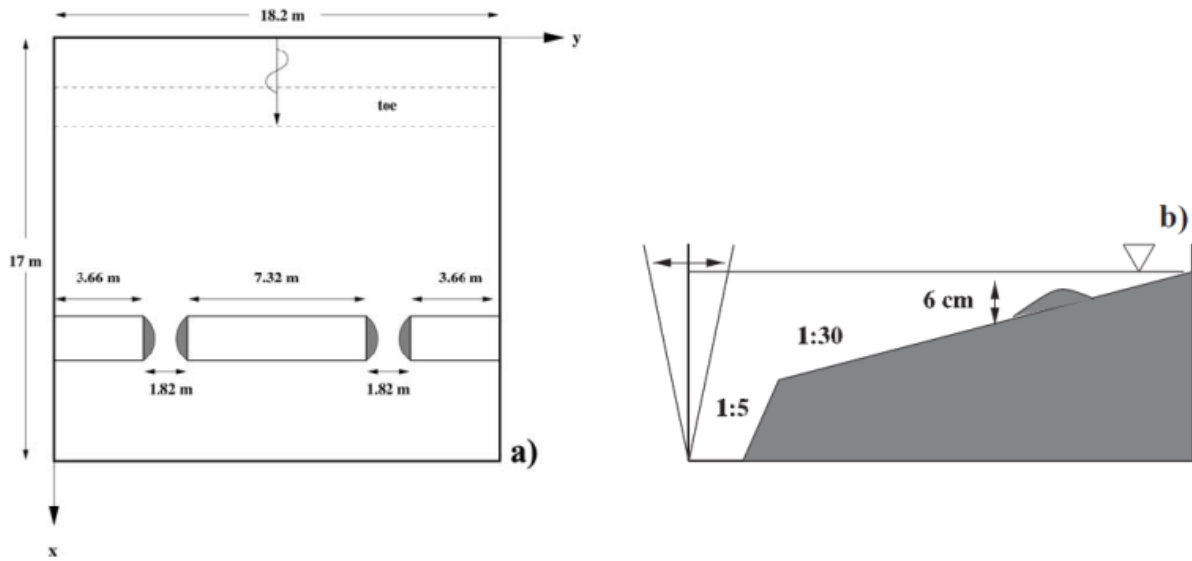


Figure 4.2 - (a) Plan view and (b) cross-section of the experimental basin used by (Haller, Dalrymple, et al., 2002).

The experiment conducted by (Haller, Dalrymple, et al., 2002) consisted of 6 tests, with varying wave height, wave direction, submergence level and cross-shore distance of the crest. The barrier length versus gap length is a constant 4:1. In this thesis the 4 tests with normal incident wave direction (test B, C, D and G) will be modelled in Delft3D on a scale of 1:15. This way the magnitudes in the model are comparable with a real life case while still eligible for validation with the analytical approximation displayed above. The physical parameters that vary per test are displayed in Table 4.1.

Test	Wave height [m]	Submergence level [m]	Crest cross-shore distance [m]
B	0.66	0.71	46.9
C	0.74	0.40	38.1
D	1.12	0.40	38.1
G	1.02	1.00	55.8

Table 4.1 - Physical parameters of the tests

Constant physical parameters include a bottom slope of 1:30, a breakwater length of 110 m, a gap length of 27.5 m and a crest width of 20 m. In the sense of designing a model with real life properties, the bottom roughness for the sand and the barrier material is modelled with a Chézy value of 65 and 20 respectively. These models will also be used in the validation of the flow patterns discussed in paragraph 4.3.

4.1.3 Comparison

To validate the output of Delft3D, the given value for the maximum set-up in the lee of the breakwater generated by the difference in radiation stress will be compared with the value when calculated with (4.9), when an optimal f_w value is selected for the smallest difference. This is the bottom value of 0.1. The results are collected in Table 4.2.

Test	Set-up D3D [m]	Set-up Bellotti [m]	Deviation [%]
B	0.018	0.015	-17.38 %
C	0.044	0.036	-18.93 %
D	0.086	0.095	10.37 %
G	0.022	0.020	-8.29 %

Table 4.2 - Comparison of the output of Delft3D and the analytical approximation by (Bellotti, 2007) regarding the set-up.

While the displayed values are in the same order of magnitude, for three of the four tests the set-up value calculated by the formula (4.9) is smaller than the output value of the corresponding Delft3D model. However, the method to determine the roughness coefficient used to calculate f_w holds some uncertainty. Instead of using the best fit in the prescribed range of 0.1 to 1.0, one can also use an empirical formula. This formula makes it possible to directly use the modelled roughness in the k_N (Nikuradse roughness) parameter. The results generated when using the empirical formula by (Kamphuis, 1975), (4.10), are collected in Table 4.3.

$$f_w = 0.247 \left(\frac{0.2 * T * \sqrt{h}}{k_N} \right)^{-0.623} \quad (4.10)$$

Test	Set-up D3D [m]	Set-up Bellotti [m]	Deviation [%]	f_w value
B	0.018	0.018	-2.74 %	0.073
C	0.044	0.046	3.91 %	0.069
D	0.086	0.104	20.52 %	0.069
G	0.022	0.023	4.32 %	0.075

Table 4.3 - Comparison of the output of Delft3D and the analytical approximation by (Bellotti, 2007) regarding the set-up, with adjusted roughness coefficient.

In this case the values given for the set-up in the lee of the breakwater by the model and the analytic approximation are almost identical (O(0.01) difference) for 3 of the 4 tests. Only the difference in the values for test D has kept a significant deviation margin. A possible cause is different distribution in water level set-up from the difference in radiation stress and shoaling further onshore, relative to the other tests. For test D the set-up by difference in radiation stress dominates the total set-up and therefore seems to be limited by other physical parameters of the model, not fully reaching the potential set-up that is available when reviewing the momentum balance. This limit might also be numerical in nature and demands further research. For all cases, however, the f_w value computed with the empirical formula is smaller than the suggested minimal value of 0.1, suggesting that the Chézy value of 20 to represent the roughness of the SBW, might be too high.

An alternative method to determine the magnitude of the set-up is using the efficiency of the wave pump concept as proposed by (Nielsen et al., 2007):

$$\epsilon = \frac{\rho g b q}{E_f} \quad (4.11)$$

With E_f being the wave energy ($E_f = \text{kinematic} + \text{potential} = \frac{1}{2} \rho g a^2$) of the incoming wave, b the set-up in the lee of the SBW and q the discharge per meter width over the barrier. (Nielsen et al., 2007) concluded that the wave pump efficiency over barriers with rip current systems is about constant and equal to 0.035.

Using values from the same test setup as before, one obtains the following results:

Test	Set-up [m]	Discharge [m ³ /s/m]	Wave pump efficiency [-]
B	0.018	0.085	0.032
C	0.044	0.048	0.037
D	0.086	0.060	0.043
G	0.022	0.140	0.029

Table 4.4 - Calculation of the wave pump efficiency with the Delft3D output

While being less comparable than the previous results, the values for the wave pump efficiency are still in the same order as the expected 0.035. A possible reason for the lower accuracy is the usage of the flow velocity at the location most susceptible to artificial spikes in the Delft3D results, when making use of the energy and/or momentum balance.

4.2 Breakwater length and gap width ratio

Another balance can be found between the distribution of the return flow over the SBW and through the gaps. When assuming an impermeable SBW these 2 flow components have to be equal to the inflow caused by the waves. It is to be expected that the smaller the gap length with respect to the SBW length, the bigger the return flow component over the SBW will be, because of the increase in hydraulic resistance of the system. This part of the return flow depends on the pilling-up in the lee of the breakwater so logically this set up will also be higher in the case of smaller (or no) gaps. The return flow through the gaps is expected to change accordingly.

4.2.1 Empirical data

As discussed in paragraph 2.3.2, the literature by (Burcharth et al., 2007) included a graph describing this balance. The graph is based on the data acquired in the Bari wave basin, where a physical scale model was created. Figure 2.5 shows the results for constant wave conditions, the data points regarding the ‘submerged conditions’ part of the graph are plotted again in Figure 4.3, this time with a linear trendline, because this type of trendline gives the best reproduction of the original graph without the data points from the emerged conditions.

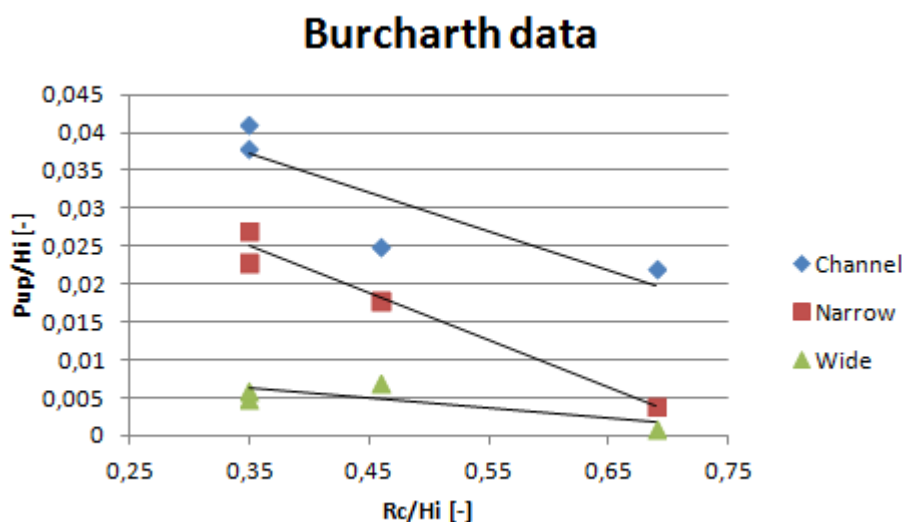


Figure 4.3 - Trendline through the measured points from the physical model

4.2.2 Numerical reproduction

When making an attempt to reproduce these points using Delft3D, nine model runs were made with different physical parameters. The ‘Channel’ confinement type is represented by a

SBW length of 600 meters (however not infinitely long, this way it approaches theoretically infinite and still has a realistic SBW length), while the ‘Narrow’ condition consists of multiple SBWs with a length of 100 meters and a gap length of 25 meters (creating a gap width versus breakwater length ratio of 1:4). Lastly, the ‘Wide’ condition is represented by multiple SBWs with a length of 100 meters and a gap width of 100 meters (a ratio of 1:1). Also, to make the comparing easier, the ratio of the submergence level, R_c , and the incoming wave height, H_i , is set in such a way that the data points match the x-values of those of the physical model, while maintaining a scale model to numerical model ratio of 1:30. An overview of the physical parameters can be found in Table 4.5.

Test	SBW length [m]	Gap length [m]	Submergence [m]	Wave height [m]
Channel	600	-	0.5	0.74
	600	-	0.5	1.09
	600	-	0.5	1.44
Narrow	100	25	0.5	0.74
	100	25	0.5	1.09
	100	25	0.5	1.44
Wide	100	100	0.5	0.74
	100	100	0.5	1.09
	100	100	0.5	1.44

Table 4.5 - Physical parameters used in the Delft3D model runs

For the roughness to be expressible in term of a Chézy coefficient, the D_{50} of the granular material in the scale model is used. The top layer of the SBW consists of stones with a D_{50} of 0.045 m. Using the 1:30 scale ratio and the following formula:

$$C = 18 \log \sqrt{\frac{12R}{k_N}} \quad (4.12)$$

With wet perimeter $R \approx d$ and the Nikuradse roughness length $k_N = 2-2.5$ times the D_{50} . From this follows that $C = 20 \text{ m}^{1/2} \text{ s}^{-1}$. The rest of the scale model bottom profile consists of concrete which is relatively smooth and is assumed to have a C value of 45 to 65. This roughness interval is displayed as a colour band in the Delft3D output graph.

4.2.3 Comparison

When plotting the results in the same manner, the Delft3D output (Figure 4.4) shows some agreement but also disparities with the physical model data points. In general the output is in the same order of magnitude and the trendlines display the same declination with a decreasing wave height. However, the trendlines of the ‘Channel’ and ‘Narrow’ conditions are shifted down slightly relative to the physical model results. For the ‘Channel’ this might be due to the model not representing an infinitely long SBW, only a relatively long one. Also the trendline of the ‘Wide’ condition is displaced relative to the physical model results, upward in this case. This can be explained by the possibility that in the Delft3D model the return flow is not governed by the SBW length to gap ratio, but by the water depth and the cross-shore distance. The close relation of the ‘Narrow’ and ‘Wide’ conditions would confirm this; the small difference would be the result of the lateral confinement factor, but the overall position on the plot determined by the water depth at the location of the SBWs.

Despite the differences, the ‘Wide’ trendline is indeed plotted below that of the ‘Narrow’ condition, showing consistency in the decay of pilling-up with a decrease in confinement.

Also the data points produced by the numerical model fit better with the trendline, displaying a more linear relationship between the wave height and the pilling up in the lee of the SBW, for every mode of confinement. Noticeable is the difference in C value is only relevant for the 'Channel' condition, most likely due to the fact that the return flow route is relatively long and experience relatively more 'hindrance' of the lower C value of the bottom.

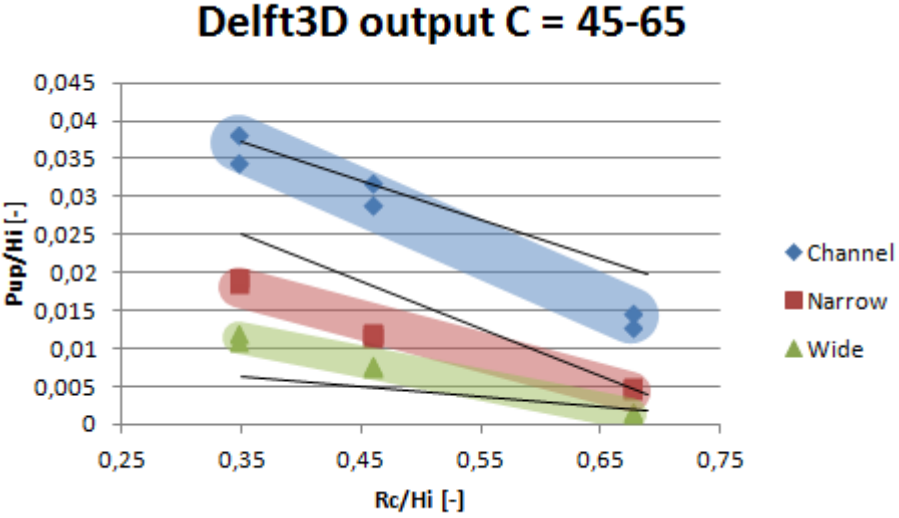


Figure 4.4 - Trendline from empirical results through the computed bands from the Delft3D model results

4.3 2-cell versus 4-cell pattern

When looking further onshore there is also set-up present at the shoreline. The presence of SBWs causes longshore differences in this set-up. To relate this to an actual expected shoreline response, one can look at the impact of these differences in set-up at the shoreline; the formation of a flow pattern. Two different flow patterns are identified in literature: the 2-cell pattern, associated with erosion, and the 4-cell pattern, associated with accretion. This paragraph reviews a criterion for these flow patterns.

4.3.1 Analytical basis for the criterion and numerical validation with SWASH

As discussed in paragraph 2.4.3, (Villani et al., 2012) proposed the following criterion to make a rapid first assessment of the potential shoreline response:

$$r = \frac{\eta_b + \eta_2}{\eta_g} \tag{4.13}$$

With $r > 1$ resulting in flow from the centre of the SBW to the gaps, giving erosion of the shoreline and $r < 1$ resulting in flow from the gaps to the centre of the SBW, giving sedimentation and the parameters described as displayed in Figure 4.5. Those η values are computed using the cross-shore momentum balance. The momentum balance can be described as follows:

$$\frac{d}{dx} \frac{q^2}{(h + \eta)} = -g(h + \eta) \frac{d\eta}{dx} - \frac{1}{\rho} \frac{dS_{xx}}{dx} - \frac{\tau_b}{\rho} \tag{4.14}$$

For the transect at the centre of the SBW the momentum balance is as described by (4.9), discussed in paragraph 4.1 and can be used to compute the set-up in the lee of the breakwater, in this case η_2 .

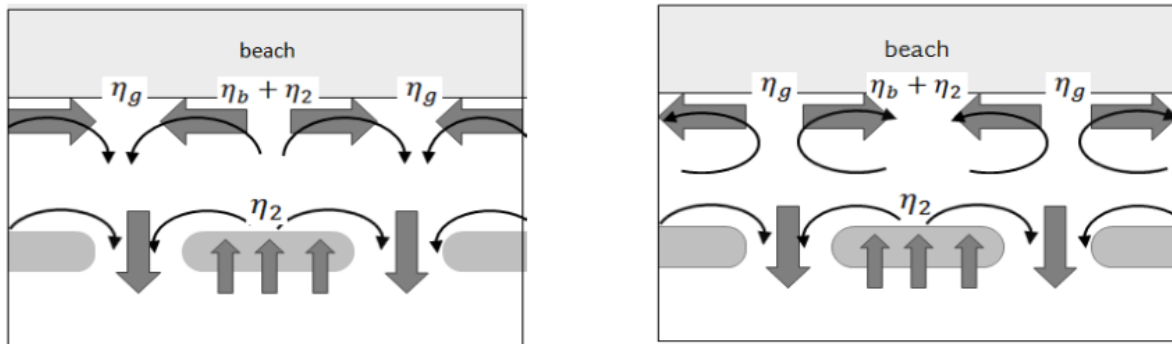


Figure 4.5 - 2-cell and 4-cell patterns in case of multiple SBWs (Villani et al., 2012).

(Villani et al., 2012) used the experimental data gathered by the tests discussed in (Haller, Dalrymple, et al., 2002) to validate the criterion analytically with (4.14) and numerically using the non-hydrostatic free surface numerical model SWASH. For this the same four tests (B, C, D and G) are used. The results are displayed in Figure 4.6. Accretion for test B, C and G and erosion for test D was in agreement with the occurrence of a 4-cell pattern in test B, C and G and a 2-cell pattern in test D (Figure B.13). However, the response of the actual shoreline was accretion in all four tests. This was thought to be due to test D being in a transition phase between a 2-cell and a 4-cell pattern.

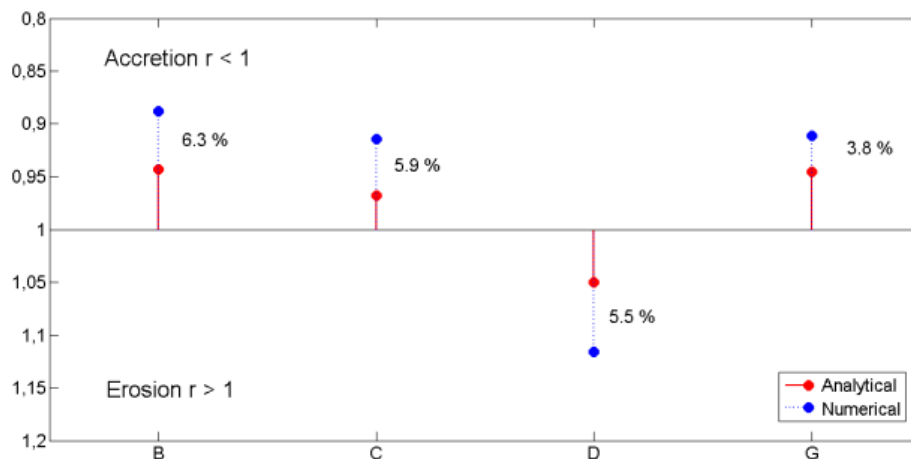


Figure 4.6 - Analytical (red) and numerical (blue) values for the ratio r and the percentage difference.

4.3.2 Numerical validation with Delft3D and validation with analytical approach

To validate the criterion in this thesis the tests by (Haller, Dalrymple, et al., 2002) will be replicated in Delft3D in the same manner as discussed in paragraph 4.1. The output will serve as the data for the numerical validation.

Figure 4.7 shows the longshore set-up profile for test B. Taking the peak values for the set-up at the shoreline behind the gap for η_g and behind the centre of the SBW for $\eta_b + \eta_2$, the ratio r per test is displayed in Table 4.6.

Test	η_g [m]	$\eta_b + \eta_2$ [m]	ratio r
B	0.0476	0.0452	0.95
C	0.0929	0.0856	0.92
D	0.1303	0.1301	1.00
G	0.0783	0.0786	1.00

Table 4.6 - Wave set-up at shoreline from Delft3D output.

While the r values already mostly agree with the flow patterns displayed in Figure B.14, Figure B.15, Figure B.16 and Figure B.17, there is a possibility that the results are sensitive to the shape of the SBW and taking the peak value will generate an error. To cancel out the sensitivity of the results to the specific cross-section selected the mean value for the set-up over the gap or barrier length is used. For clarity, this is shown with the red lines in Figure 4.7 for Test B. The graphs for the other test are collected in Appendix B.

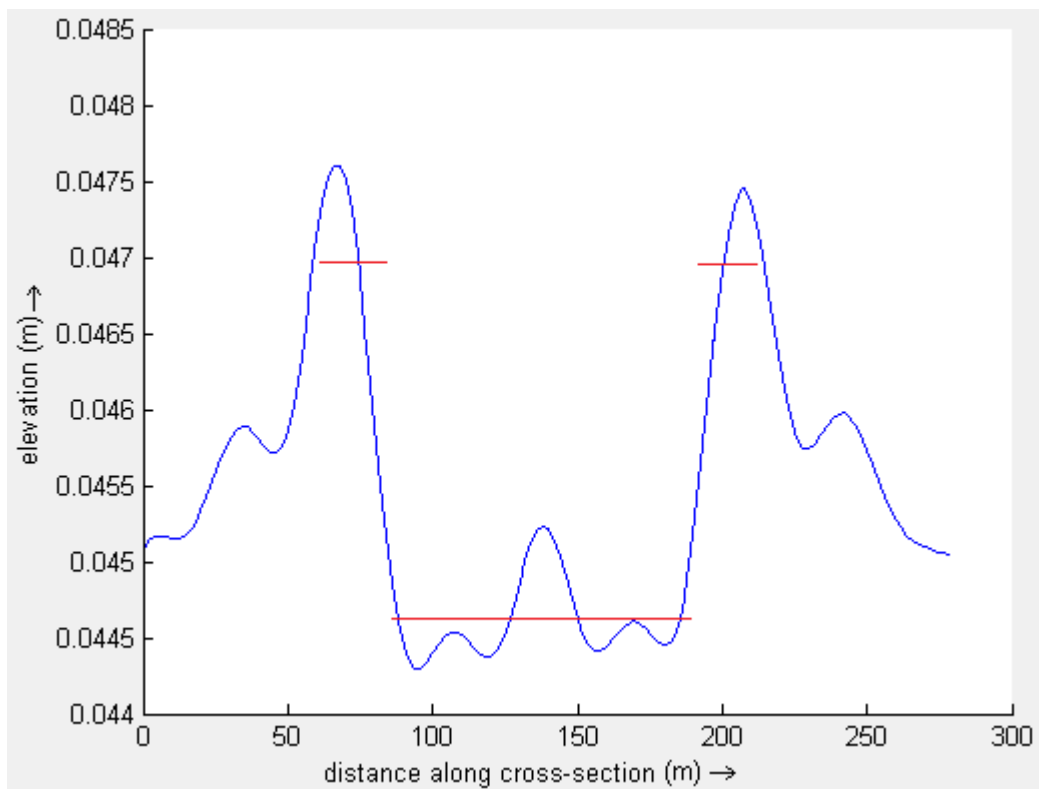


Figure 4.7 - Set-up at shoreline, with average over section (red lines), for test B

The results using the average set-up values are collected in Table 4.7.

Test	η_g [m]	$\eta_b + \eta_2$ [m]	ratio r
B	0.0470	0.0446	0.95
C	0.0905	0.0820	0.91
D	0.1282	0.1234	0.96
G	0.0778	0.0770	0.99

Table 4.7 - Averaged wave set-up at shoreline from Delft3D output.

When comparing these r values with the ones from Table 4.6, the only difference can be found for test D, going from a 'neutral' 1.00 to an 'accretive' 0.96. Looking at the actual flow pattern and the shoreline response when morphology is included will prove which r value is more accurate.

To validate the criterion analytically, (4.14) is used. This equation can be simplified to (4.15) when looking only at the set-up value at the shoreline.

$$\eta_{b,g} = \eta_{br} + \frac{\frac{3\gamma_{b,g}^2}{8}}{1 + \frac{3\gamma_{b,g}^2}{8}} (h_{br,b,g} - h(x)) \quad (4.15)$$

With h_{br} being the depth at wave breaking, applying linear wave theory and η_{br} the set-up (set-down in this case) at the point of wave breaking. The wave height to water depth ratio at wave breaking, γ , is assumed constant but two different values are used for the ratio in the lee of the SBW and the ratio in the gap, because the rip currents in the gap will steepen the incoming waves, such that wave breaking will occur for lower values of γ (Haller & Özkan-Haller, 2002). It is proposed that $\gamma_g = 0.63$ and $\gamma_b = 0.68$, despite the fact that the rip current velocity is not the same for the different cases. The results are collected in Table 4.8.

Test	η_g [m]	$\eta_b + \eta_2$ [m]	ratio r	Deviation in ratio r
B	0.0725	0.0609	0.84	11.58 %
C	0.0951	0.0902	0.95	-4.23 %
D	0.1102	0.1160	1.05	-9.38 %
G	0.1145	0.1056	0.92	7.07 %

Table 4.8 - Wave set-up at shoreline computed analytically.

The differences between the individual set-up values are significant, whereas the values for the ratio r are more comparable. This is to be expected when using constant values per test for the breaker index in the analytical calculation and a breaker index depending on the hydrodynamics of the model in the numerical approach. Because the proposed values for the breaker index are best fitted over the tests the average deviation for the values for the ratio r is close to 0, but the set-up values have an increasing disparity when the rip current velocity increases, as can be seen in Table 4.9.

Test	U_r [m/s]	Deviation in ratio r
B	0.21	11.58 %
C	0.49	-4.23 %
D	0.68	-9.38 %
G	0.30	7.07 %

Table 4.9 - Rip current velocity in relation to the deviation in the ratio r

Interpolation shows that the proposed breaker index value for the gap of 0.63 would, hypothetically, fit for a rip current velocity of about 0.45 m/s in combination with the other current physical parameters of the model (Figure 4.8). With an increasing rip current velocity, the wave breaker index value decreases. Apart from the evidence for the existence of that relation, which was already known from other studies, no conclusions can be drawn from this graph without further research.

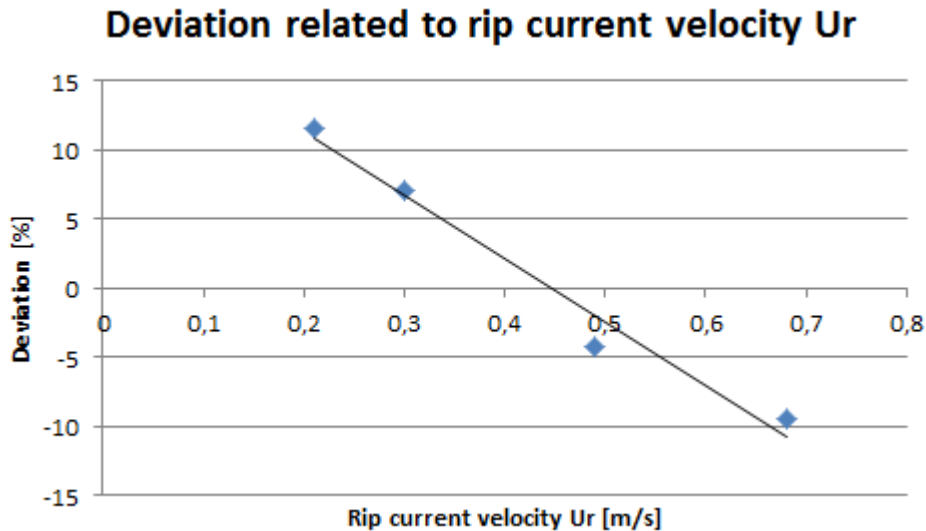


Figure 4.8 - Deviation in generated r value related to rip current velocity

This shows the importance of the chosen value for the breaker index, as already mentioned in the conclusions of the study by (Villani et al., 2012).

4.3.3 Flow pattern analysis in Delft3D

The, in general, good agreement of the ratio r produced by the numerical approach of the literature and Delft3D, should result in similar flow patterns as showed in the literature (Figure B.13), because these values are directly related to the occurrence of a 2-cell or 4-cell pattern. Based solely on the value for r , Delft3D should display 4-cell patterns for all four tests, albeit not a clearly defined one for test D and possibly test G given the value for r is close to 1 in these cases. Similarities and disparities between the flow patterns from literature and Delft3D are briefly summarized below.

Test B (Figure B.14)

The flow pattern of test B shows a weak 4-cell pattern, but a clear distinction between the set-up caused by the momentum flux over the barrier and the set-up caused further onshore by shoaling. Test B from literature has a clearer 4-cell pattern with separated cells, but the other aspects are in agreement.

Test C (Figure B.15)

Again the flow pattern displays a weak 4-cell pattern. This time there is hardly any flow directly onshore of the SBW, as well as a less confined outflow through the gap and a less clearly visible distinction between set-up caused by the momentum flux and set-up caused by shoaling. Test C in literature is comparable regarding the low flow velocity and the set-up in the lee of the SBW, but again has a more defined 4-cell pattern with separated cells.

Test D (Figure B.16)

As expected the flow pattern is close to a 2-cell pattern which corresponds well with the r value. The set-up by momentum flux dominates the total set-up and there is hardly any cross-shore flow present in the lee of the SBWs. Test D in literature presents the only 2-cell pattern and although the flow pattern is more defined as a 2-cell pattern there, it is

comparable to the one presented by Delft3D and can be seen as a transition between a 2-cell and a 4-cell pattern.

Test G (Figure B.17)

This test presents a 4-cell pattern with the most separated cells from all the tests, extending up to far behind the SBWs, especially clear at the shoreline. There is also a high offshore velocity present at the shoreline behind the centre of the SBW. In the literature the 4-cell pattern is more located at the gap and the relatively strong offshore velocity at the shoreline behind the middle of the SBW is absent. In both cases the gradient of the set-up is highest at the shoreline.

4.4 Conclusions

Conclusions can be made when comparing the Delft3D model output to analytical and empirical data for multiple SBW systems.

When computing the water level set-up directly in the lee of the SBW, the difference in value via the analytical approach and via the numerical approach seems related to the level of distinction of the set-up by difference in radiation stress over the SBW and the set-up by shoaling. The deviation in computed set-up is $O(0.01)$ when the set-up by difference in radiation stress is comparable to the set-up by the waves further onshore (test B, C and G). However, when the set-up by difference in radiation stress dominates (test D), the difference between the two tends to be larger; $O(0.1)$. This result is only generated by 1 of the 4 test and this conclusion is therefore unreliable, further research should be done to validate this hypothesis. However, the wave pump efficiency agrees with the good comparison of 3 of the 4 tests, giving values around the expected 0.035 value, albeit slightly less accurate, and more susceptible to errors by the numerical calculation.

For the comparison regarding the lateral confinement parameter, the values are again in the same order for numerical and empirical approach. However, conclusive judgment cannot be made because of the lack of some of the physical parameters of the physical model. It is to be expected that the total gap profile is governing, which is only partly defined by the lateral confinement. The other factor is depth, which is not defined in the description of the physical model, making it hard to accurately reproduce it. A lower Chézy value for the bottom is only clearly noticeable when the return flow route is relatively long.

The numerical reproduction of the validation of the r -value criterion yields values for r that are smaller than 0 with corresponding (albeit weakly defined for test D) 4-cell flow patterns for all tests. For test D, this is in contrast with the study by (Villani et al., 2012) displaying a 2-cell pattern, but in agreement for the same 4 tests in the study by (Haller, Dalrymple, et al., 2002), which reported converging flows for all tests. The analytic approach showed relatively large difference for individual set-up values. This is mainly due to the constant wave breaker parameter used in contrast with the wave breaker parameter in the numerical model, which is influenced by hydrodynamic processes, mainly the rip current velocity. For test D this even leads to a prediction of erosion using the analytical method, showing the importance of the use of a breaker index value based on the model hydrodynamics. In overview, when solely looking at the level of definition of the 4-cell patterns; they are relatively well defined in test B and C and less defined in test D and G. One could note that the r value computed from the peak values from the Delft3D output is a better predictor for the corresponding flow pattern.

5 Shoreline response

When assessing the viability of a certain shape and location for the SBW(s), one starts with the mode of shoreline response. When using the previously discussed r criterion (4.13) as a prediction for the mode of shoreline response, it is important to visualize the response with the help of Delft3D for a certain value of r , and confirm the prediction of the type of response. In this section that comparison is made for the four tests discussed in paragraph 4.3. Because the r values are all in the range of 0.9-1.0, a more extensive comparison will be made in section 6, exploring a wider range of r values and with that a (prediction of) a more varying shoreline response. In addition, this section includes the prediction for the shoreline response when using the graph from (Ranasinghe et al., 2010), to depict the similarities and differences for single and multiple SBW systems.

5.1 Model set-up and results

To model the shoreline response, the same set-up per tests is used as in paragraph 4.3 with the addition of the morphological module by enabling the sediment process. The sediment properties used by this module are set up as described in paragraph 3.3.6 and Appendix A, including a grain diameter (D_{50}) of 0.25 mm, a spin up interval of 720 minutes and a morphological scale factor of 15. Because the tests are according to the physical model, they also have a bottom profile slope of 1:30 which is not in accordance with the equilibrium profile as proposed by (Dean et al., 1994). Hence, morphologic changes are to be expected regardless of the construction of SBWs. To overcome this, a run is made for each test without the human intervention in the like of a SBW system, but identical settings aside from that (henceforth called the 0-test). Finally, a comparison can then be made looking at the difference in the computed depth contour line of -0.5 m after a model run time of 90 (morphologic) days. Figure 5.1 is a plot showing this comparison for all 4 tests.

Test B

The previously computed r value for this test predicted accretion and some sedimentation can indeed be observed in the lee of the breakwater (at the shore as well as directly at the onshore trunk of the SBW) relative to the 0-test. However, this accretive response does not hold for the complete length of the shoreline and the profile in the lee of the gaps shows some erosion. It should also be noted that the shape of the shoreline does not follow a clear salient type longshore profile.

Test C

Accretion can be seen at the shoreline over the complete length of the barriers and even in the lee of the gaps there is no noticeable erosion. The bottom height contour line of -0.5m is displaced as far as 10 meter seaward at the location behind the centre of the barrier. Overall a clear salient type beach profile has been formed.

Test D

Relative to the contour line of the model without the SBW, accretion can be seen in lee of the major part of the SBWs but erosion of the shoreline is shown in the remaining part and in the lee of the gaps. Overall the gain in shore width behind the barriers is lost at the locations behind the gaps which results in a salient character for the beach profile, but no real

accretion or erosion in the system as a whole. This might be linked to the previously found r value close to 1.0, but to confirm this, more research is needed.

Test G

The comparison plot for test G shows the largest offshore progression of the coastline, progressing as far as 20 meters in the lee of the centre of the SBW. The contour line almost connects to that of the sedimentation at the onshore trunk of the SBW for a tombolo profile at 0.5 m depth. Given that the r value is relatively close to 1.0 and the big difference in shoreline response compared to test D, this is unexpected.

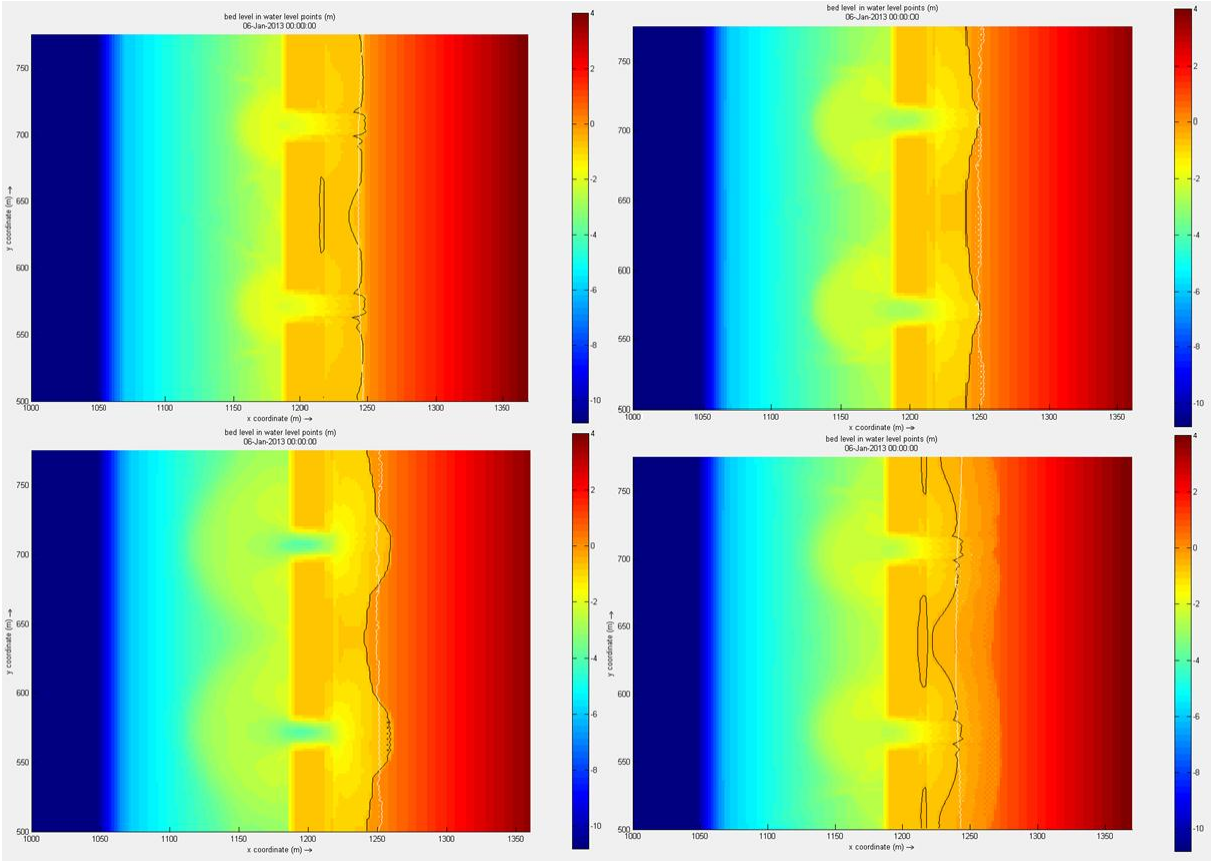


Figure 5.1 - Plot of the bed level height for test B (top left), C (top right), D (bottom left) and G (bottom right) after 3 months with the -0.5m contour lines with SBWs (black) and without (white)

To quantify the shoreline response, it can be expressed in cumulative volumetric change. To be able to do this, the complete area in the lee of the middle SBW is monitored, as shown in Figure 5.2 and the cumulative change is expressed in cubic meters (Table 5.1).

Test	Cumulative volumetric change [m ³]	Shoreline response
B	73.3	Accretive
C	79.7	Accretive
D	6.9	Neutral/Accretive
G	158.6	Accretive

Table 5.1 - Cumulative volumetric change per test

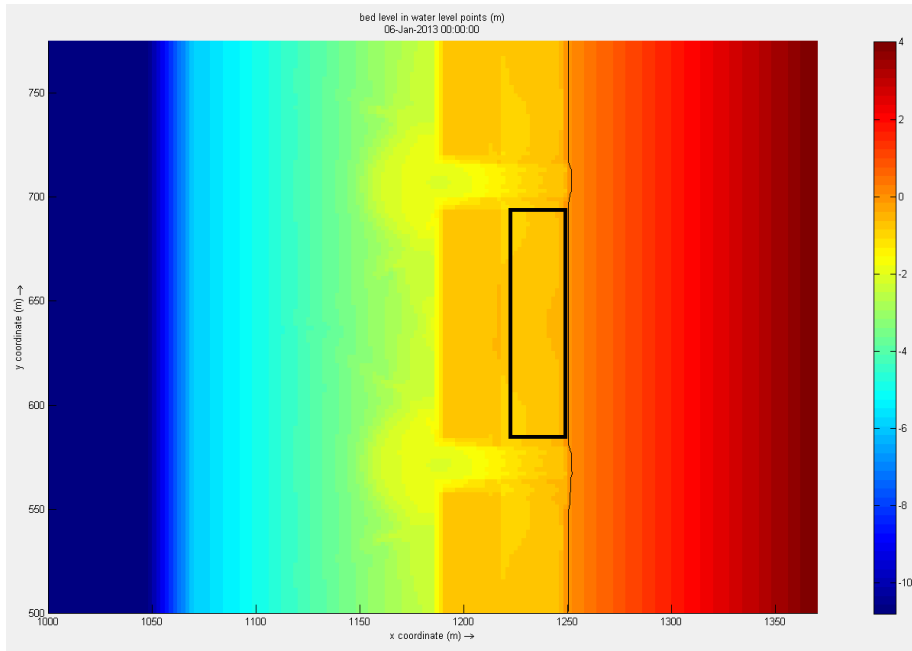


Figure 5.2 - Monitor area from the inshore trunk of the SBW to the 0 water depth contour line, in the lee of the central SBW

Looking at the values for the cumulative sediment displacement, this confirms the conclusions based on the shoreline profile. Occurrence of relatively mild accretion in the lee of the middle SBW for tests B and C, a neutral response with a cumulative sediment displacement value of close to 0 for test D and a relatively large accretive response for test G, shown by the highest value.

5.2 Prediction when using single SBW criterion

To show the relevance of treating multiple SBW coastal systems separately from single SBW coastal systems, this paragraph will show the results of plotting the data points of the previous 4 tests in the graph for predicting the shoreline response to a *single* SBW by (Ranasinghe et al., 2010). Discrepancies are to be expected and would show the importance of this thesis. The graph is already discussed in paragraph 2.4.3 but is summarized here shortly.

The graph for the prediction of the shoreline response to a single SBW shows the relation between the ratio of water depth (at the location of the SBW) over the significant wave height and the ratio λ :

$$\lambda = \left(\frac{s_b}{h_b}\right)^{\frac{3}{2}} \left(\frac{L_b}{h_b}\right)^2 \left(\frac{A^3}{h_b}\right)^{\frac{1}{2}} \quad (5.1)$$

And a line following:

$$\frac{h_b}{H_0} = 2 \log_{10} \left[\left(\frac{s_b}{h_b}\right)^{\frac{3}{2}} \left(\frac{L_b}{h_b}\right)^2 \left(\frac{A^3}{h_b}\right)^{\frac{1}{2}} \right] + 0.65 \quad (5.2)$$

With s_b as the submergence level, L_b the breakwater length and A as a shape parameter based on the grain size. These parameters allow a single SBW system to be plotted in the

graph (by making use of its physical properties) as a single data point. If a specific data point is plotted left of the line, the prediction is accretion, for a data point at the right side of the line, the shoreline change can be expected to be erosive.

Following this method, the tests are plotted in the graph as data points Figure 5.3. The parameters used in the criterion are collected in Table 5.2. The grain size of 0.25 mm used in the model results in a value for A of $0.115 \text{ m}^{1/3}$ (Dean et al., 1994).

Test	h_B [m]	H_0 [m]	s_B [m]	L_B [m]	A [$\text{m}^{1/3}$]
B	1.6	0.66	0.71	110	0.115
C	1.29	0.74	0.40	110	0.115
D	1.29	1.12	0.40	110	0.115
G	1.89	1.02	1.00	110	0.115

Table 5.2 - Parameters used in the criterion for the shoreline response to a single SBW

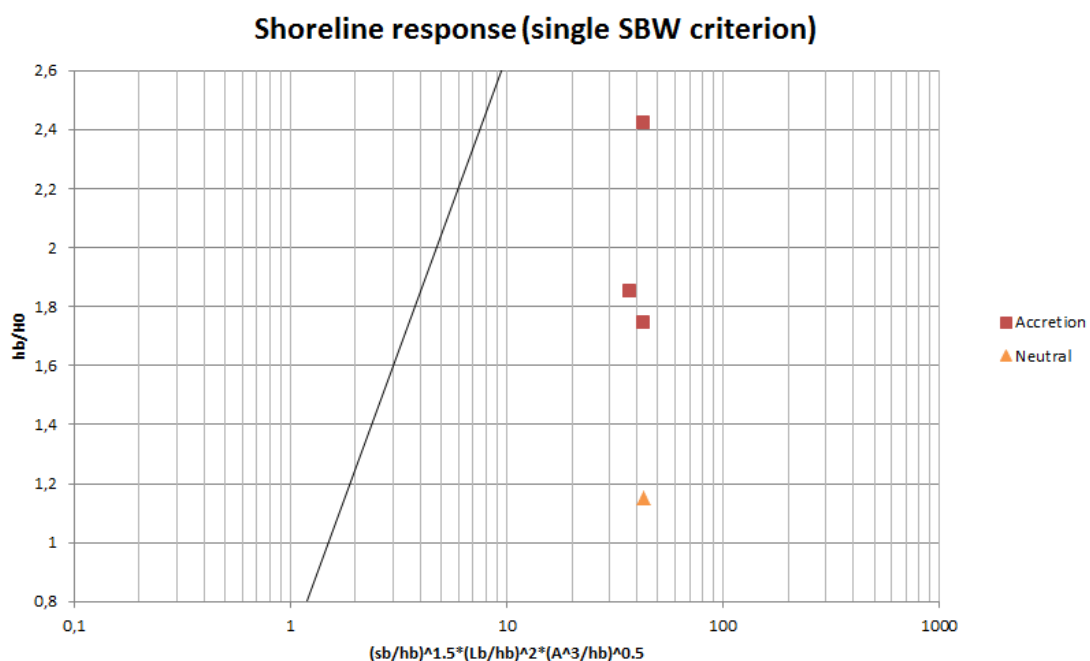


Figure 5.3 – Results of tests B, C, D and G plotted as data points in the graph for the prediction of shoreline response to a single SBW

As expected, the criterion for single SBWs does not hold when applied to coastal systems with multiple SBWs. The relative big difference when comparing the volumetric change for test B and C to G is also not shown in the graph with the placements of the respective data points. However, this graph is meant for indicating shoreline change in the sense of accretion or erosion so the same response for test C and G was to be expected (accretion) when looking at the placement of the data points, albeit in the wrong area of the graph. Furthermore, test D, the test closest to an erosive shoreline response case, is furthest away from the line, suggesting a possible use for the graph when slightly adapted for multiple SBW cases with the addition of 1 or more relevant physical parameters.

5.3 Conclusion

To come to a prediction for the shoreline response to multiple SBWs the r value criterion looks promising. Where an r value of below 1 was found, the morphological response was indeed accretion. However, as a rule of thumb, this criterion is probably not the best option.

The analytical method is based on a wave set-up equation which is too much simplified for a complex cross-shore profile present in SBW systems (Bellotti, 2007). The empirical formula for wave transmission over a submerged barrier has an inaccuracy of $O(0.1)$ (Villani et al., 2012). And lastly, in the case of a large rip current velocity the constant wave breaker parameter does not hold. For instance: the results of test D is (erroneously) erosive with a constant wave breaker parameter of 0.63 but (correctly) accretive when a wave breaker parameter dependent on flow velocity and direction at the point of breaking is used (paragraph 4.3.2). It is, however, difficult to determine this wave breaker parameter analytically, therefore demanding the use of a numerical model.

The criterion for the shoreline response to a single SBW did not hold for cases with multiple SBWs, as expected. However, if the addition of one or more terms based on the physical parameters of the case could make it valid for cases with multiple SBWs, this method would be promising. The criterion would consist of the relation of physical parameters of the system to certain powers and with that, avoids the complexity of wave transmission and non-constant wave breaker parameters. This setup makes it a good candidate for a rule of thumb for the initial assessment of the shoreline response to a certain multiple SBW system.

The possibility to make this criterion valid for multiple SBW systems with the addition of one or more terms based on the physical parameters of the system is looked at in section 6.

6 Analysing the shoreline response to multiple SBWs by means of scenario's

As mentioned in section 5, this section includes further research of the mode of the shoreline response to multiple SBW systems by varying certain physical parameters. Analysis of the results will show which added processes influences the system in what way, and if it is indeed possible to predict the shoreline response to a multiple SBW system with an addition to the existing criterion.

First the extra processes will be looked into with a prediction of the influence on the system. Subsequently, a model will be set-up to visualize these processes as best as possible. If the results show a trend of any kind, the data can be used to set up a criterion.

6.1 Added processes relative to a single SBW system

Based on the findings in section 5, the added processes relative to a single SBW system tend to make the system able to retain an accretive shoreline response under more 'severe' circumstances (e.g. higher wave energy exerted on the system). The contributing factors to making the shoreline response more prone to be accretive in cases of multiple SBWs are lateral confinement (for a certain range of ratios) and the rip current influence on the wave breaker parameter differences longshore. The first and last barrier in the series also experience an increased difference in wave set-up between the set-up in the lee of the breakwater and outside of the system since the waves outside of the system only diffract to one side (behind the adjacent SBW) as opposed to the waves entering through the gaps diffracting to two sides and therefore reducing more in height. However, this will not be included since the researched system will be handled as an infinite series of SBWs with a certain degree of lateral confinement. However, it is important at what lateral confinement ratio the gap is too wide to be speaking of a multiple SBW system and the response of the shoreline is equal to an array of single SBWs.

The system also depends on the availability of sediment. As can already be seen by single SBWs (Figure 6.1), when the area in the lee of the SBW is indeed accretive, this area is fed with sediment mostly from the adjacent shoreline and the area's directly longshore of the location of the SBW. For a multiple SBW system this is found to be the gap area and the lee of the gap. This would mean an increasing availability of sediment with an increasing gap length to barrier length ratio.

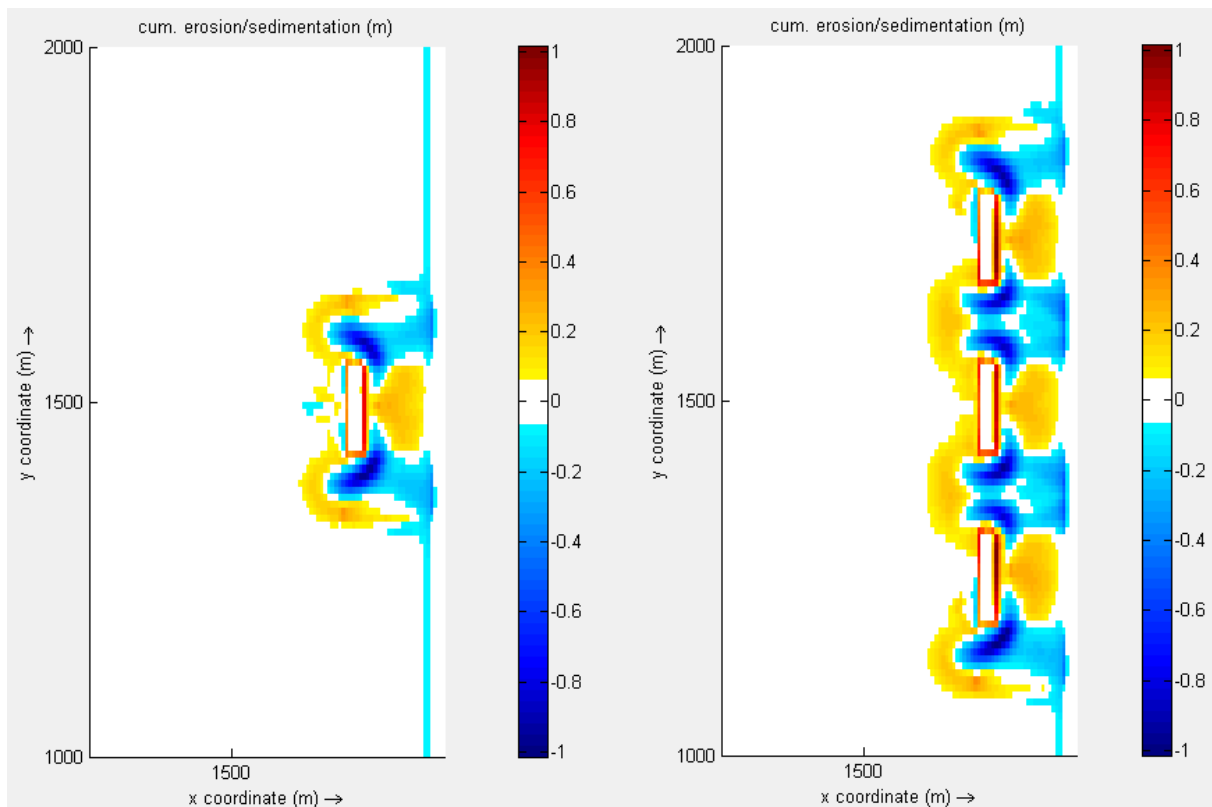


Figure 6.1 - Cumulative sediment/erosion profile for a single SBW (left) and multiple SBW (right) system

When determining the extra term(s) for the shoreline response criteria these additional processes need to be looked at. The lateral confinement is dependent on the ratio between the gap length and the barrier length, whereas the difference in protruding wave energy in the lee of the SBWs, with respect to a single SBW, is related to the relative wave height entering the system and the again the lateral confinement ratio. This amounts to term G, consisting of the lateral confinement ratio and relative wave height ratio, both to a certain power:

$$G = \left[\left(\frac{L_g}{kL_b} \right)^i \left(\frac{h_b}{H_0} \right)^j \right] \quad (6.1)$$

With k as a factor to address the possibility of an unequal contribution of the gap length and the barrier length to the shoreline response. The term G serves as a first approximation of the reduction on the x-value of a certain data point, when plotted in the graph for the shoreline response, also used in section 5. In this graph, moving a data point in the direction of the accretive area means it is expected that a multiple SBW system is more prone to an accretive shoreline response. Since the lateral confinement ratio works both for (a higher ratio means more available sediment and more wave penetration to feed sediment) and against (a higher ratio means a smaller return velocity and more wave penetration to erode existing sediment in the lee of the SBW) a larger chance of accretion, it is, at first hand, unclear if the term should be noted as L_g over L_b or vice versa, depending on which process dominates in which circumstances. The sign of the appointed power should point this out when fitting the results. For the second term; a higher relative wave results in a bigger difference in wave height in the gap and in the lee of the SBW (for example, a difference of 100 % can be found at emergent breakwaters. An increased difference enhances the inward

directed diffraction and the difference in water level set-up at the shoreline, enhancing the driving mechanics of a 4-cell pattern. Hence this term is noted as h_b over H_0 , a higher relative wave leads to more reduction of the x-value of the data point which, in result, moves closer to the accretive area.

While the lateral confinement contribution and the different degree of wave sheltering with respect to a single SBW are both governed by the L_g over L_b ratio, they are reviewed as separate as possible by consecutively keeping the relative wave height and lateral confinement ratio constant. This is required to equip the new criterion with the terms needed to accurately predict the mode of shoreline response with a wider range of physical parameters. Incorporating both contributions in one term would narrow the range of different scenarios where the criterion can be used and would generate a too complex fit as a result, unnecessarily complicating the criterion for multiple SBWs.

Before looking into these parameters and their powers, the transition point between a multiple SBW system and a system of multiple single SBWs will be determined (paragraph 6.3).

6.2 Model set-up

When trying to determine the magnitude of the separate contribution factors, it is important that the ratios on which they are based vary per model run, while maintaining a close proximity of the resulting data points to the area of the graph where the transition between an accretive and an erosive response is expected. The line of the single SBW criterion is used as a first estimate. In addition, it is preferred that the used parameters are identifiable with real life cases. Table 6.1 shows the parameters used per ratio of the length of the barrier in relation to the length of the gap, with their respective x- and y-values using the single SBW criterion. These 12 tests will be performed for multiple modes of lateral confinement expressed in length of the barrier versus length of the gap: 1:2, 1:1.5, 1:1, 2:1 and 4:1. For reference, also a single SBW system will be modelled with these parameters, which can be seen as a multiple SBW system with infinite gap length.

Test	hb	xb	H0	sb	Lb	A	y	x
1	2	100	1	0,2	120	0,115	2	3,13931
2	2	100	1	0,4	120	0,115	2	8,879311
3	2	100	1	0,6	120	0,115	2	16,31234
4	2	100	1,5	0,2	120	0,115	1,333333333	3,13931
5	2	100	1,5	0,4	120	0,115	1,333333333	8,879311
6	2	100	1,5	0,6	120	0,115	1,333333333	16,31234
7	3	200	1,8	0,2	200	0,115	1,666666667	1,72253
8	3	200	1,8	0,4	200	0,115	1,666666667	4,87205
9	3	200	1,8	0,6	200	0,115	1,666666667	8,950527
10	3	200	3	0,2	200	0,115	1	1,72253
11	3	200	3	0,4	200	0,115	1	4,87205
12	3	200	3	0,6	200	0,115	1	8,950527

Table 6.1 - Physical parameters for the tests per ratio of L_b over L_g

Results will be plotted in the graph shown in Figure 6.2 to find the relation separating accreting and erosive cases for systems of multiple SBWs. In this plot the data points have

not been given a mode of response yet. The expectation is that there will be more data points with an accretive response than the 2 that the graph predicts now.

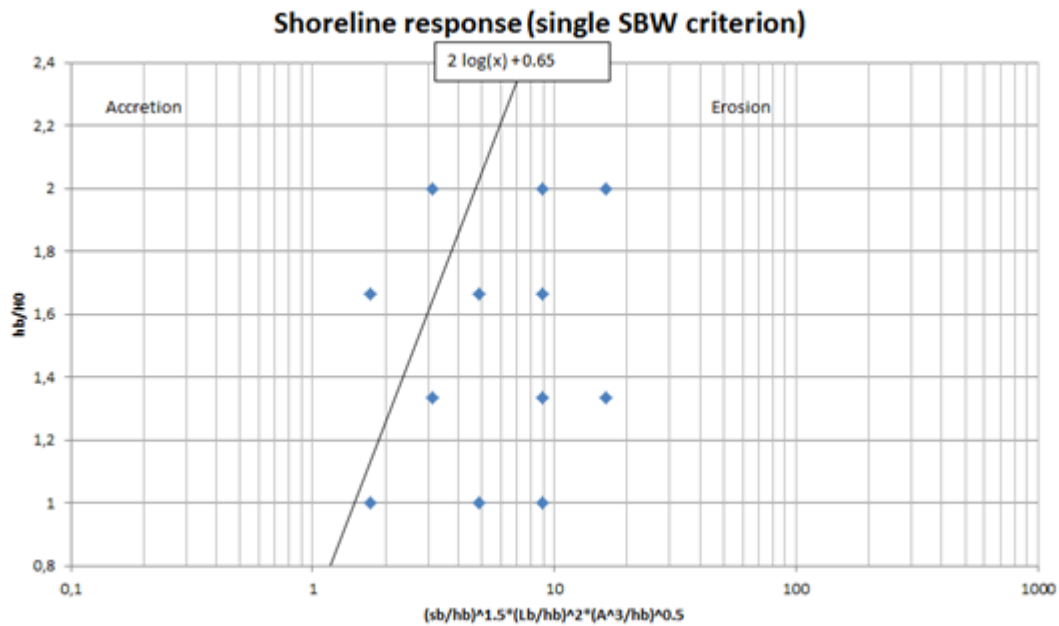


Figure 6.2 - Results of tests 1 to 12, plotted as data points in the graph for the prediction of shoreline response to a single SBW

6.3 Transition between multiple and single SBW system

One can speak of multiple SBW systems instead of multiple single SBWs when the hydrodynamic and morphodynamic disturbances protrude far enough longshore to influence these processes of the next SBW. This could be the distribution and location of return flow, bottom profile in the gaps or return velocity profile over the gap transect. Before this point of interaction between the SBWs the criterion for single SBWs can still be used to determine the mode of shoreline response. After this point the criterion for multiple SBW systems should hold. This transition can be found at a certain ratio of lateral confinement and this paragraph will look into this point, if it is constant and if not, which factor is governing in determining its location.

6.3.1 Morphologic changes

The return flow dominates the morphologic changes in the gap. A scour hole in the gap is expected and the location of the maximum depth of the scour holes is related to the location of the peaks in the return velocity. If the scour holes caused by different SBWs connect, they tend to enhance one another and will most certainly influence the overall system as a whole. Three cases with a varying lateral confinement ratio are observed to look at the differences in development of these scour holes. The parameters of these cases are collected in Table 6.2. Only the lateral confinement ratio is varied over the cases.

LC ratio	hb	xb	H0	sb	Lb	A	Shoreline response
1:4	2	100	1.5	0,4	120	0,115	Erosive
1:1	2	100	1.5	0,4	120	0,115	Accretive
2:1	2	100	1.5	0,4	120	0,115	Accretive

Table 6.2 - Parameters of the three reviewed cases.

Figure 6.3 shows the relative bottom level change for the lateral confinement ratio of 1:4. The scour holes in the gaps between the SBWs are fully overlapping and have a maximum depth of 1.6 m. Figure 6.4 shows the same plot for the 1:1 ratio. In this case the maximum depth points of the scour holes caused by each SBW are separated, but the locations where scour occurs still overlap. The maximum depth of the scour holes is 1.3 m. However, for the 2:1 ratio (Figure 6.5), the scour holes are not connected, the relative bottom level change is 0 between the gaps. The maximum scour hole depth is 1.2 m which is the same as the maximum depth found in the reference model with a single SBW with the same parameters. Repeating this comparison for different wave heights, cross-shore distance and submergence levels showed that the degree of separation per ratio is hardly different, only the maximum scour hole depth changes. So concerning the impact of the return flow on the morphology in the gap SBWs can be reviewed as 'single' when $L_g/L_b \geq 2$.

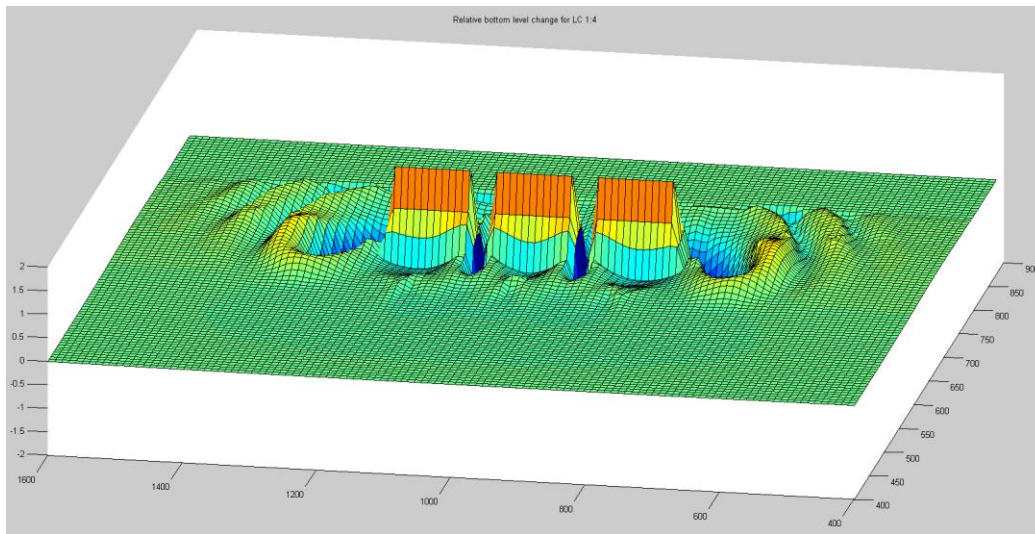


Figure 6.3 - Relative bottom level change for lateral confinement ratio 1:4

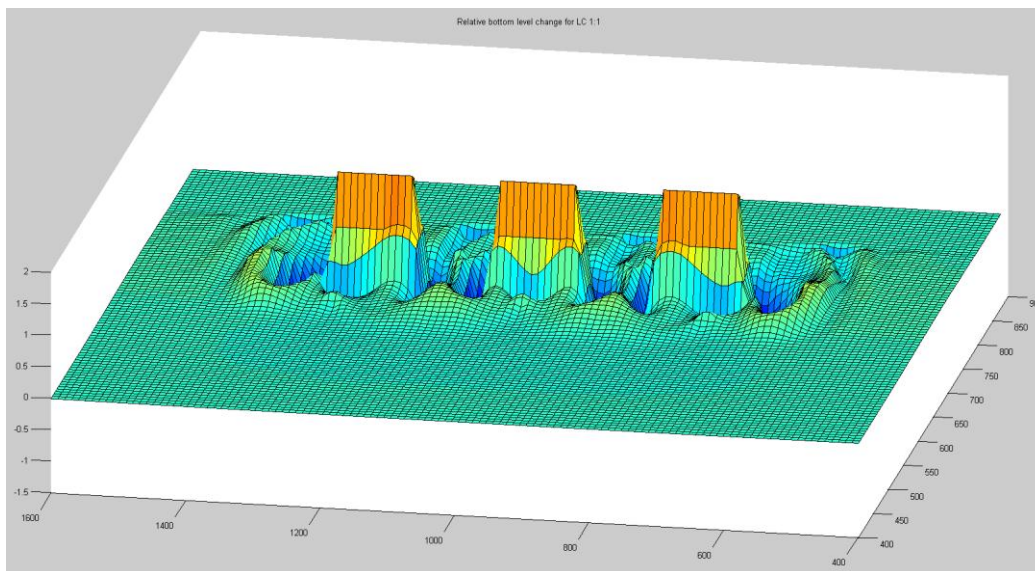


Figure 6.4 - Relative bottom level change for lateral confinement ratio 1:1

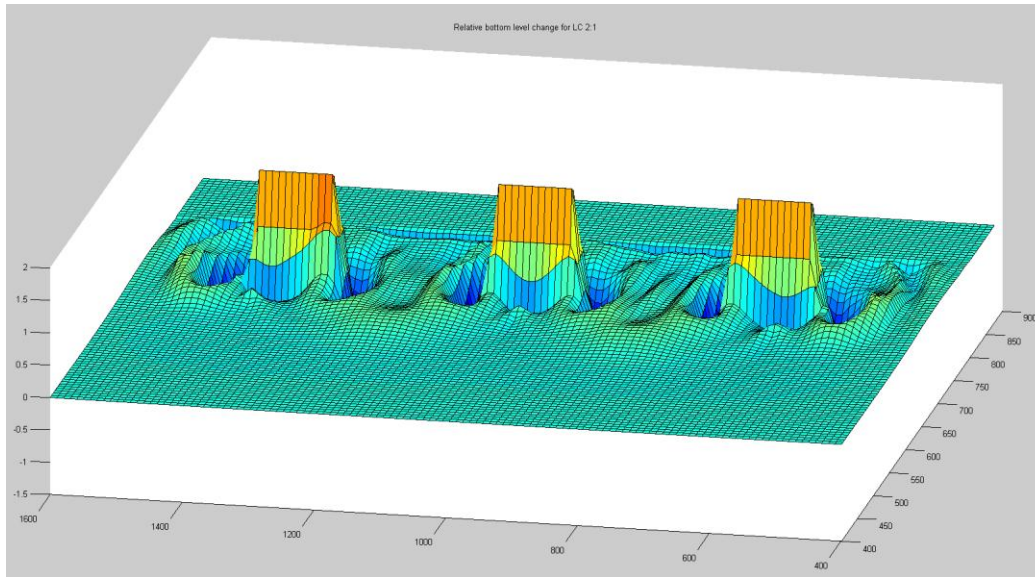


Figure 6.5 - Relative bottom level change for lateral confinement ratio 2:1

6.3.2 Flow velocity profile over the gap transect

As shown in many studies, the flow pattern behind SBWs is highly relevant for the shoreline response. The mode of circulation in the lee of the SBW(s) determines if the system is accretive or erosive. However, the maximum flow velocity can be found in the gap. In the sense of finding the transition between a system of multiple SBWs and a system of multiple single SBWs it is assumed that if the return flow in the gap is separated per SBW, the flow pattern in the lee of an SBW has little to no impact on the flow pattern in the lee of the SBW next to it (under the circumstances used in the models), based on the nature of the flow patterns and the fact that the flow velocity in those patterns is an order smaller than the flow velocities found in the gap. To get an idea of the magnitude of the 'area of disturbance' the longshore plots of the cross-shore flow velocity at the cross-shore location of the SBW crest are observed for different wave heights. Figure 6.6, Figure 6.7 and Figure 6.8 show this plot for the wave heights of 1.0 m, 1.5 m, and 1.8 m respectively. It can be seen that the longshore length of the affected area increases with wave height.

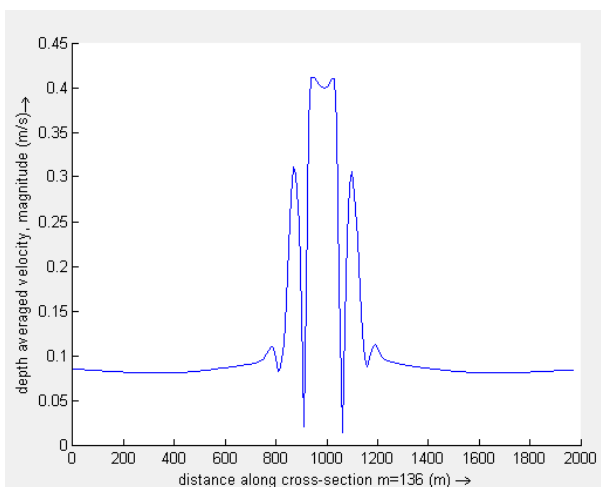


Figure 6.6 - Longshore profile of the cross-shore flow velocity for $H_i = 1.0$, at the cross-shore height of the SBW crest

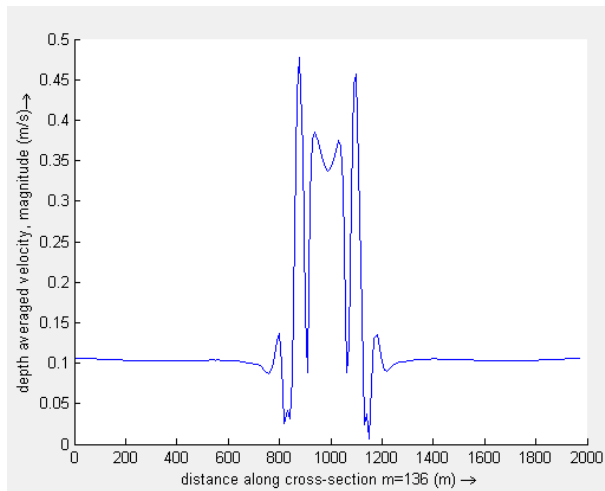


Figure 6.7 - Longshore profile of the cross-shore flow velocity for $H_i = 1.5$, at the cross-shore height of the SBW crest

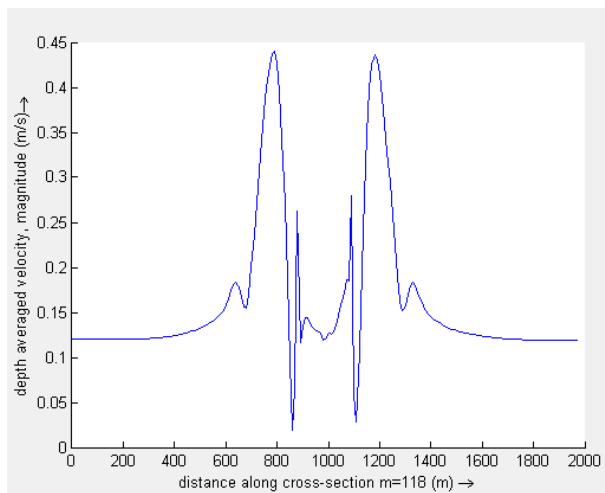


Figure 6.8 - Longshore profile of the cross-shore flow velocity for $H_i = 1.8$, at the cross-shore height of the SBW crest

The parameters of the used cases and the longshore length up until the observed disturbance is less than 5 % of the total when following the velocity profile outward of the SBW, are collected in Table 6.3. The value of 5 % is arbitrarily chosen to avoid generating erroneously length values as a result of small disturbances in the velocity profile.

H_i	h_b	x_b	s_b	L_b	A	Disturbance length	Relative to barrier length
1.0	2	100	0,4	120	0,115	160	1.34
1.5	2	100	0,4	120	0,115	180	1.49
1.8	3	200	0,4	200	0,115	390	1.95

Table 6.3 - Longshore disturbance length per wave height

The gap length needs to be 2.68 (2 times 1.34) the barrier length in a case with a wave height of 1.0 m for the influence of the flow velocity for the next SBW to be negligible. This length increases to approximately 3 times the barrier length for a wave height of 1.5 m and even further to 3.9 times in a case with waves of 1.8 m. These lengths are larger than the disturbance length on the morphological scale so these lengths are used to determine where the transition takes place between a system of multiple SBWs and a system of multiple

single SBWs. This knowledge can then be used to get a better fit through the data points of the contribution of the lateral confinement to the shoreline response (paragraph 6.4). The transition point will henceforth be indicated with a dashed line where relevant.

6.4 Varying the lateral confinement ratio

To single out the contribution of the first of the extra terms, the lateral confinement is plotted against the cumulative volumetric change in sediment in the lee of the SBW after a morphologic run time of 45 days, for the 4 wave heights used. Since the relative wave height is constant per plot, so is the contribution of the second added term, so the relative differences in the cumulative volumetric change of sediment (erosive or accretive) are caused solely by the first added term, monitored in a control area such as used in section 5. The control area is the area in the lee of the middle SBW from 20 m off the inshore SBW trunk to the shoreline. Figure 6.9 shows the plot for the wave height of 1.0 m. The plots of the other wave heights can be found in Appendix C. A line is fitted through the data points and the value of the single SBW case is used to simulate an infinite wide gap to serve as an asymptote for the fitted line. The location of the point of transition between a multiple SBW and a single SBW system is based on the findings in paragraph 6.3 and indicated with a dashed line.

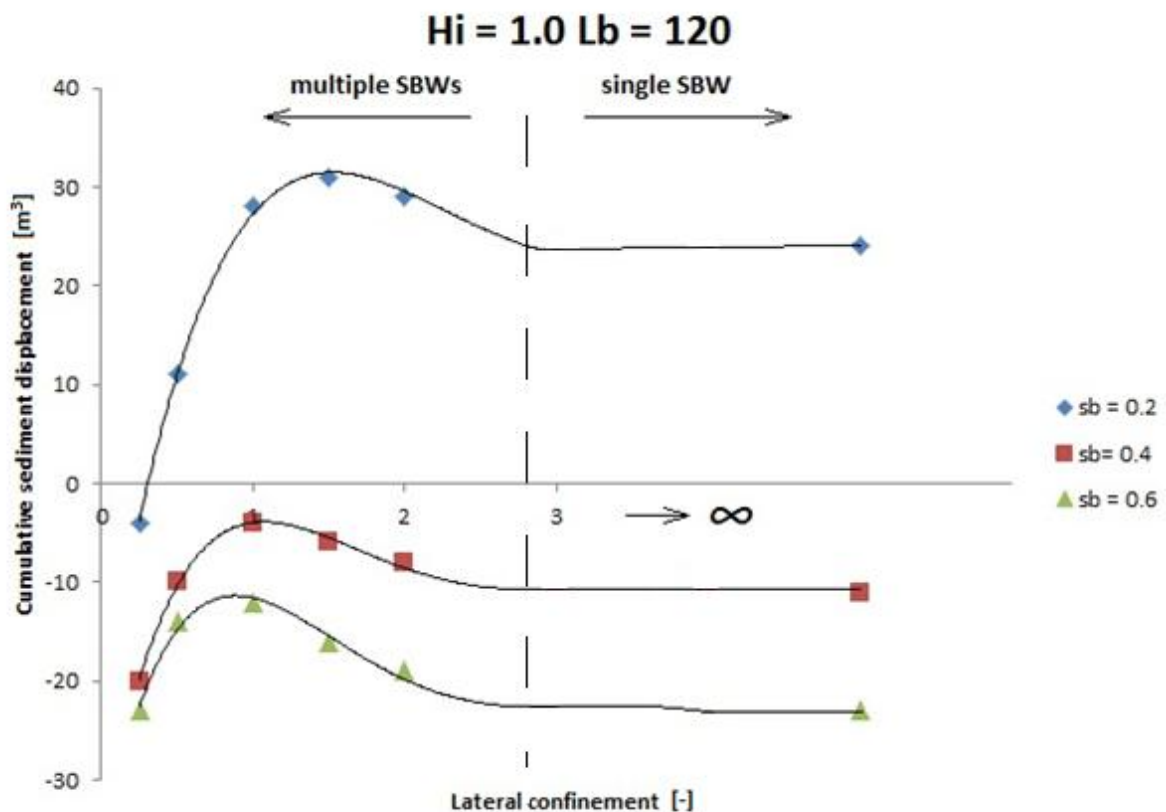


Figure 6.9 - Contribution of the lateral confinement ratio to the shoreline response for $H_i = 1.0 \text{ m}$

A general pattern can be seen for all wave conditions and all submergence levels. The cumulative volumetric displacement increases (or becomes less negative) when L_g over L_b increases, above the value found in a single SBW case. It reaches its maximum between ratio 1:1 and 2:1; 1:1 for lower wave heights and 2:1 for higher wave heights, and decreases to the level of a single SBW when the ratio increases further.

It should be noted that the model for the wave condition of 3m, while the plot of the results still roughly representing the shape previously discussed at a morphological run time of 45 days, becomes increasingly unstable if the model has a longer run time. The model runs with a submergence level of 0.2 m even gave spurious results for the sediment displacement values from the first morphological time step. This could only be slightly reduced by lowering the morfac factor to 1. Therefore it is advisable to limit the second term to $h_b/H_0 \geq 1.25$. This includes a large amount of all the real life cases, since it is likely that waves do not exist below that ratio because it is past wave breaking point under normal circumstances.

If the cumulative sediment displacement is normalized with the amount of the single SBW case as 1 and averaged over all conditions per lateral confinement (excluding the unstable results), the following plot can be made. The fit through the points is of the 2nd order. This will be used in paragraph 6.6 to develop the term added by the lateral confinement ratio.

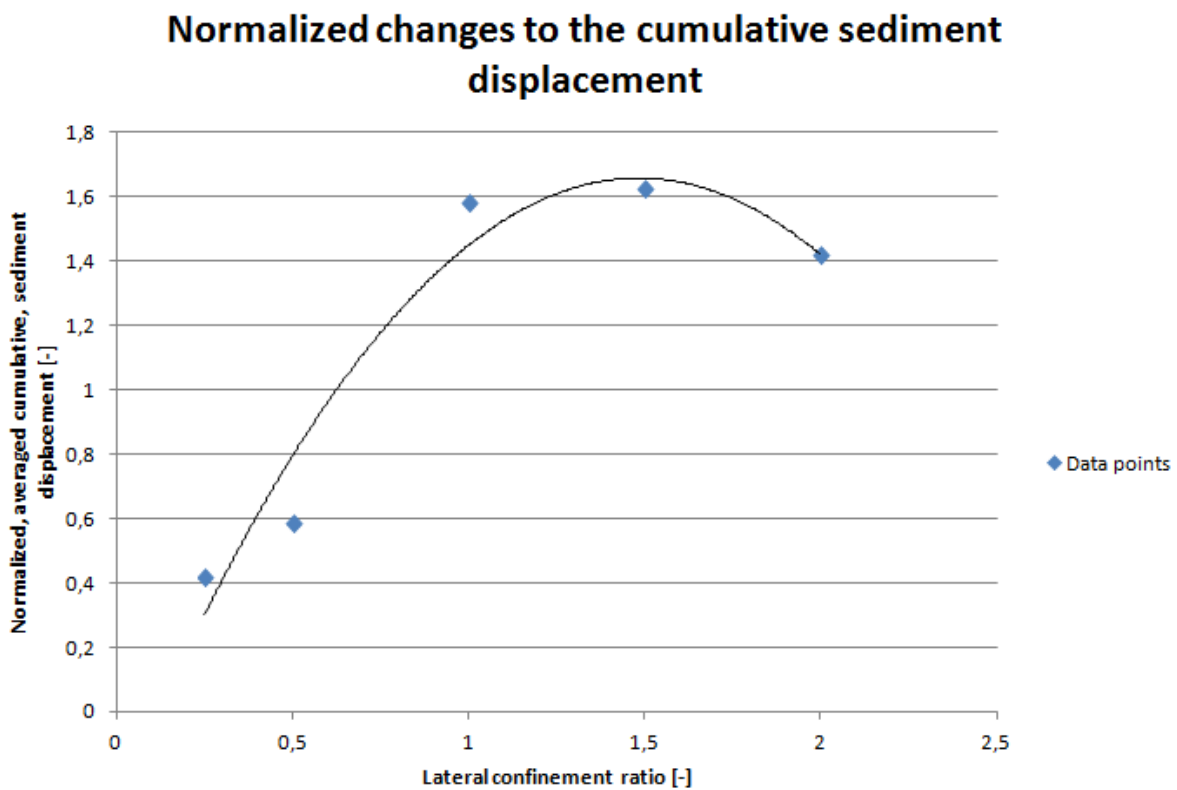


Figure 6.10 - Normalized, averaged, cumulative sediment displacement

6.5 Varying the relative wave height

As mentioned earlier the contribution of the relative wave height h_b/H_0 to the response of the shoreline is different from single SBW cases. The wave climate in the lee of the SBW is determined by the wave transmission (including the directional spreading induced by the wave passing over the barrier) and diffraction in the shadow zone from the waves next to the SBW. For single SBWs the diffraction of the wave next to the SBW is one sided (into the shadow zone of the SBW) and there is a certain change in the wave spectrum by directional spreading. For multiple SBWs the waves entering through the gap diffract to two sides in the shadow zones of two SBWs, reducing the wave energy in the actual gap even more. Figure 6.11 shows the increased directional spreading in the case of multiple SBWs with equal physical parameters. The wave spectrum is therefore wider and less concentrated on the

shoreline in the lee of the SBWs. This results in a different degree in wave sheltering with relative to a single SBW case. Figure 6.12 shows the wave sheltering areas for a single SBW and for multiple SBWs, including the interaction area if the transitional zone overlaps.

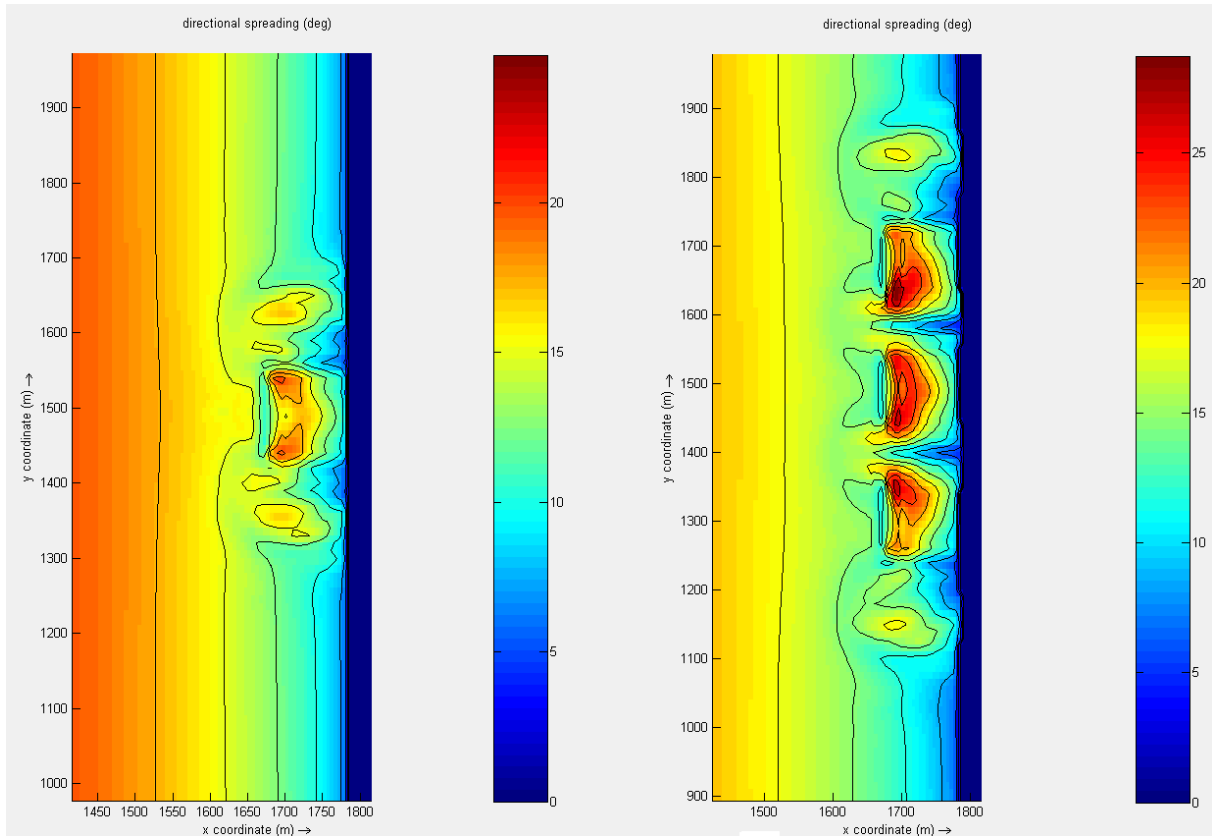


Figure 6.11 - Difference in directional spreading for a single SBW and multiple SBWs with a lateral confinement ratio of 1:1

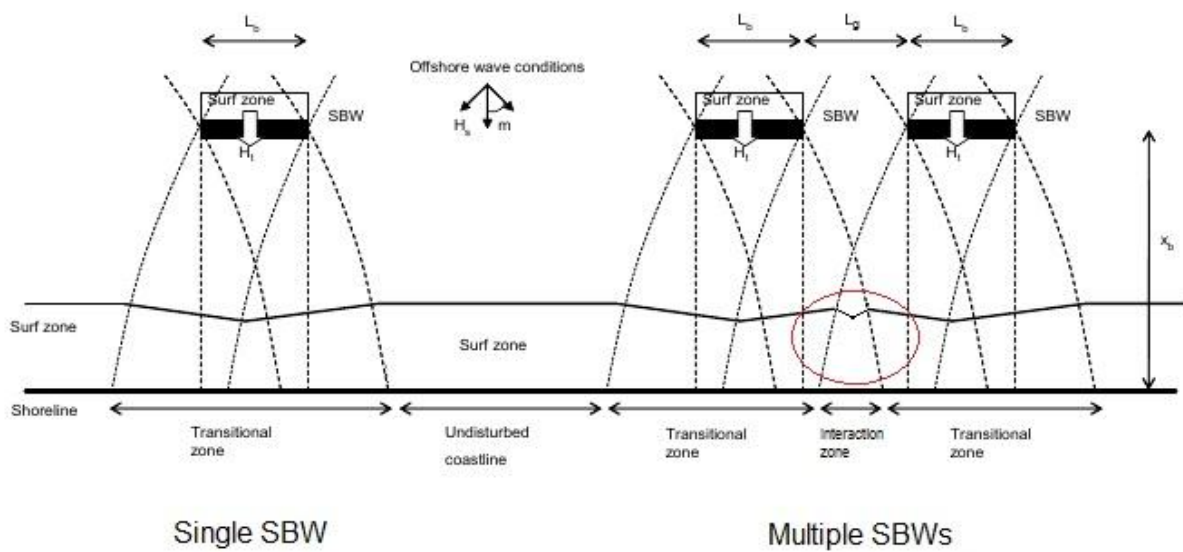


Figure 6.12 - Visualisation of the wave sheltering effect of a single SBW (left) and multiple SBWs (right)

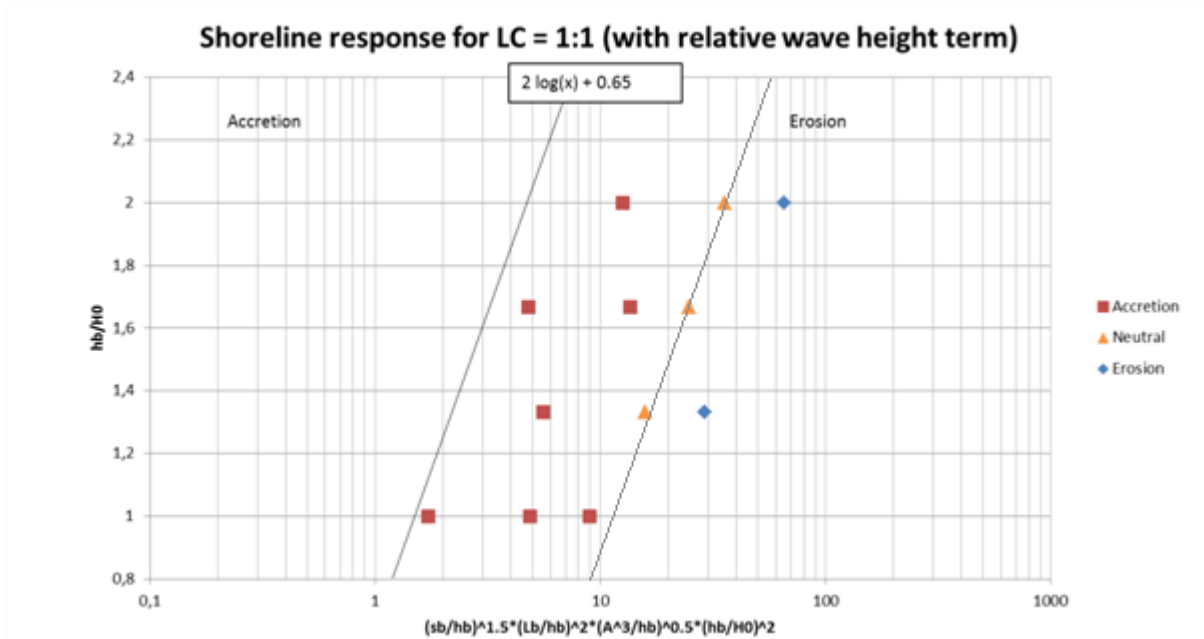


Figure 6.14 - Data points of the LC = 1:1 case with the added relative wave height term, lines are parallel

This fit, and possible reduction factor, will be checked further when combined with the term for the lateral confinement ratio. Note that including this fit in the criterion is only necessary when using the same line for the transition between an erosive and an accretive response is a prerequisite. When developing the graph solely for the shoreline response to multiple SBW systems, the different degree in wave sheltering can be incorporated in the placement of the transition line.

6.6 Developing the criterion

To validate the conclusions from the previous paragraphs, the shape of the term G has to be determined and tested on the data points from all model runs for every lateral confinement.

For the term describing the contribution by the lateral confinement ratio the shape is known (Figure 6.10). However, because more sedimentation values should lead to a bigger probability for an accretive shoreline response, the data points should be displaced to the left in the graph for the shoreline response. This means the graph has to be inverted on the y-axis. Figure 6.15 shows the result with a 2nd order fit through the data points. This fit describes the contribution to the displacement of the value of the data points on the x-axis of the data points due to the lateral confinement ratio.

2nd order fit for the contribution by the lateral confinement ratio

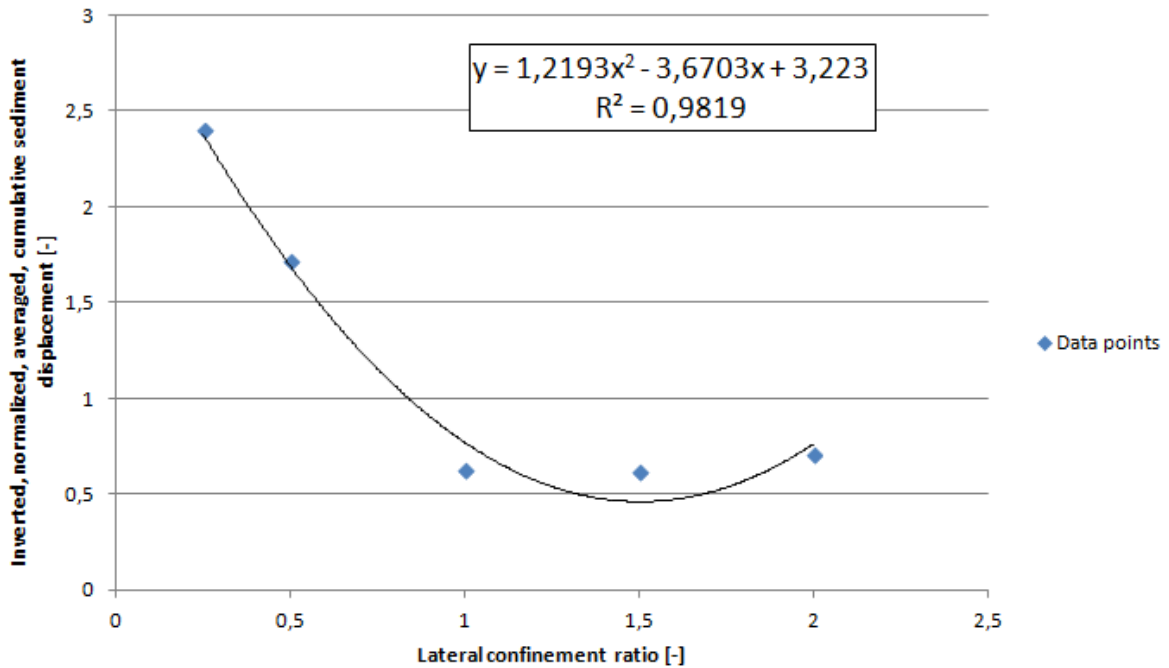


Figure 6.15 - Inverted, normalized, averaged, cumulative sediment displacement

This amounts to the first term of G as displayed in (6.2):

$$f_1(L_g, L_b) = 1.22 \left(\frac{L_g}{L_b} \right)^2 - 3.67 \left(\frac{L_g}{L_b} \right) + 3.22 \quad (6.2)$$

The term for the relative wave height was determined in paragraph 6.5, only the factor is still unknown.

$$f_2(h_b, H_0) = i \left(\frac{h_b}{H_0} \right)^2 \quad (6.3)$$

These terms together form the additional term G. Plotting all the data points of all lateral confinement ratios with the new addition to the existing criterion in the form of the term G, with the value of 0.4 for i, yields the resulting plot as shown in Figure 6.16. The plots with the data points per individual lateral confinement ratio are collected in Appendix C.

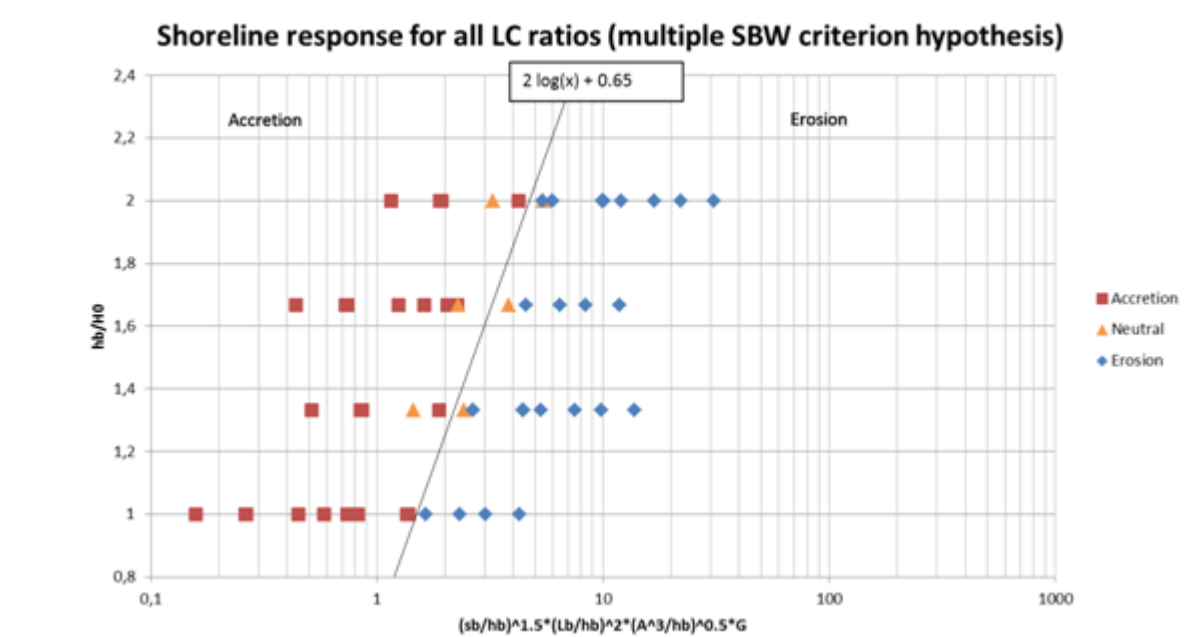


Figure 6.16 - Data points of all the LC ratios with the added term G

All accretive points are in the area for accretion and all erosive cases are in the area for erosion. The neutral points are around the transition line. The fact that these points are not directly on the line is caused by the error made by averaging the cumulative sediment displacement values per lateral confinement ratio while the maxima were not exactly equal per ratio. This is also shown by the small deviation from the fit shown in Figure 6.10 and Figure 6.15, where the points of the lateral confinement ratios of 1:1 and 1.5:1 are not exactly on the fit. However, the error does not lead to discrepancies in the plot for the mode of response and, in the sense of keeping the criterion as straightforward as possible, the small deviation in the location of the peak is not represented in the criterion.

6.7 Conclusion

The trend seems to indicate a balance between a protection from wave energy by wave attenuation consisting of both wave transmission (dissipation), directional spreading over the barriers and diffraction of the undamped wave through the gaps, and an allocation of the available sediment. The sediment being used is located at the cross-shore length at the gaps and the offshore trunk of the SBW. This availability increases with a decreasing lateral confinement. However, when this ratio exceeds a certain limit, the system cannot be seen as a multiple SBW system anymore and instead can be assessed by the single SBW criterion again. These processes lead to an extra term (G) in addition to the existing criterion for single SBW for the possibility to assess the shoreline response to multiple SBW systems. This is shown in (6.4).

$$\lambda = \left(\frac{s_B}{h_B}\right)^{\frac{3}{2}} \left(\frac{L_B}{h_B}\right)^2 \left(\frac{A^3}{h_B}\right)^{\frac{1}{2}} \left[1.22 \left(\frac{L_g}{L_b}\right)^2 - 3.67 \left(\frac{L_g}{L_b}\right) + 3.22 \right] \times 0.4 \left(\frac{h_b}{H_0}\right)^2 \quad (6.4)$$

For $h_b/H_0 \geq 1.25$ and $0.25 \leq L_g/L_b \leq 2.5$.

However, this criterion is based on model runs with a relatively low variation in physical parameters. For instance, the condition for $h_b/H_0 < 2$ has not been looked at. Also, the terms concerning the lateral confinement ratio are based on a fit through the average of the model results per lateral confinement ratio. The factors of this fit should be further solidified by including more model results.

Note that the term accounting for the difference in the degree of the wave sheltering relative to a single SBW case is only necessary when using the same line for the transition between an erosive and an accretive response is a prerequisite. When developing the graph solely for the shoreline response to multiple SBW systems, the different degree in wave sheltering can be incorporated in the placement of the transition line.

The model runs were done under simplified conditions for an undisturbed comparison between single and multiple SBW systems. However, such perfect conditions do not exist in real life cases and for this reason section 7 will be looking at the validity of the criterion when expanding the model parameters.

7 Expanding the model parameters

This section introduces additional hydrodynamic parameters such as obliquely incident waves, tidal variation and a longshore tidal current in attempt to make the criterion suggested in section 6 more robust. When the criterion holds outside of perfect and simplified model parameters it is more widely applicable. However, this section only serves as a short exploration into a few hydrodynamic variables.

7.1 Model set-up

The methodology to test the influence of the added hydrodynamic processes is to add them separately to a (stable) model set-up and compare the results to the model without that process. Before analysing the results, a prediction can be made for the consequence of the added process based on knowledge of coastal dynamics. Subsequently, the model result can be compared to the case without the added process and to the prediction. Finally, something can be said regarding the impact on the applicability of the criterion.

For the 'normal' case a stable model with intermediate wave height is chosen. The relevant parameters are collected in Table 7.1.

Hi	hb	xb	sb	Lb	A
1.5	2	100	0,2	120	0,115

Table 7.1 - Physical parameters of the 'normal' case

The parameter of the added hydrodynamic process and how it is represented in the model is explained in the associated paragraphs.

7.2 Obliquely incident waves

The obliquely incident waves are represented by waves with a (nautical) direction of 255 degrees, opposing the direction of 270 degrees in the normal case. The angle with the shore normal line is consequently 15 degrees. Other wave parameters are kept the same.

Based on theory, a northward directed longshore current is expected in the surf zone. The cross-shore distribution of the longshore current consists of a peak at the cross-shore location of the wave breaker zone and a smaller peak more closely to the shoreline. The corresponding sediment transport is mainly found at the location of the higher peak at the wave breaker zone. The magnitude of the sediment transport is dependent on the longshore current velocity which varies almost linearly with the incident wave angle for small angles (up to 20° - 30°).

The longshore current will interfere with the flow pattern in the lee of the SBW. The wave sheltering effect will be reduced in the lee of the SBW as a result of the oblique nature of the waves. However, the longshore current can also feed the system sediment from updrift. It can be expected that erosive cases will be more erosive and accretive cases will be more accretive.

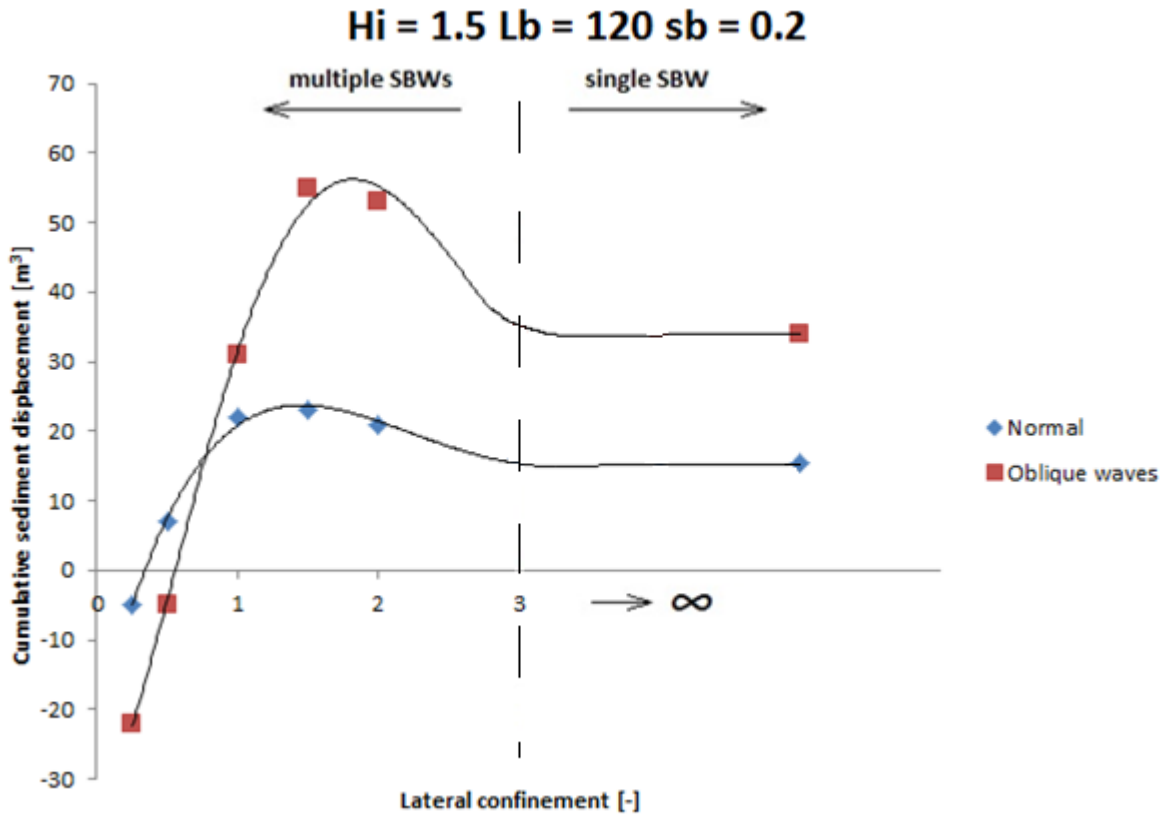


Figure 7.1 - Cumulative sediment displacement comparison, obliquely and normal incident waves

Figure 7.1 mostly agrees with this prediction. Except for the data points of the lateral confinement ratio of 1:2, every cumulative sediment displacement value is amplified in its respective mode of response. When relating this to the validity of the criterion it is mostly positive. The criterion predicts the mode of response and not the severity, however, the disparities in the area where the original result was neutral can lead to some errors in the transition area between erosive and accretive response.

7.3 Tide

The tide is represented by a wave at the offshore boundary with an amplitude of 0.5 m and a phase speed of 30 degree/hour. The (wind) wave conditions remain the same for both cases.

The result of the tide will be a varying submergence level of the SBWs. The SBW will less submerged (up to -0.3 m submergence) during the ebb period and will be more submerged compared to the normal case (up to 0.7 m submergence) during flood. This means that the wave attenuation will vary over the tide. Based on the fact that the normal case is erosive for $s_b = 0.6$ m, accretive for $s_b = 0.2$ m and expected to be even more accretive for $s_b = -0.3$ m, the equilibrium over the full duration of the tide should be equal to the result for $s_b = 0.2$ m and therefore still accretive.

Figure 7.2 shows an equal shape of the fit through the data points of both cases. However, the disparity increases with an increasing gap to barrier length ratio. This might be due to the fact that the SBW will be emergent for a small period of time, greatly increasing the wave sheltering effect and leading to more sedimentation during that period. The criterion holds in this case, however if the same increase in cumulative sediment displacement by the addition

of the tide is shown for a slightly erosive case, the response could change from erosive to accretive where the criterion would still predict erosion.

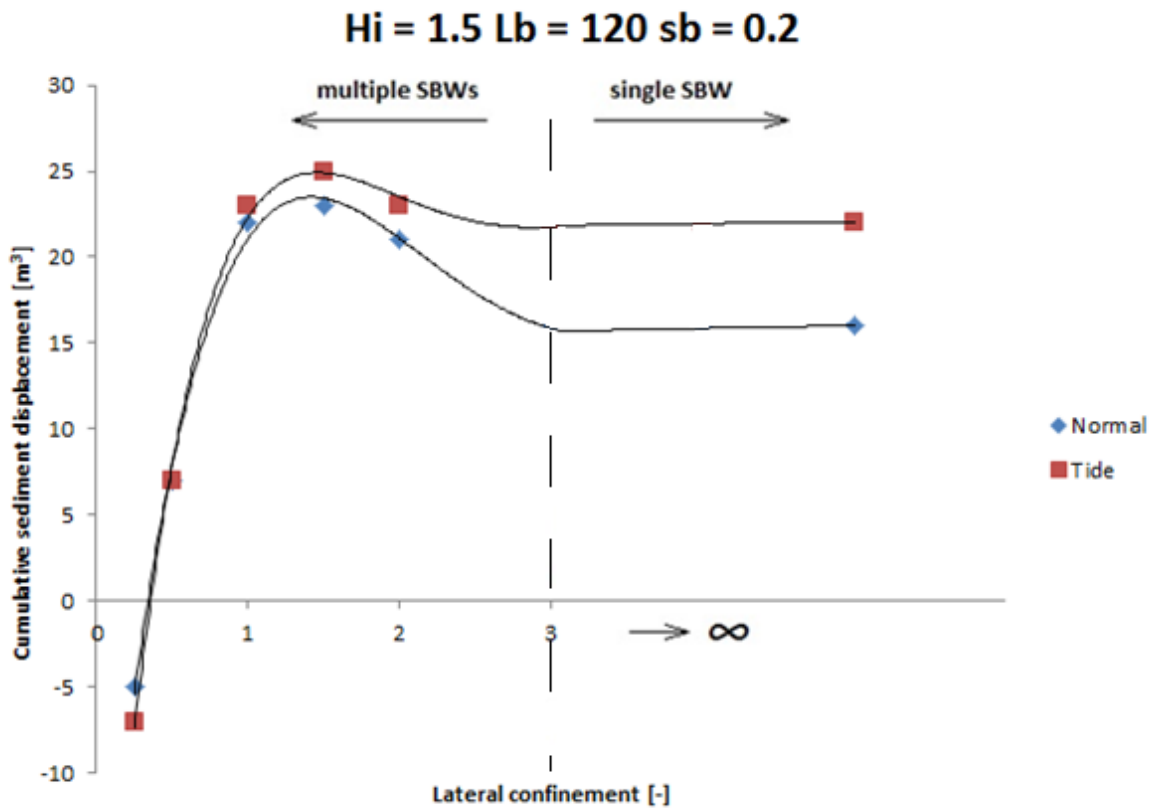


Figure 7.2 - Cumulative sediment displacement comparison, 0.5 m tidal amplitude and no tide

7.4 Longshore tidal current

The longshore tidal current is represented by a gradient in both Neumann boundaries (the North and South boundaries) and a corresponding varying water level for the offshore boundary. The longshore gradient amounts to $i = 1.5 \cdot 10^{-5}$.

The longshore current velocity can be calculated as follows:

$$u_y = C\sqrt{Ri} \quad (7.1)$$

The Chézy value for the bottom is $65 \text{ m}^{0.5}/\text{s}$ and the hydraulic radius, R , is equal to the local depth. This amounts to a decreasing longshore current velocity profile with a decreasing depth. The expected (northward directed) longshore current velocity is 0.35 m/s at the inshore trunk of the SBWs and decreases to 0 at the shoreline. Because the wave attenuation is the same as for the normal case (shore normal) and this resulted in an accretive response, the expectation for this case is more accretion since the longshore current feeds sediment from updrift in the system and the sediment transport capacity is reduced in the lee of the SBWs by reduced wave action. Consequently, erosion is expected downdrift of the SBW system, where the transport capacity is increased again and the flow becomes sediment hungry.

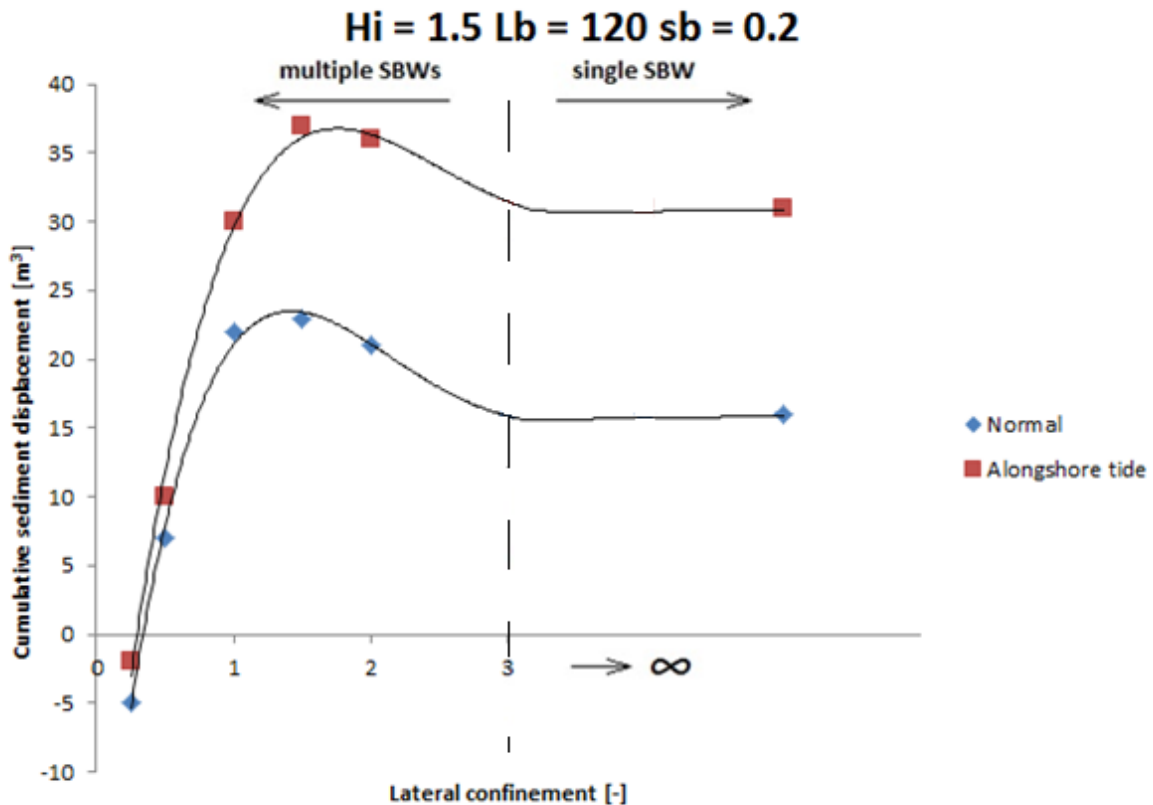


Figure 7.3 - Comparison sediment displacement comparison, a longshore tidal current and no current

Figure 7.3 agrees with the prediction. For increasing lateral confinement ratios the cumulative sediment displacement greatly increases, reaching a factor 2 for single SBWs. Concerning the criterion; the same problem as encountered when analysing the case for the normal tide surfaces. When the feeding of sediment into the system changes the response from erosion to accretion the criterion gives the wrong prediction for the mode of response.

7.5 Conclusion

Based on very select data there are some positive points and some negative points regarding the robustness of the criterion. In the case of a hydrodynamic process that amplifies the coastal response (e.g. obliquely incident waves) the criterion holds. When the added hydrodynamic process causes the available sediment to increase or decrease over the whole lateral confinement ratio spectrum (e.g. tide and longshore current), the criterion could give an erroneous prediction if the 'normal' case is close to the transition between an erosive response and an accretive response. For the used case this did not happen, but more testing is advisable to visualize the impact of these processes further, especially around the transition area. A possible solution could be an error band around the transition area or the separate treatment of the process not included in the criterion (e.g. a variation of the submergence level by a large tidal amplitude).

8 Conclusions and recommendations

To conclude this thesis, an overview will be given of the conclusions made per section. Based on the findings and conclusions some recommendations will be made.

8.1 Conclusions

Although the knowledge regarding shore parallel detached SBWs increases, there is still no easy accessible rule of thumb for the first assessment of the mode of the shoreline response to more complex SBW systems, such as a coastal protection system consisting of multiple SBWs. The r -value criterion, based on the difference in water level set-up at the shoreline in the lee of the breakwater and the lee of the gap(s), is promising but is dependent on a thorough understanding of the coastal momentum balance and it requires numerical modelling to avoid errors in the wave transmission and the wave breaker index. This makes it less suited for a rule of thumb. A criterion for the mode of shoreline response based on a relation between solely physical parameters of the system exists for a single SBW, however, is not valid for a system of multiple SBWs and a separate criterion for such cases is lacking.

In this thesis the existing criterion based on physical parameters is extended to be applicable to multiple SBW cases. This is done by modelling a number of scenarios with varying parameters in a numerical model (Delft3D) and monitoring the shoreline response. The physical parameters of the models are picked in such a way that they serve the purpose of this thesis, while still being relatable to real life coastal protection systems. To relate these physical parameters to a shoreline response, Delft3D uses a flow module online coupled with SWAN accounting for all the processes induced by the SBW(s).

Assessment of the results showed that the change in the mode of the shoreline response relative to a single SBW case was due to two factors (both governed by the ratio of the width of the gap over the length of the SBW):

- The lateral confinement ratio, directly based on the ratio of the width of the gap and the length of the SBW. A general trend shows a smaller degree of sedimentation relative to single SBW cases for the smaller ratios (<1), but an increase for ratios of 1 to 2. For ratios of 2 and larger, the value for sedimentation returns to the value found at single SBW cases.
- A different degree of wave sheltering relative to single SBW cases. The models show an increased directional spreading of the waves over the SBW crests. Additionally, up to a certain ratio of gap width over SBW length, the transitional zones of the wave sheltering by different SBWs overlap one another, leading to a different degree in wave sheltering.

Based on these two factors an additional term to the existing criterion is developed. The contribution of the lateral confinement ratio is based on a fit through the quantitative difference in sedimentation relative to the single SBW value. The contribution of the different degree of wave sheltering is represented by a term describing the relative wave height. The extended criterion for multiple SBW cases is then as follows, with the additional term between the square brackets (henceforth called G):

$$\lambda = \left(\frac{S_B}{h_B}\right)^{\frac{3}{2}} \left(\frac{L_B}{h_B}\right)^2 \left(\frac{A^3}{h_B}\right)^{\frac{1}{2}} \left[1.22 \left(\frac{L_g}{L_b}\right)^2 - 3.67 \left(\frac{L_g}{L_b}\right) + 3.22 \right] * 0.4 \left(\frac{h_b}{H_0}\right)^2 \quad (8.1)$$

For $h_b/H_0 \geq 1.25$ and $0.25 \leq L_g/L_b \leq 2.5$.

When plotting the result of all the model runs as data points in the graph for the mode of shoreline response (accretion left of the line, erosion right of the line) using the extended criterion, no discrepancies can be found (Figure 8.1).

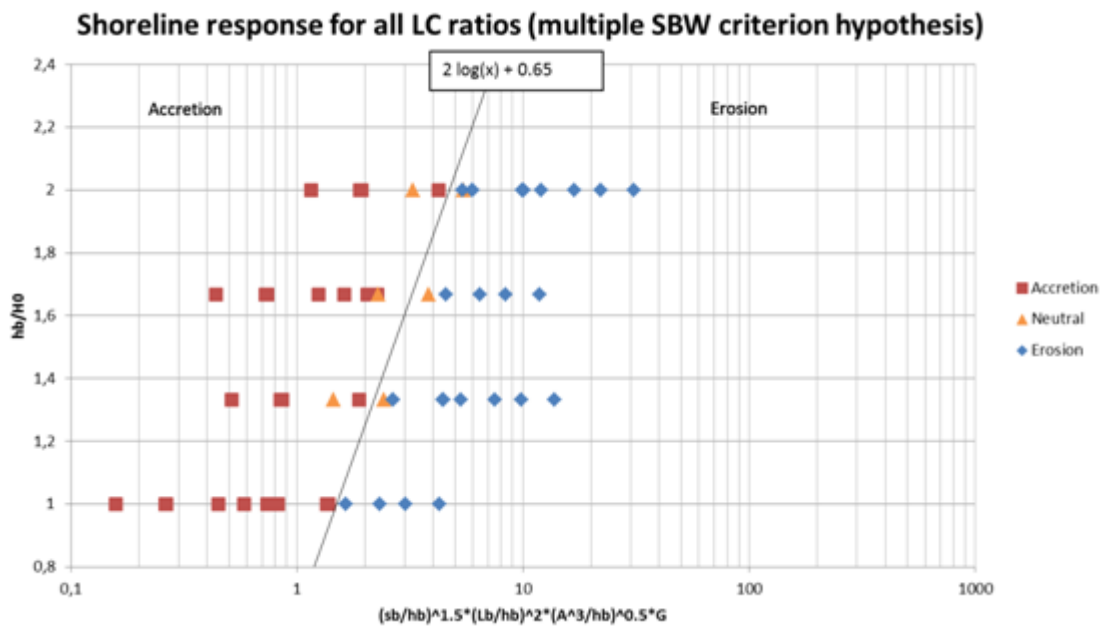


Figure 8.1 - Data points of all the lateral confinement ratios with the added term G

A first look into the application of the criterion in non-simplified hydrodynamic conditions by adding a tidal amplitude, a longshore current or obliquely incident waves is made to research the robustness of the criterion. In the select cases used for this research the criterion predicted the correct mode of the shoreline response. However, when looking at the impact of the added processes on the displacement of the data points, one can draw two conclusions.

- The criterion does not suffer from processes that amplify the shoreline response by a certain factor, because the prediction is solely the mode and not the magnitude of the mode.
- Processes that add or reduce the availability of sediment independent of the physical parameters of the system can prove to lead to an erroneous prediction, especially in the transition area between an erosive or accretive response.

8.2 Recommendations

During the literature study, information on certain subjects was proven to be scarce or limited to specific aspects of the subject. As for the development of the extended criterion some recommendations can be made regarding assumptions made, the numerical model used and future research. The recommendations are therefore split in two sections.

8.2.1 Recommendations on general future research

- Literature on diffraction in complex situations, especially longshore distributed diffraction is scarce. Research on this subject would make some of the assumptions made in this thesis void, if the impact of the processes could be analytically based.
- The partial wave breaking, inflow and return flow over the crest and the inshore trunk of the barrier generates complicated flow behaviour. Due to the grid size and the depth averaged set-up of the model, this flow behaviour is simplified. A more detailed research would benefit visualising this flow and could add to this research.
- However many model runs a conclusion is based on, a field case is a necessary part of the validation. For a field case to be eligible for such validation field measurements should be done frequently. The data should include wave data, bathymetrical updates with a reasonable time interval and data on possible nourishments of the system.

8.2.2 Recommendations on improving the criterion

- The model runs with Delft3D were all done in a depth averaged set-up. However, some processes (e.g. undertow) can only be modelled correctly in a vertically layered model set-up. A research of the impact of this simplification is advisable.
- Longer (morphological) run time to research the time scale of reaching a new equilibrium. Use a salient type beach profile as a starting file instead of longshore uniform equilibrium profile. This allows a higher morfac factor and a larger coupling interval resulting in less computational time for a longer morphological modelling period.
- As of now, the fit to describe the contribution of the lateral confinement ratio is based on 66 model runs. Further research on this contribution, including a field case, would benefit the validity of the criterion as a whole.
- Section 7 explores the validity of the criterion in non-simplified hydrodynamic conditions briefly. It is recommended to continue this research of the influence of non-simplified model conditions, by varying (for example):
 - Non-uniform longshore shoreline profiles,
 - Tidal amplitudes,
 - Obliquely incident waves,
 - Longshore currents,
 - Added beach nourishments.
- To add to the value of the criterion from an engineering point of view, research regarding the possibility of adding the magnitude of the mode of response in the criterion while maintaining a criterion based solely on physical parameters could show beneficial.

9 References

- Baldock, T. E., Holmes, P., Bunker, S., & Van Weert, P. (1998). Cross-shore hydrodynamics within an unsaturated surf zone. *Coastal Engineering*, 34(3), 173-196.
- Battjes, J. A., & Janssen, J. P. F. M. (1978). Energy loss and set-up due to breaking of random waves. Paper presented at the Proceedings of the 16th International Conference of Coastal Engineering.
- Bellotti, G. (2004). A simplified model of rip currents systems around discontinuous submerged barriers. *Coastal Engineering*, 51(4), 323-335.
- Bellotti, G. (2007). An improved analytical model for estimating water level set-up and currents induced by waves over submerged low crested coastal defence structures. Paper presented at the Coastal Structures 2007, Venice.
- Black, K. P., & Andrews, C. (2001). Sandy shoreline response to offshore obstacles, part 1: salient and tolo gradient and shape. *Journal of Coastal Research*, 29(82-93).
- Blouin, N. (2012). Process based modeling of shoreline response to submerged breakwaters. (MSc), UNESCO-IHE.
- Bosboom, J., & Stive, M. J. F. (2012). Coastal Dynamics I: VSSD.
- Bowen, A. (1969). Rip currents, I. Theoretical investigations. *Journal of Geophysical Research*, 74, 5467-5478.
- Bowen, A., & Inman, D. (1969). Rip currents, II. Laboratory and field observations. *Journal of Geophysical Research*, 74, 5479-5490.
- Burcharth, H. F., Hawkins, S. J., Zanuttigh, B., & Lamberti, A. (2007). *Environmental Design Guidelines for Low Crested Coastal Structures*. Oxford.
- Calabrese, M., Buccino, M., & Pasanisi, F. (2007). Qualitative and quantitative features of wave breaking over a submerged breakwater, and effects on nonlinear wave-structure interaction. Paper presented at the Proceedings of the 2nd International Conference on Marine Research and Transportation, Napels.
- Calabrese, M., Vicinanza, D., & Buccino, M. (2008). 2D Wave setup behind submerged breakwaters. *Ocean Engineering*, 35(10), 1015-1028.
- Dalrymple, R. A. (1975). A mechanism for rip current generation on an open coast. *Journal of Geophysical Research*, 80, 3485-3487.
- Dalrymple, R. A., Dean, R. G., & Stern, R. (1976). Wave-induced currents on barred coastlines. *EOS*, 57.
- Dalrymple, R. A., MacMahan, J. H., Reniers, A. J. H. M., & Nelko, V. (2011). Rip Currents. *Annual Review of Fluid Mechanics*, 43(1), 551-581.
- Dean, R. G., & Charles, L. (1994). *Equilibrium Beach Profiles: Concepts and Evaluation*. In D. o. C. a. O. Engineering (Ed.): University of Florida.
- Deltares. (2011a). *Delft3D-FLOW, simulation of multi-dimensional hydrodynamic flows and transport phenomena, including sediments*. User Manual.
- Deltares. (2011b). *Delft3D-WAVE, Simulation of short-crested waves with SWAN*. User Manual.
- Dick, T. M., & Breber, A. (1968). Solid and permeable submerged breakwaters. *Proceeding of 11th International Conference on Coastal Engineering*, London, United Kingdom, 11, 1141-1158.
- Diskin, M. H. (1970). Piling-up behind low and submerged permeable breakwaters. *Journal of Waterways and Harbour Division*, 96(359-372).
- Groenewoud, M. D., Van de Graaff, J., Claessen, E. W. M., & Van der Biezen, S. C. (1996). Effect of submerged breakwater on profile development. *Coastal Engineering*, 2428-2441.
- Haller, M. C., Dalrymple, R. A., & Svendsen, I. A. (2002). Experimental study of nearshore dynamics on a barred beach with rip channels. *Journal of Geophysical Research*, 107(C6).

- Haller, M. C., & Özkan-Haller, H. T. (2002). Wave breaking and rip-current circulation. Paper presented at the Proceeding Of The 28th International Conference on Coastal Engineering.
- Harris, M. M., & Herbich, J. B. (1986). Effects of breakwater spacing on sand entrapment. *Journal of Hydraulic Research*, 24(5).
- Herbers, T. H. C., Elgar, S., & Guza, R. T. (1999). Directional spreading of waves in the nearshore. *Journal of Geophysical Research*, 104(C4), 7683-7693.
- Holthuijsen, L. H. (2007). *Waves in oceanic and coastal waters*: Cambridge.
- Homma, M., & Sokou, T. (1959). An experimental study on submerged breakwaters. *Coastal Engineering in Japan*, 2, 103-109.
- Kamphuis, J. W. (1975). Friction factor under oscillatory waves. *Journal of the Waterways, Harbors and Coastal Engineering Division*, 101(WW2), 135-144.
- Lesser, G. R., Roelvink, J. A., Van Kester, J. A. T. M., & Stelling, G. S. (2003). Development and validation of three-dimensional morphological model. *Coastal Engineering*, 51(8-9), 883-915.
- Liu, P., & Mei, C. (1976). Water motion on a beach in the presence of a breakwater. *Journal of Geophysical Research*, 81, 3079-3094.
- Longuet-Higgins, M. S. (1967). On the wave induced difference in mean sea level between two sides of a submerged breakwater. *Journal of Marine Research*, 25, 148-153.
- Nairn, R. B., Roelvink, J. A., & Southgate, H. N. (1990). Transition zone width and implications for modelling surfzone hydrodynamics. Paper presented at the Proceedings of the 22nd Conference on Coastal Engineering, Delft.
- Nielsen, P., Guard, P. A., Callaghan, D. P., & Baldock, T. E. (2007). Observations of wave pump efficiency. *Coastal Engineering*, 55(1), 69-72.
- Noda, E. (1974). Wave-induced nearshore circulation. *Journal of Geophysical Research*, 79, 4097-4106.
- Pilarczyk, K. W. (2003). Design of low crested (submerged) structures: an overview. Paper presented at the Proceedings of the 6th Conference on Coastal and Port Engineering in Developing Countries.
- Pilarczyk, K. W., & Zeidler, R. B. (1996). *Offshore breakwaters and shore evolution control*: Balkema.
- Ranasinghe, R., Larson, M., & Savioli, J. (2010). Shoreline response to a single shore-parallel submerged breakwater. *Coastal Engineering*, 57(11-12), 1006-1017.
- Ranasinghe, R., Swinkels, C., Luijendijk, A. P., Roelvink, J. A., Bosboom, J., Stive, M. J. F., & Walstra, D. (2011). Morphodynamic upscaling with the MORFAC approach: Dependencies and sensitivities. *Coastal Engineering*, 58(8), 806-811.
- Ranasinghe, R., & Turner, I. L. (2006). Shoreline response to submerged structures: A review. *Coastal Engineering*, 53(1), 65-79.
- Sasaki, T. (1975). Simulation on shoreline and nearshore current. *Proceedings of Civil Engineering in the Oceans*, 3, 179-196.
- Silvester, R., & Hsu, J. R. C. (1997). *Coastal Stabilization*: World Scientific.
- Stamos, D. G., & Hajj, M. R. (2001). Reflection and transmission of waves over submerged breakwaters. *Journal of Engineering Mechanics*, 127(2), 99-105.
- Sumer, B. M., Fredsoe, J., Lamberti, A., Zanuttigh, B., Dixen, M., Gislason, K., & Di Penta, A. F. (2005). Local scour at roundhead and along the trunk of low crested structures. *Coastal Engineering*, 52(10-11), 995-1025.
- Svendsen, I. A. (1986). Mass flux and undertow in a surf zone. *Coastal Engineering*, 8(4), 347-365.
- Van der Meer, J. W., Briganti, R., Zanuttigh, B., & Wang, B. (2005). Wave transmission and reflection at low-crested structures: Design formulae, oblique wave attack and spectral change. *Coastal Engineering*, 52(10), 915-929.
- Van der Meer, J. W., Regeling, H. J., & Waal, J. P. (2000). Wave transmission: spectral changes and its impact on run up and overtopping. Paper presented at the Proceedings of the 27th International Conference of Coastal Engineering.

- Vicinanza, D., Cáceres, I., Buccino, M., Gironella, X., & Calabrese, M. (2009). Wave disturbance behind low-crested structures: Diffraction and overtopping effects. *Coastal Engineering*, 56(12), 1173-1185.
- Vicinanza, D., Calabrese, M., & Buccino, M. (2008). Low-crested and submerged breakwaters in presence of broken waves. Budapest.
- Villani, M., Bosboom, J., Zijlema, M., & Stive, M. J. F. (2012). Circulation patterns and shoreline response induced by submerged breakwaters. Paper presented at the Proceedings of the 33rd International Conference on Coastal Engineering, Santander.
- Vlijm, R. J. (2011). Process-based modelling of morphological response to submerged breakwaters. (MSc), TU Delft.
- Wu, Y., Hsiao, S., Huang, Z., & Hwang, K. (2012). Propagation of solitary wave over a bottom-mounted barrier. *Coastal Engineering*, 62, 31-47.
- Young, D. M., & Testik, F. Y. (2009). Onshore scour characteristics around submerged vertical and semi-circular breakwaters. *Coastal Engineering*, 56(8), 868-875.
- Zanuttigh, B., Martinelli, L., & Lamberti, A. (2008). Wave overtopping and pilling-up at permeable low-crested structures. *Coastal Engineering*, 55(6), 484-498.

Appendices

A. Numerical model parameters Delft3D

This appendix includes an overview of the grids for the Flow and Wave module of Delft3D and a 3D representation of the bathymetry with multiple SBWs. The physical and numerical parameters for both modules are collected in tables.

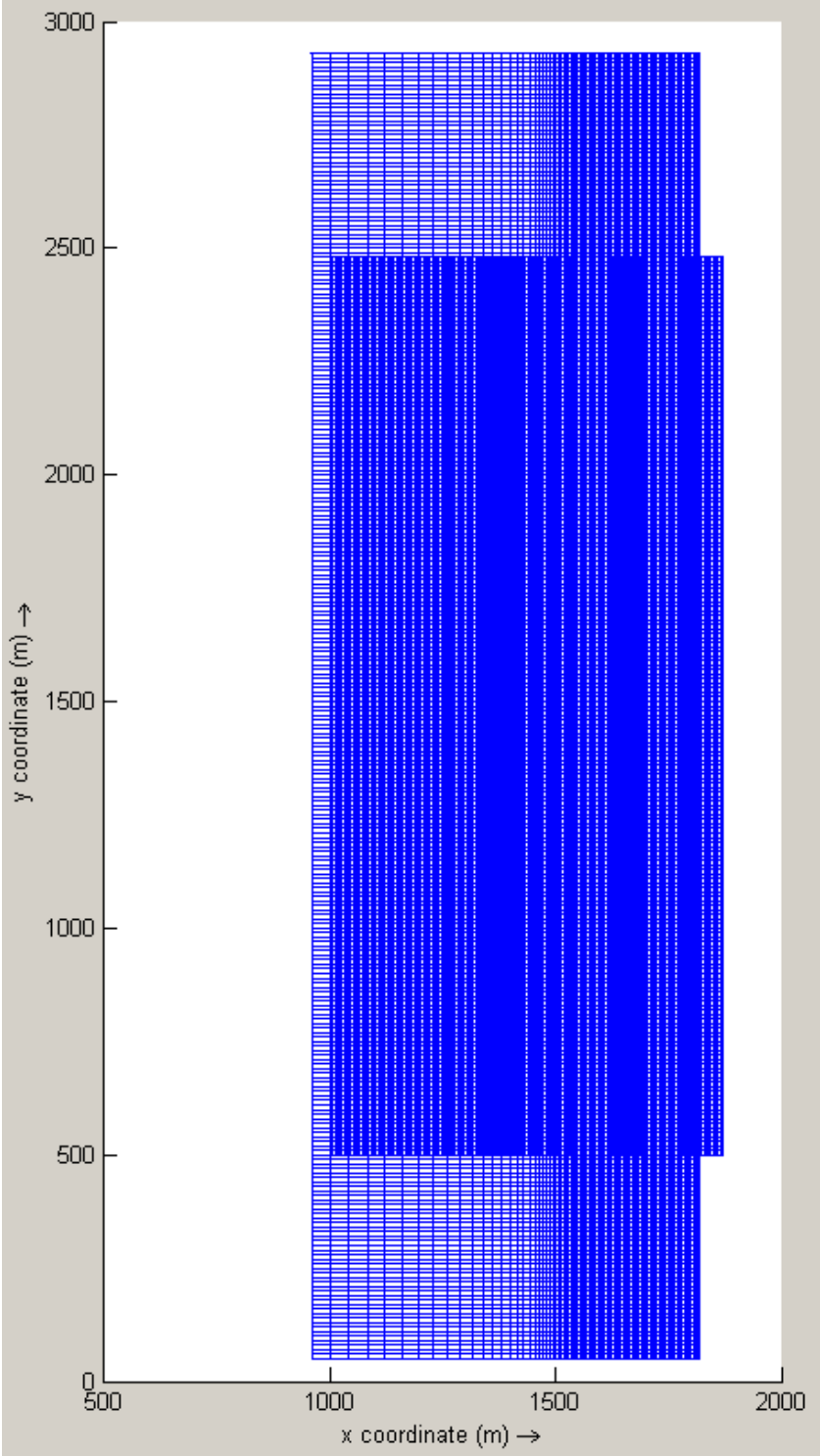


Figure A.1 - WAVE and FLOW grid superimposed, with length scales.

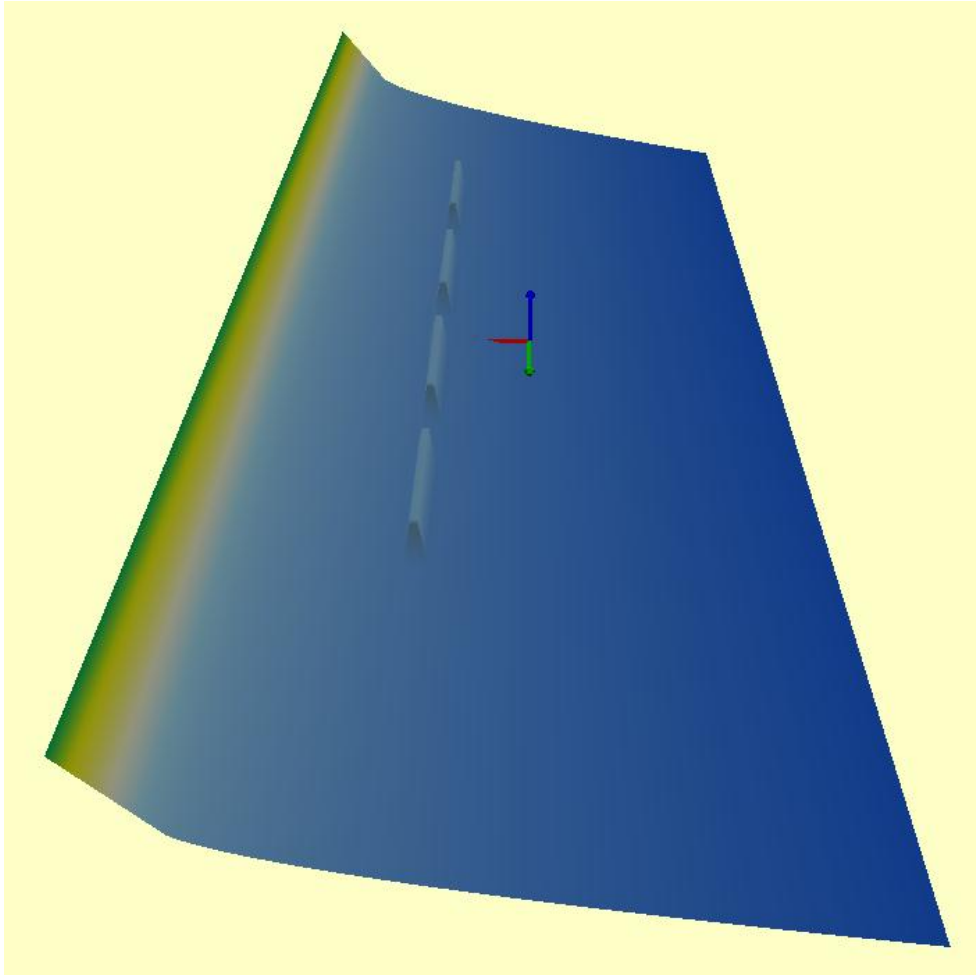


Figure A.2 - 3D representation of the initial bathymetry with 4 SBWs.

Subject	Parameter	Value or setting
Constants	Gravity	9.81 m/s ²
	Water density	1025 kg/m ³
Roughness	Bottom roughness formula	Chézy
	Uniform/from file	From file
	Stress formulation due to wave forcing	Fredsoe
	Slip condition (wall roughness)	Free
Viscosity	Background horizontal viscosity/diffusivity	Uniform
	Horizontal eddy viscosity	1 m/s ²
	Horizontal eddy diffusivity	0.5 m/s ²
Sediment	Reference density for hindered settling	1600 kg/m ³
	Specific density	2650 kg/m ³
	Dry bed density	1600 kg/m ³
	Median sediment diameter d ₅₀	250 μm
	Initial sediment layer thickness at bed	From file
Morphology	Update bathymetry during Delft3D-Flow	True
	Include effect of sediment on fluid density	False

	Equilibrium sand concentration profile at inflow boundaries	True
	Morphological scale factor	15
	Spin-up interval before morphological changes	720 min
	Minimum depth for sediment calculation	0.1 m
	Van Rijn's height factor	1
	Threshold sediment thickness	0.05
	Estimated ripple height factor	2
	Factor for erosion of adjacent dry cells	1
	Current-related reference concentration factor	1
	Current-related transport vector magnitude factor	1
	Wave-related suspended transport factor	0
	Wave-related bed load transport factor	0

Table A.1 - Physical parameters Delft3D-Flow

Subject	Parameter	Value or setting
Constant	Gravity	9.81 m/s ²
	Water density	1025 kg/m ³
	North w.r.t. x-axis	90 degrees
	Minimum depth	0.05 m
	Convention	Nautical
	Wave set-up	None
	Forces	Radiation stresses
Processes	Depth induced wave breaking	Battjes and Jansen
	Alpha	1
	Gamma	0.78
	Non-linear triad interactions	Off
	Bottom friction	On
	Bottom friction type	JONSWAP
	Bottom friction coefficient	0.067 m ² s ⁻³
	Diffraction	On
	Smoothing coefficient	0.02
Smoothing steps	5	
Various	Whitecapping	Off
	Refraction	On
	Frequency shift	On

Table A.2 - Physical parameters Delft3D-Wave

Subject	Parameter	Value or setting
Numerical parameters	Drying and flooding check	Grid cell centres and faces
	Depth specified	Cell centre
	Depth at grid cell faces	Mor
	Threshold depth	0.1 m
	Marginal depth	-999 m
	Smoothing time	60 min
	Advection scheme for momentum	Cyclic
	Advection scheme for transport	Cyclic
	Forester filter horizontal	On

Table A.3 - Numerical parameters Delft3D-Flow

Subject	Parameter	Value or setting
Spectral space	Directional space	0.5
	Frequency space	0.5
Accuracy criteria	Relative change H_s, T_{m-01}	0.005
	Percentage of wet grid points	99 %
	Relative change w.r.t. mean value H_s, T_{m-01}	0.005
	Maximum number of iterations	15

Table A.4 - Numerical parameters Delft3D-Wave

B. Delft3D output for comparison with literature

This appendix contains the plots of the Delft3D output when reproducing the analytical, physical and numerical models. This includes:

- The longshore profiles of the water level set-up in the lee of the SBW for all four tests,
- The trends describing the relation between the pilling up and the lateral confinement (for multiple Chézy values),
- The longshore profiles of the water level set-up at the shoreline for all four tests,
- The flow patterns for all four tests.

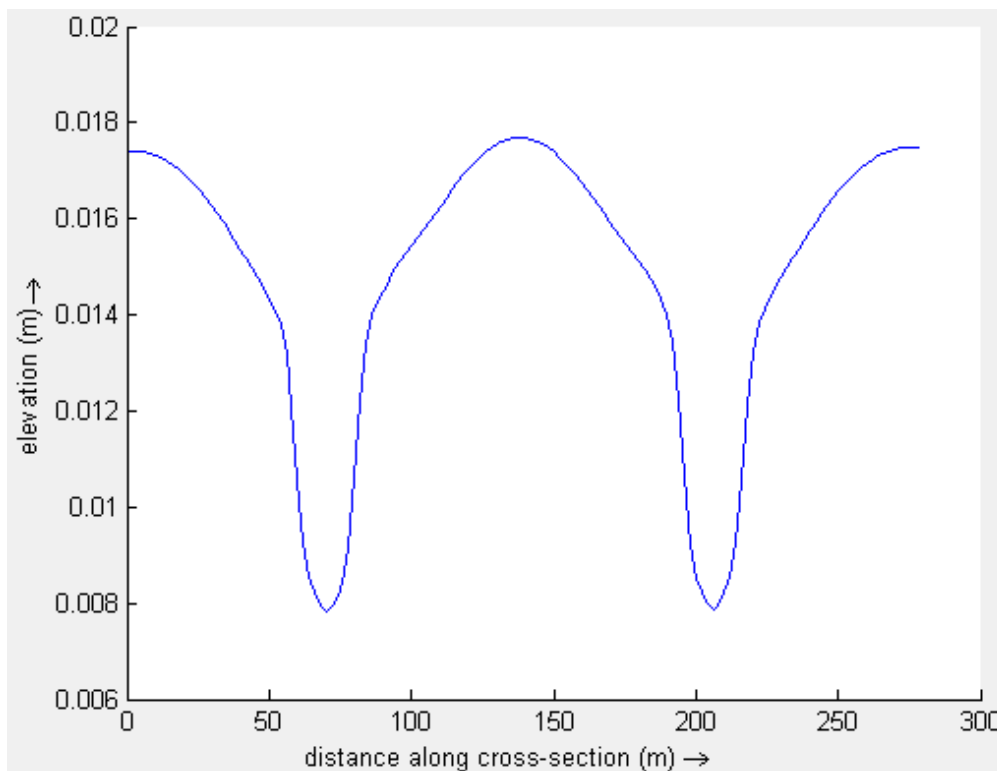


Figure B.1 - Set-up in the lee of the SBW, test B

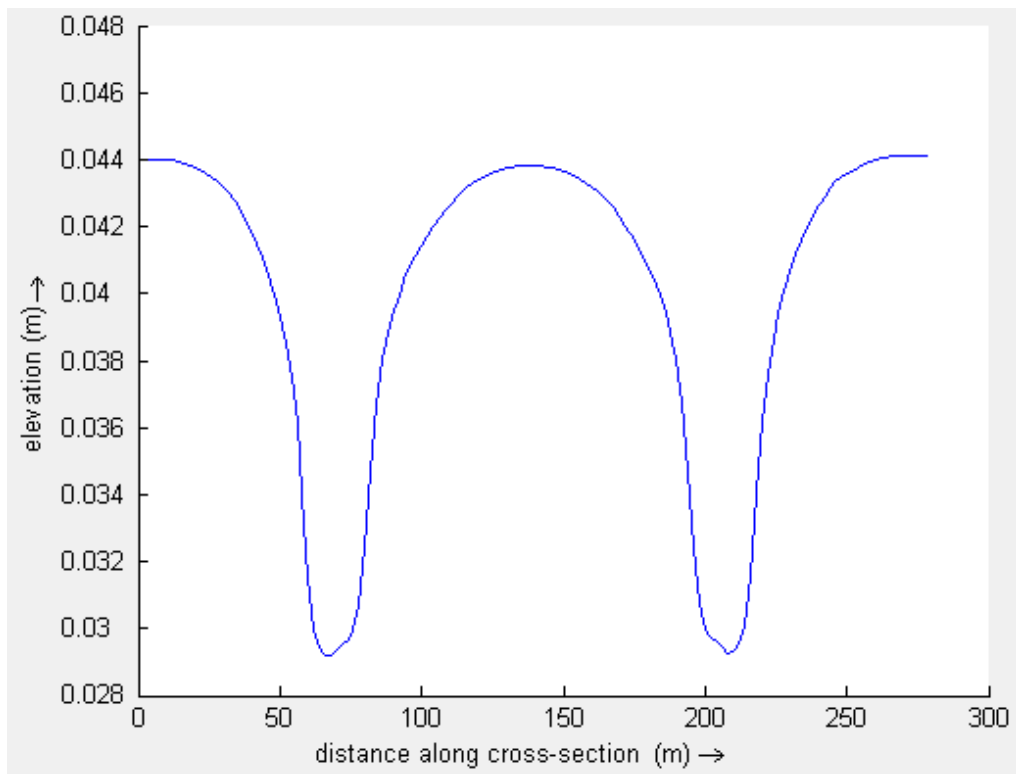


Figure B.2 - Set-up in the lee of the SBW, test C

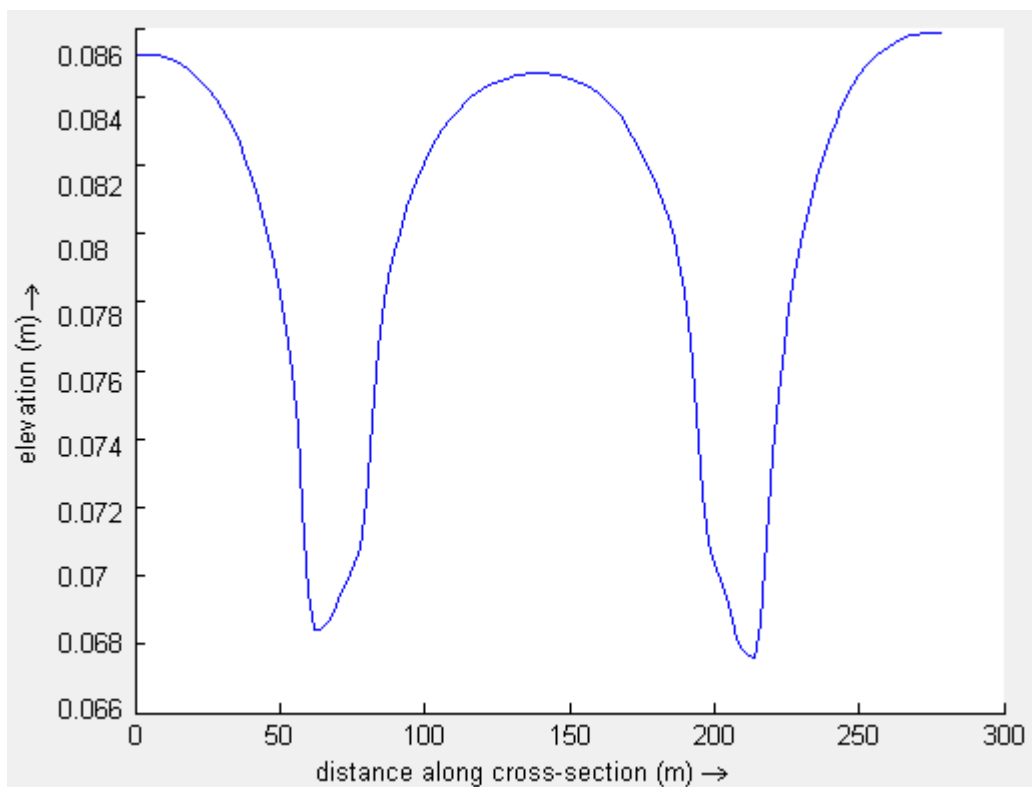


Figure B.3 - Set-up in the lee of the SBW, test D

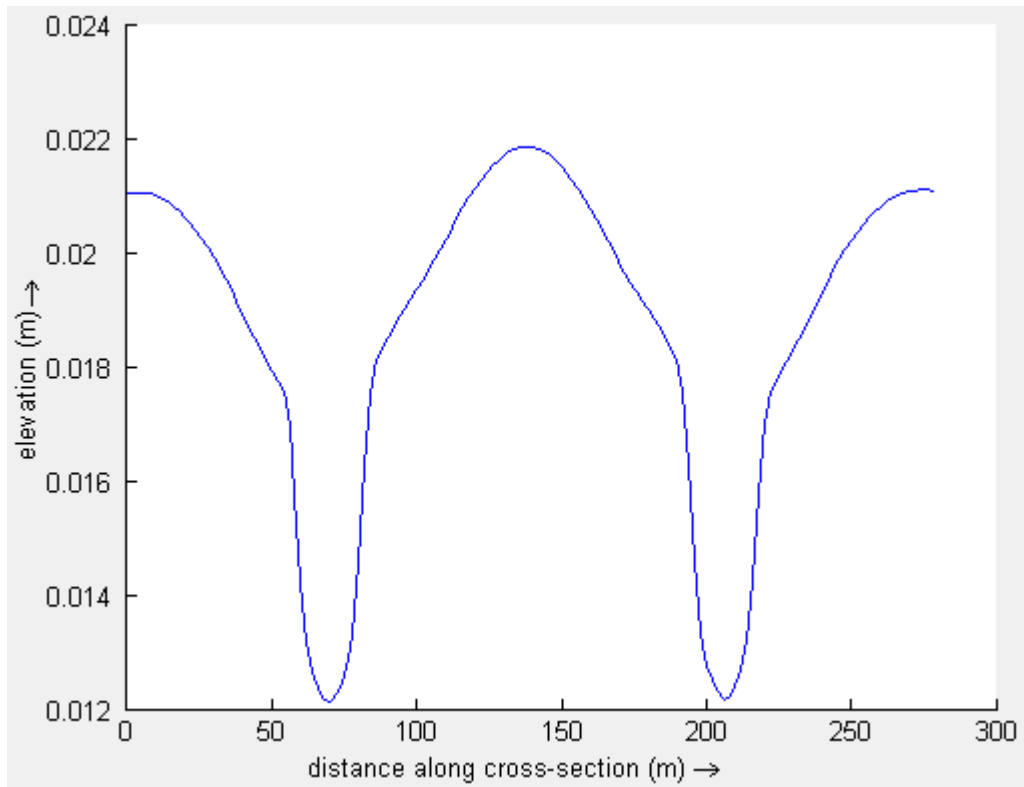


Figure B.4 - Set-up in the lee of the SBW, test G

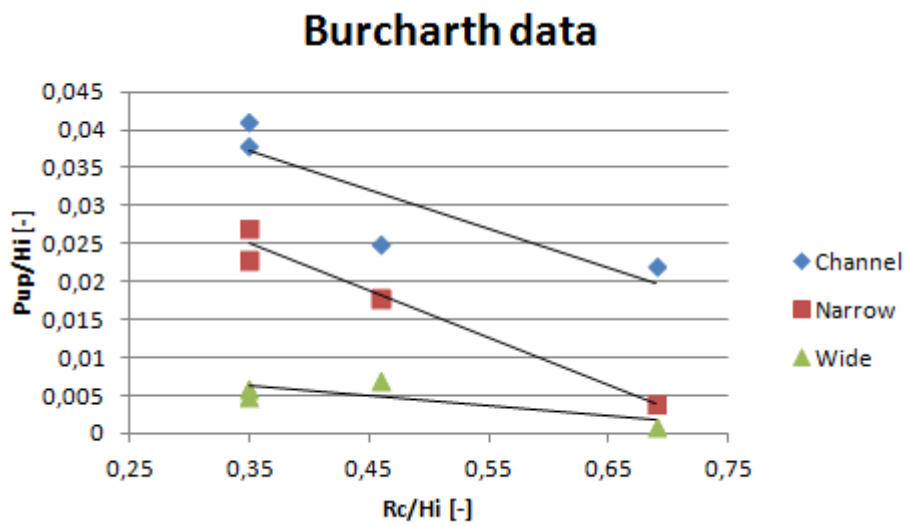


Figure B.5 - Plot of the data by Burcharth (2007)

Delft3D output, C = 65

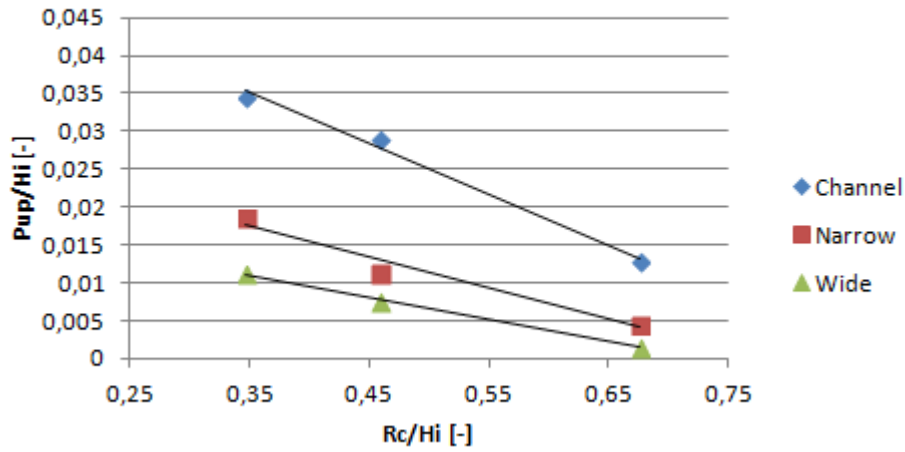


Figure B.6 - Plot of the data from Delft3D with a Chézy value of $65 \text{ m}^{0.5}/\text{s}$

Delft3D output, C = 45

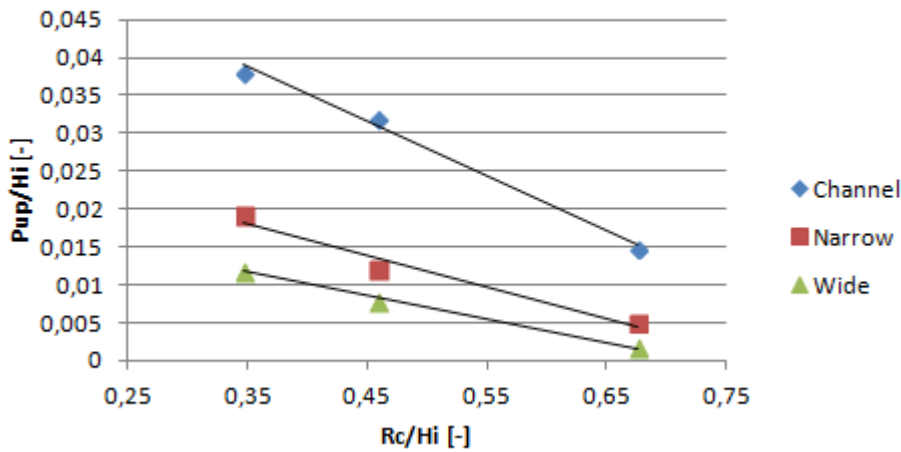


Figure B.7 - Plot of the data from Delft3D with a Chézy value of $45 \text{ m}^{0.5}/\text{s}$

Delft3D output C = 45-65

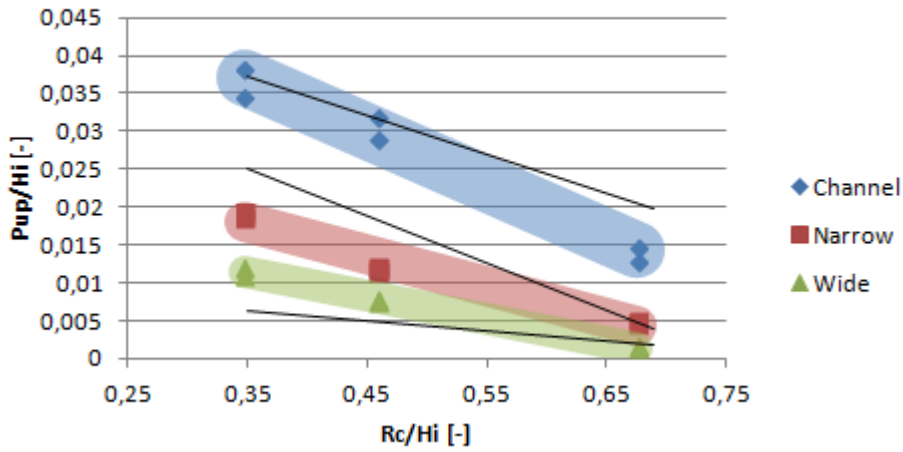


Figure B.8 - Plot of the data from Delft3D with the varying Chézy value as uncertainty band

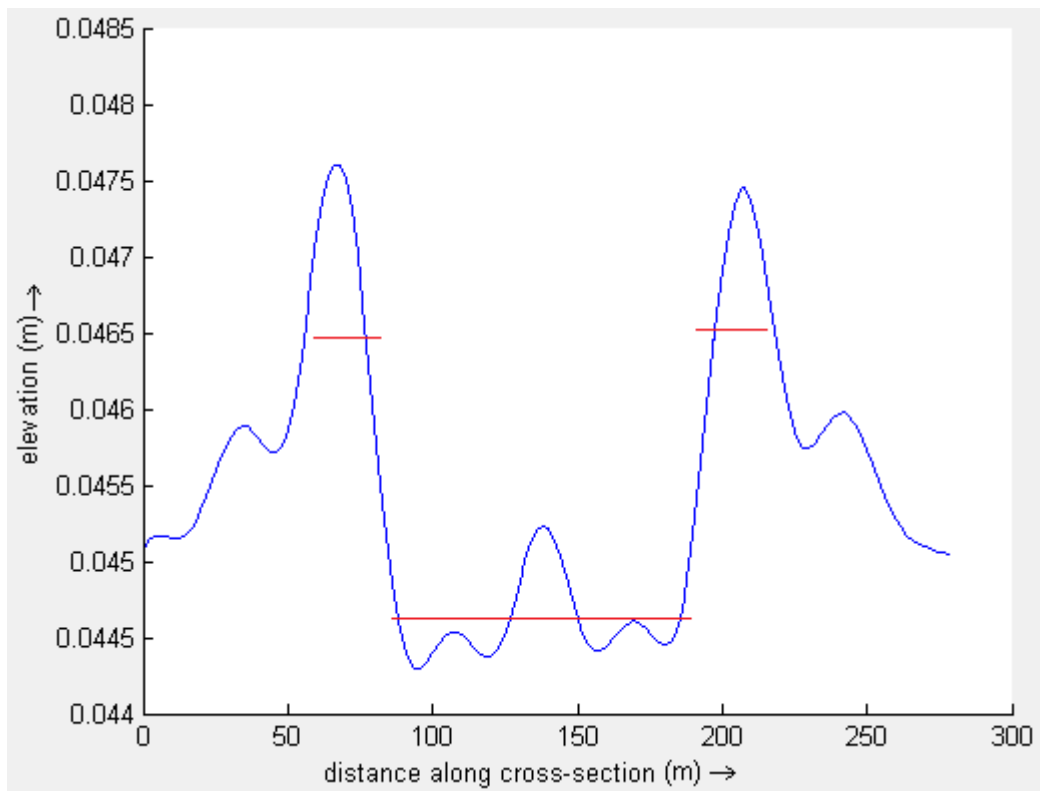


Figure B.9 - Set-up at the shoreline, with average over sections, test B

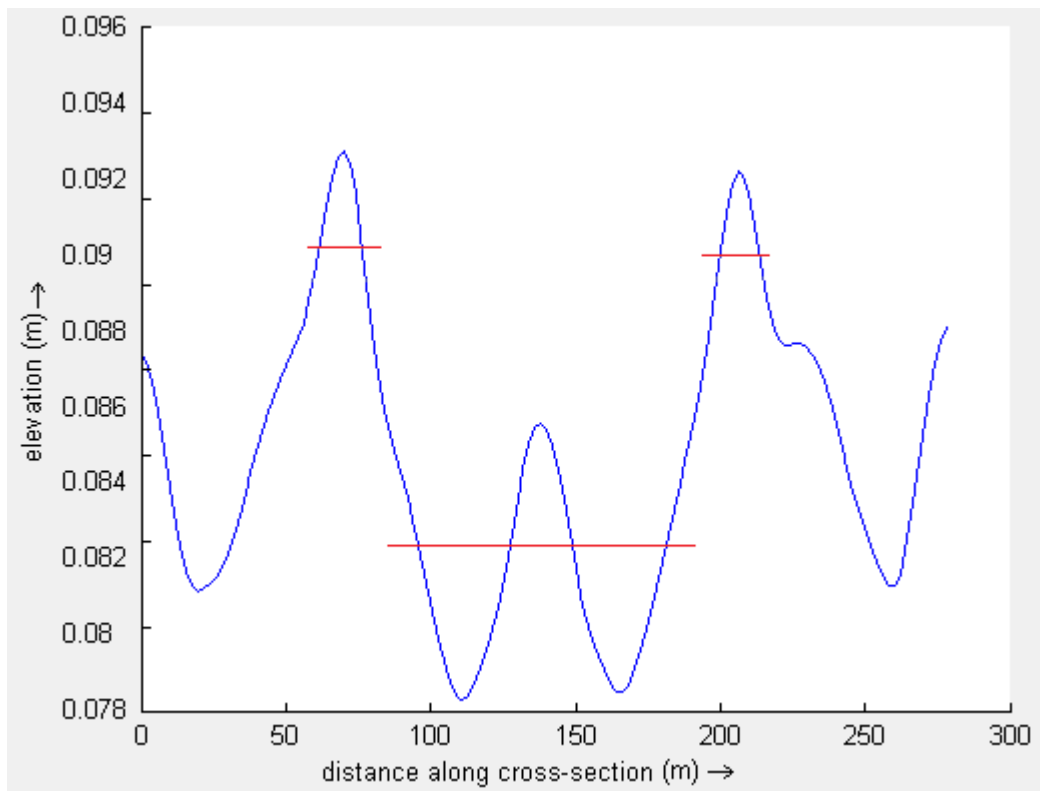


Figure B.10 - Set-up at the shoreline, with average over sections, test C

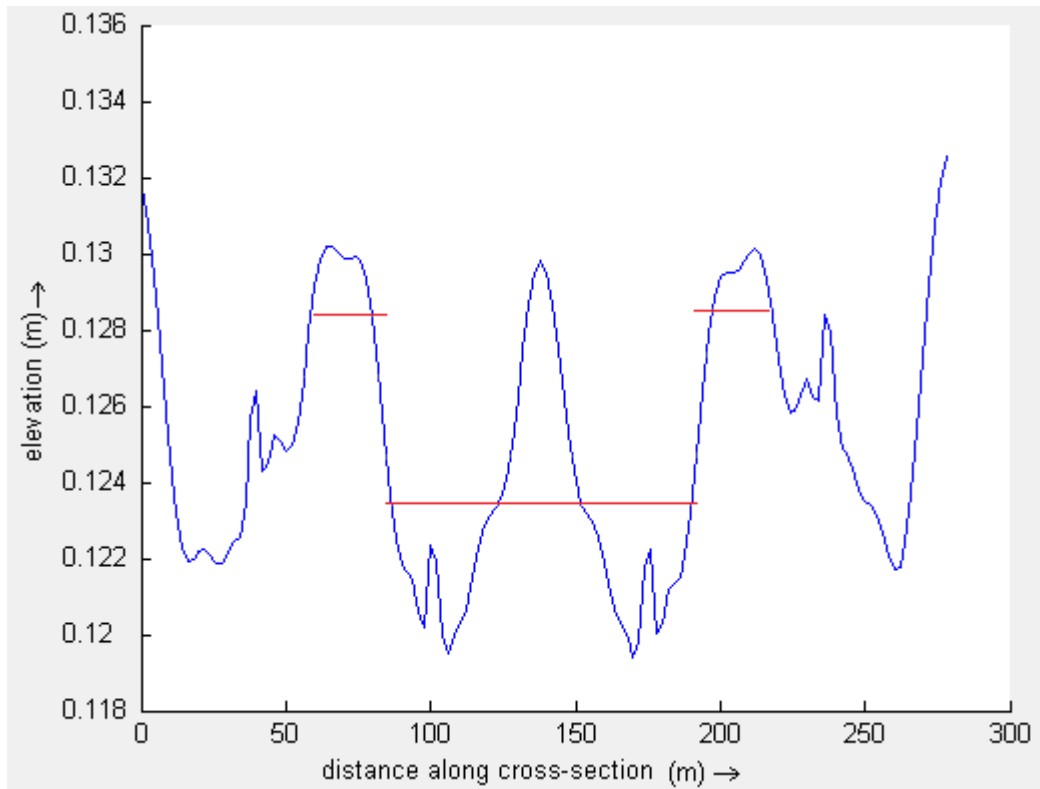


Figure B.11 - Set-up at the shoreline, with average over sections, test D

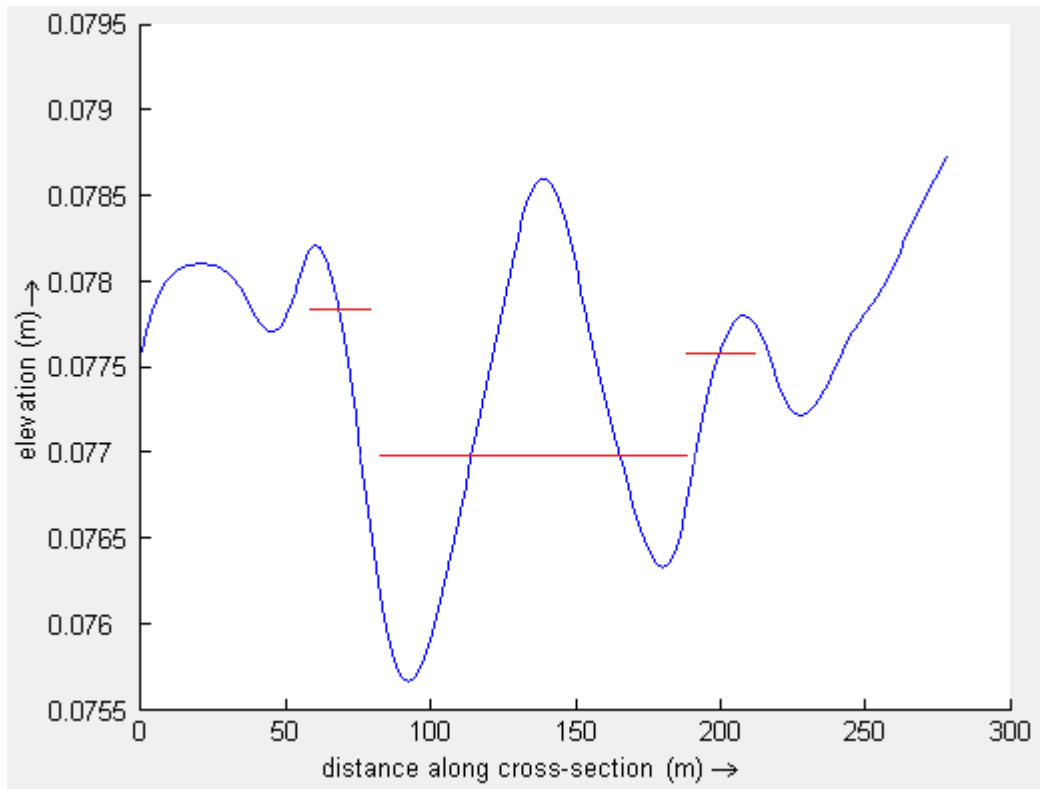


Figure B.12 - Set-up at the shoreline, with average over sections, test G

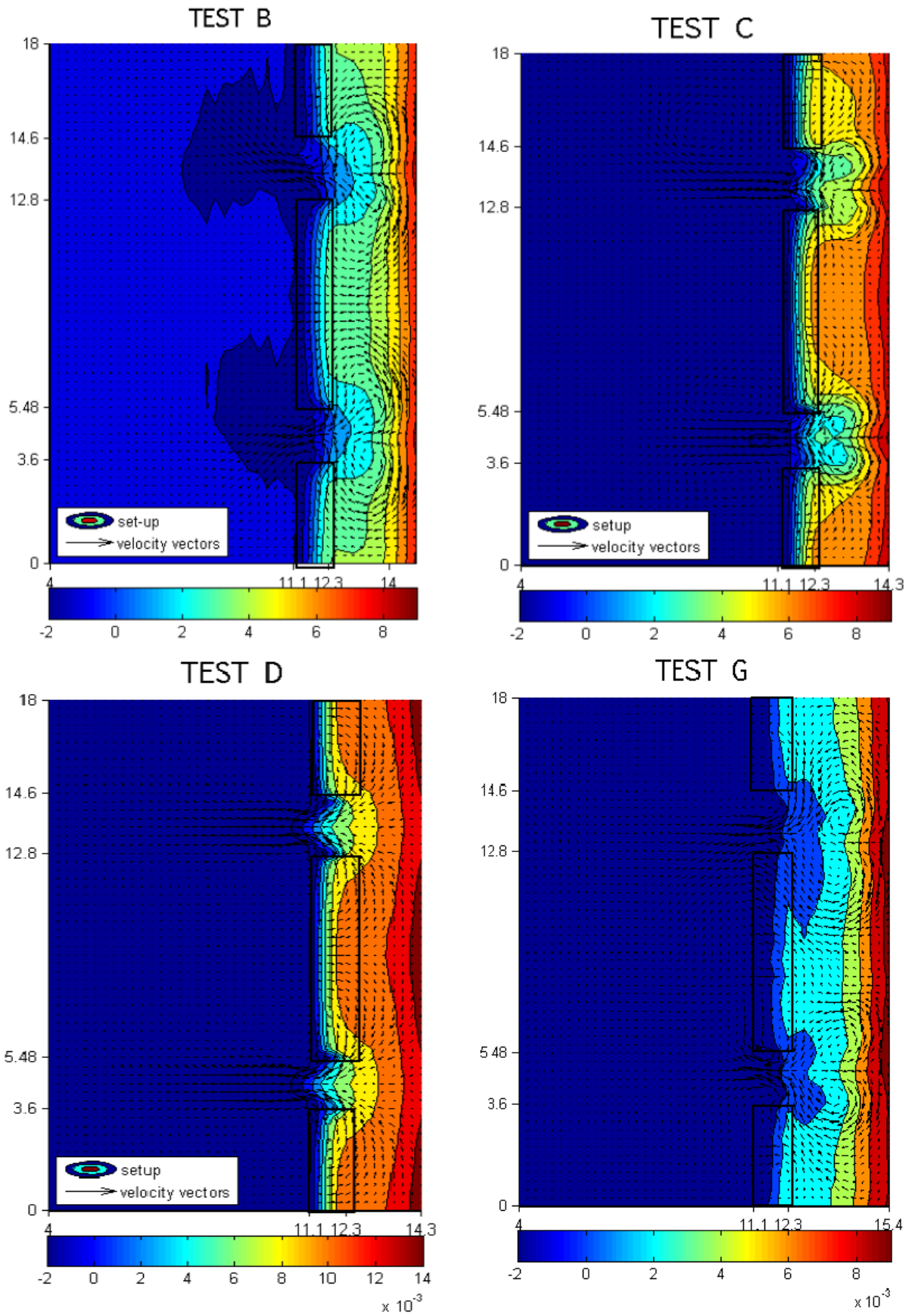


Figure B.13 - Plan view of the time-averaged velocity vectors and set-up (colour map) from (Villani et al., 2012)

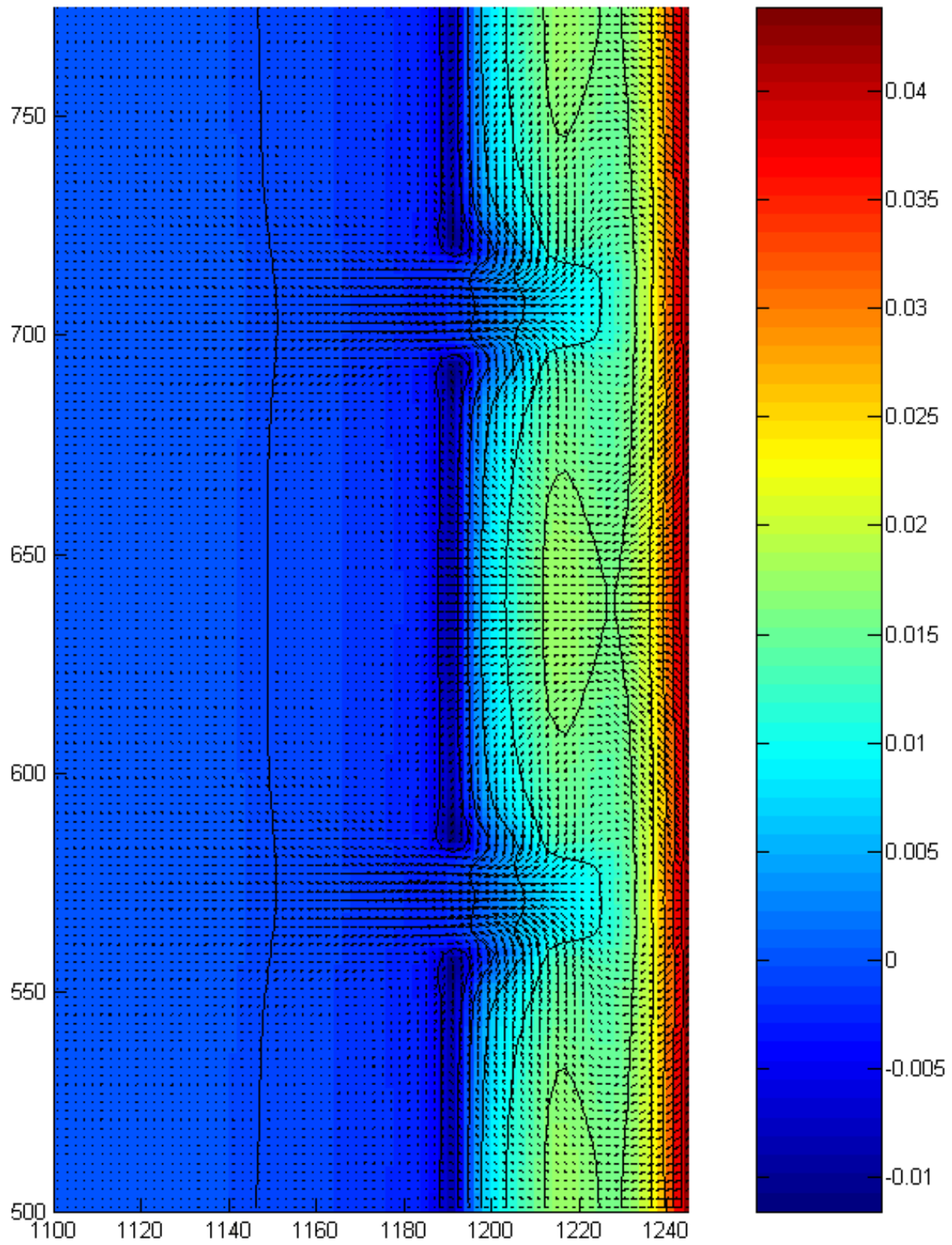


Figure B.14 - Flow pattern test B

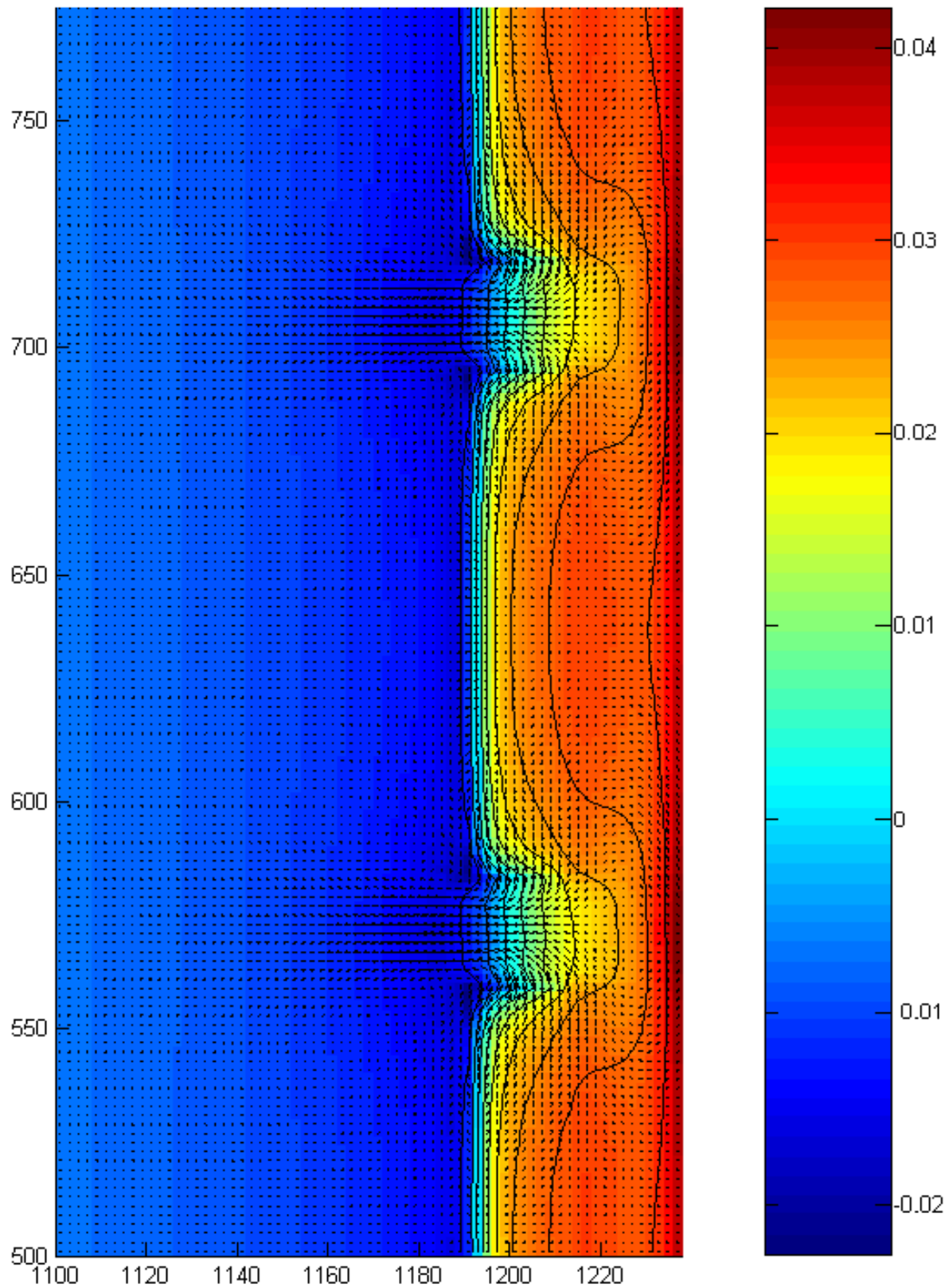


Figure B.15 - Flow pattern test C

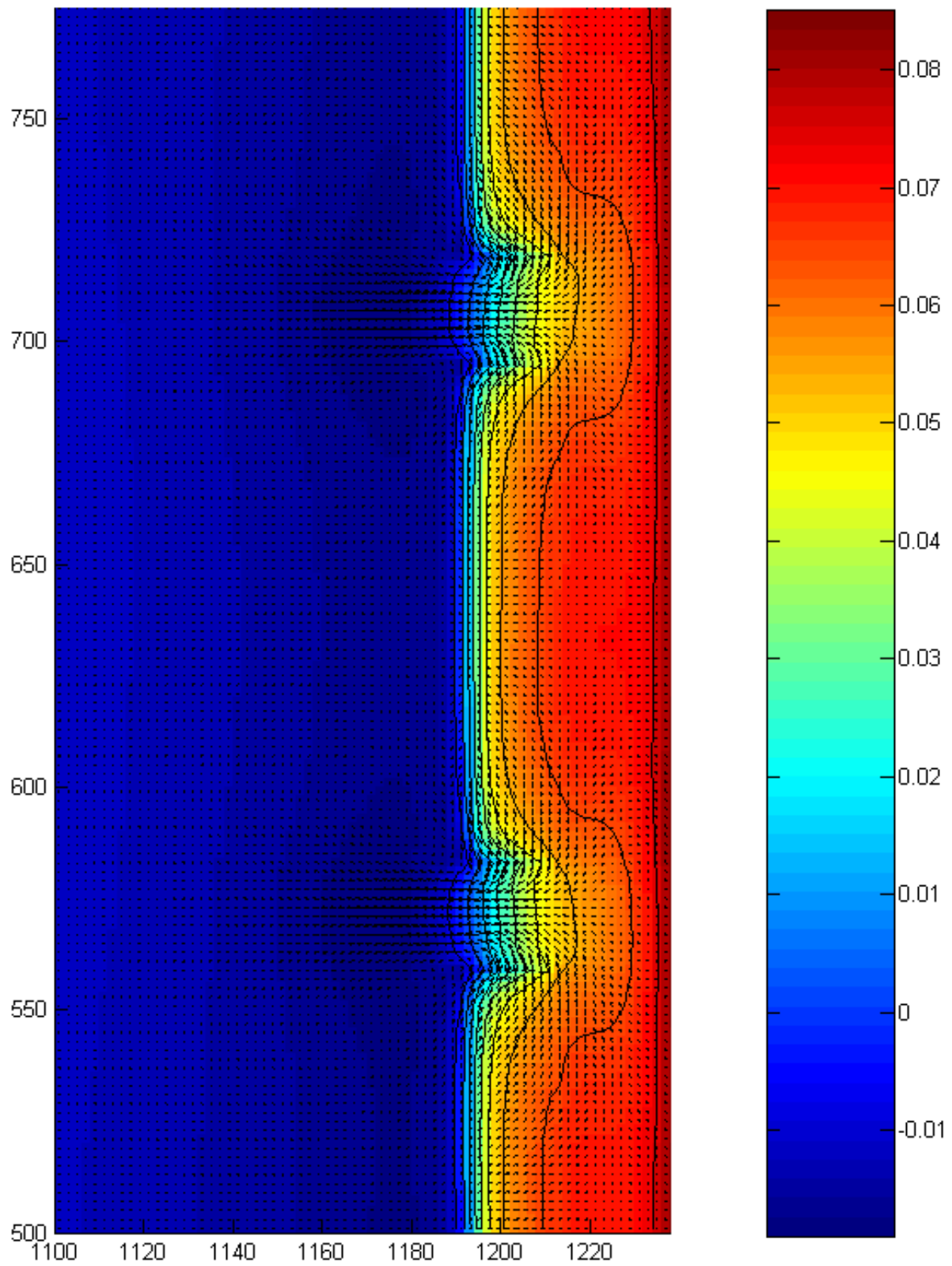


Figure B.16 - Flow pattern test D

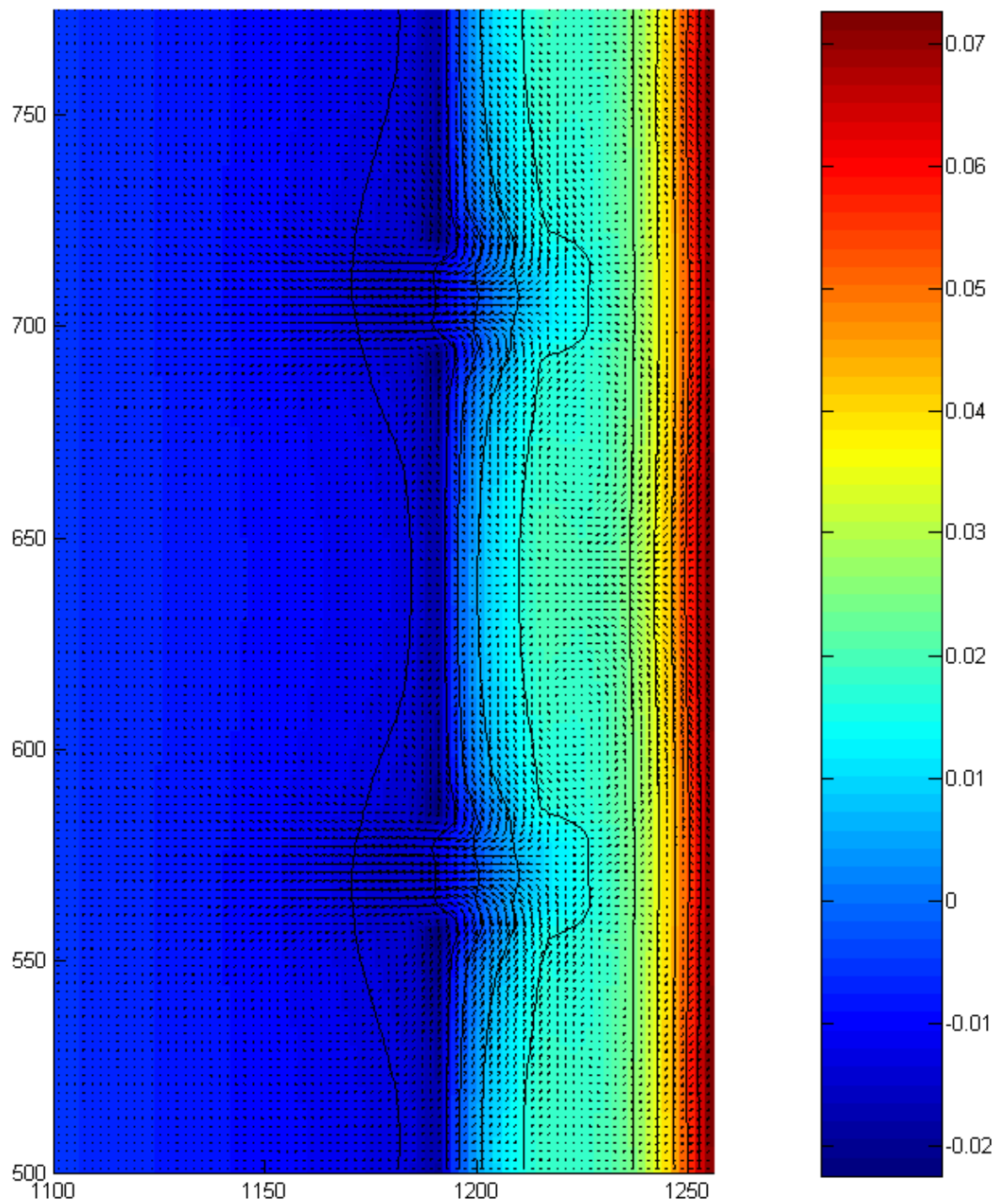


Figure B.17 - Flow pattern test G

C. Developing the criterion

This appendix is a collection of all the plots used to determine the contribution of the lateral confinement ratio and the validation of the criterion on the bases of the model runs, first per lateral confinement ratio and finally for all ratios combined.

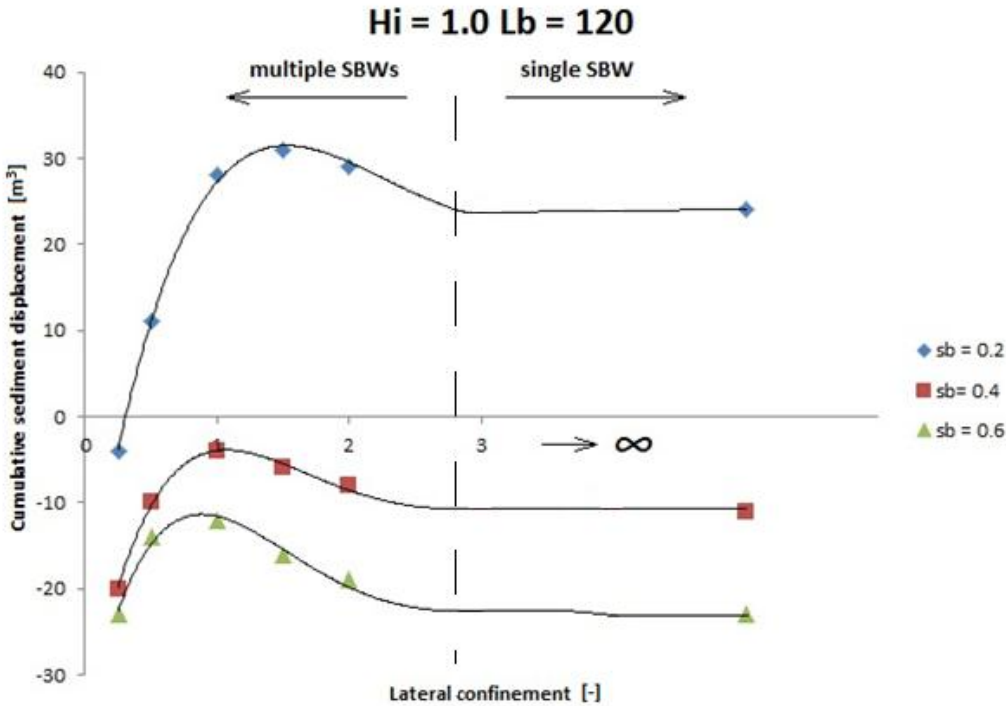


Figure C.1 - Contribution of the lateral confinement ratio to the shoreline response for $H_i = 1.0m$

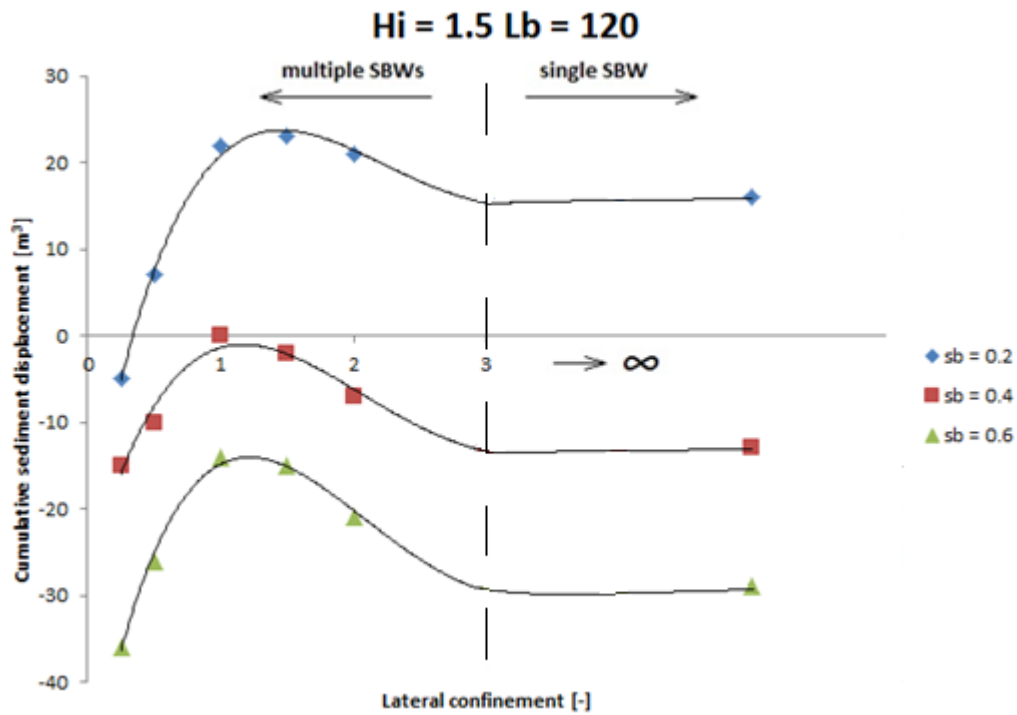


Figure C.2 - Contribution of the lateral confinement ratio to the shoreline response for $H_i = 1.5\text{m}$

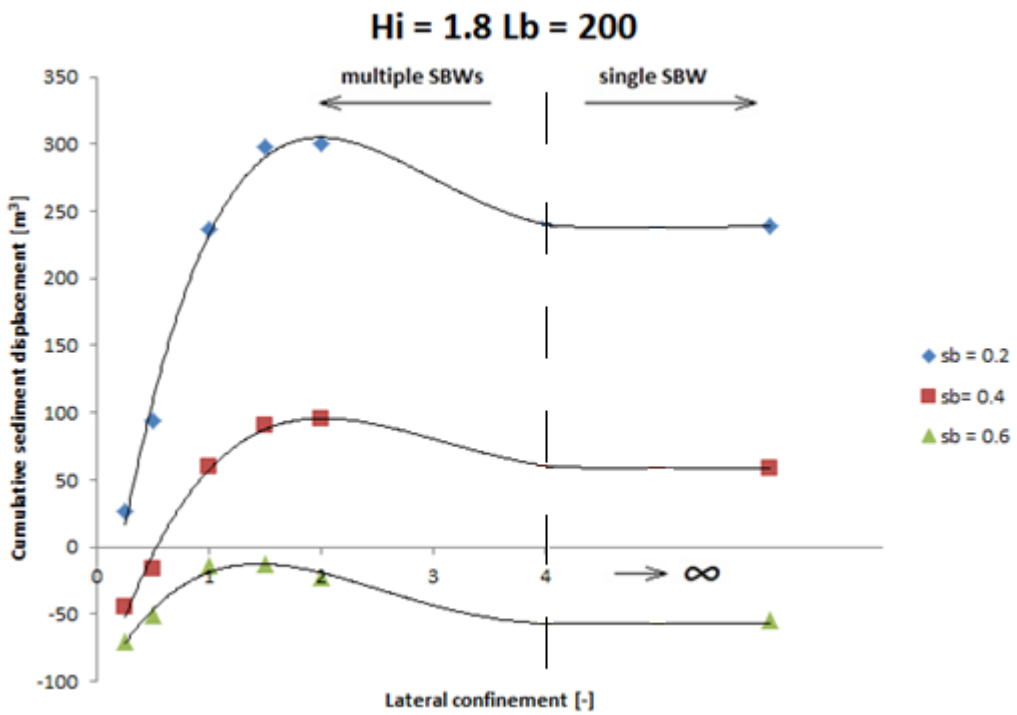


Figure C.3 - Contribution of the lateral confinement ratio to the shoreline response for $H_i = 1.8\text{m}$

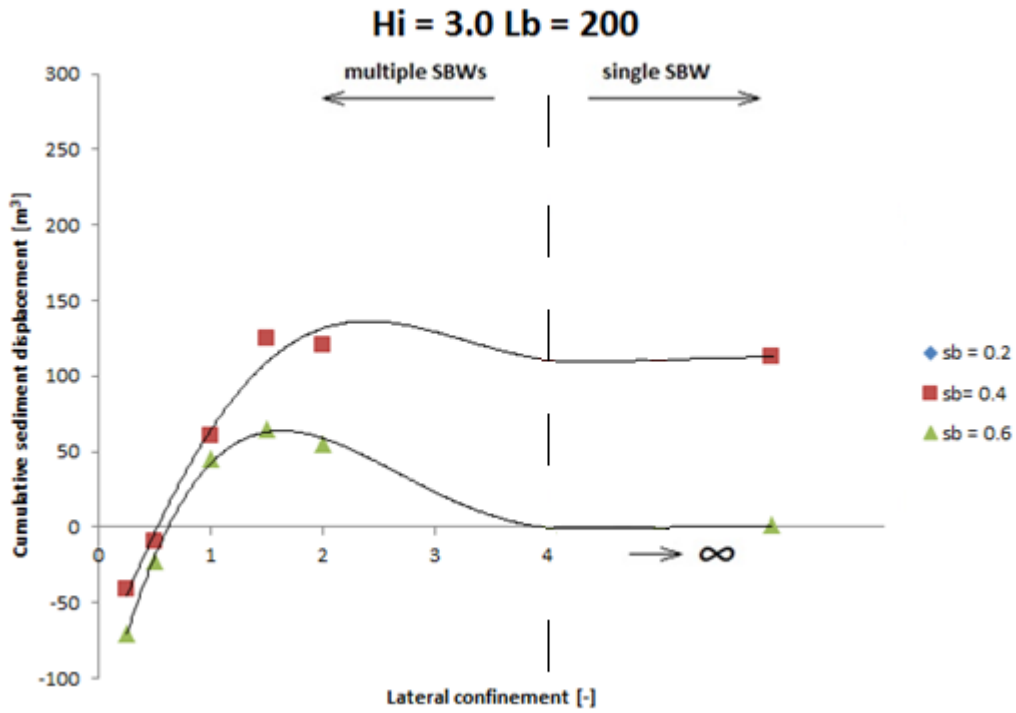


Figure C.4 - Contribution of the lateral confinement ratio to the shoreline response for $H_i = 3.0m$

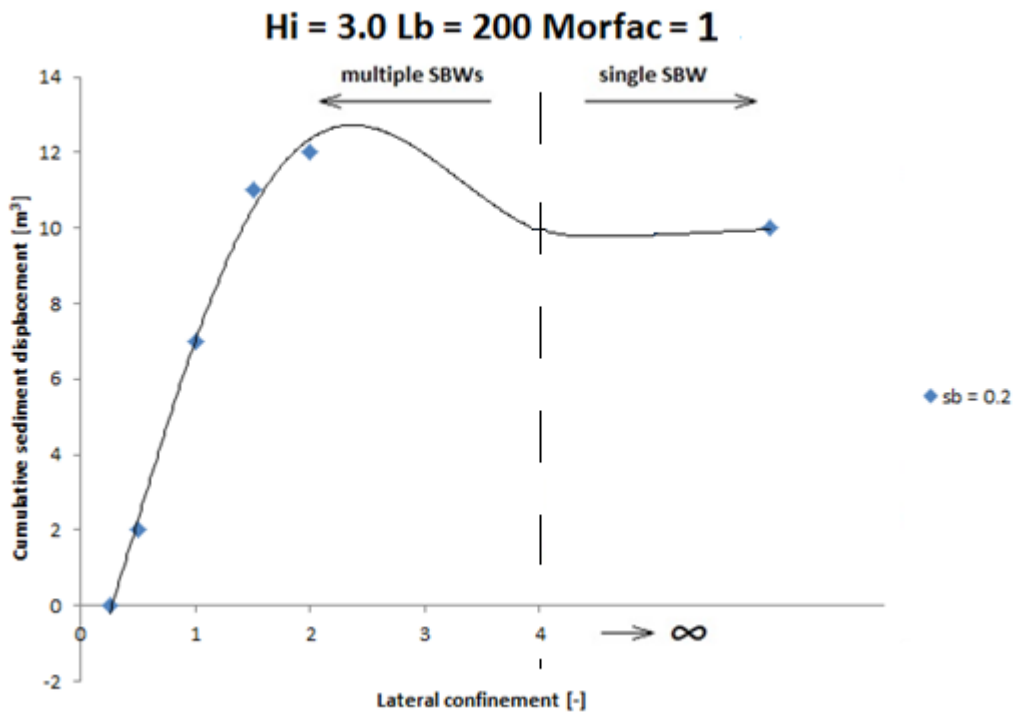


Figure C.5 - Contribution of the lateral confinement ratio to the shoreline response for $H_i = 3.0m$ and $sb = 0.2$ with $morfac = 1$

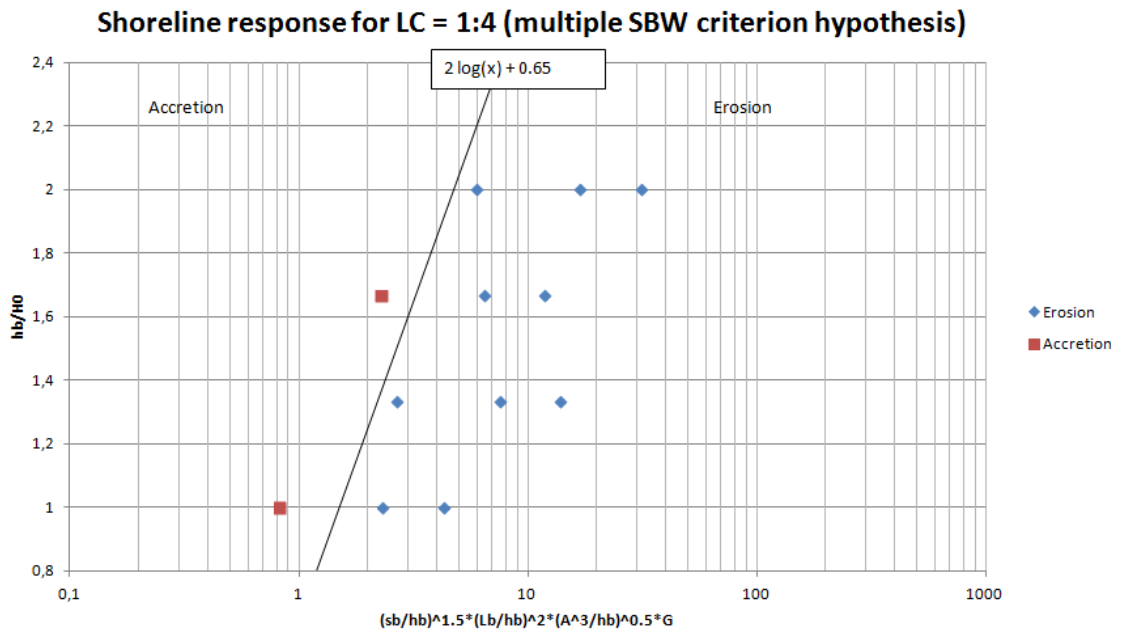


Figure C.6 - Data points for the LC ratio of 1:4 with the added term G

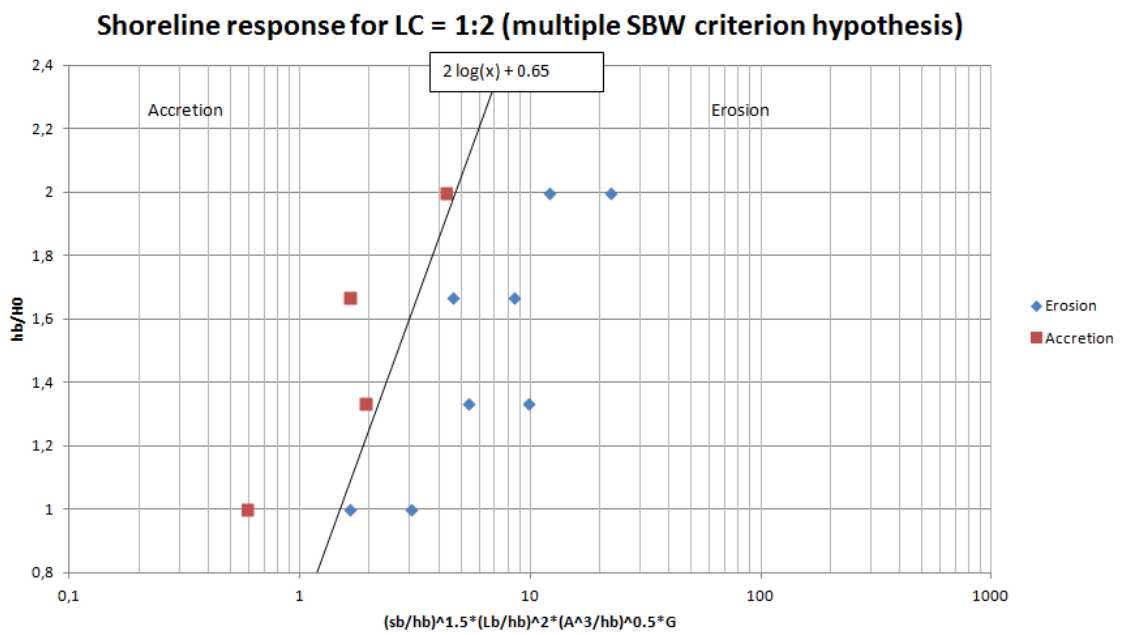


Figure C.7 - Data points for the LC ratio of 1:2 with the added term G

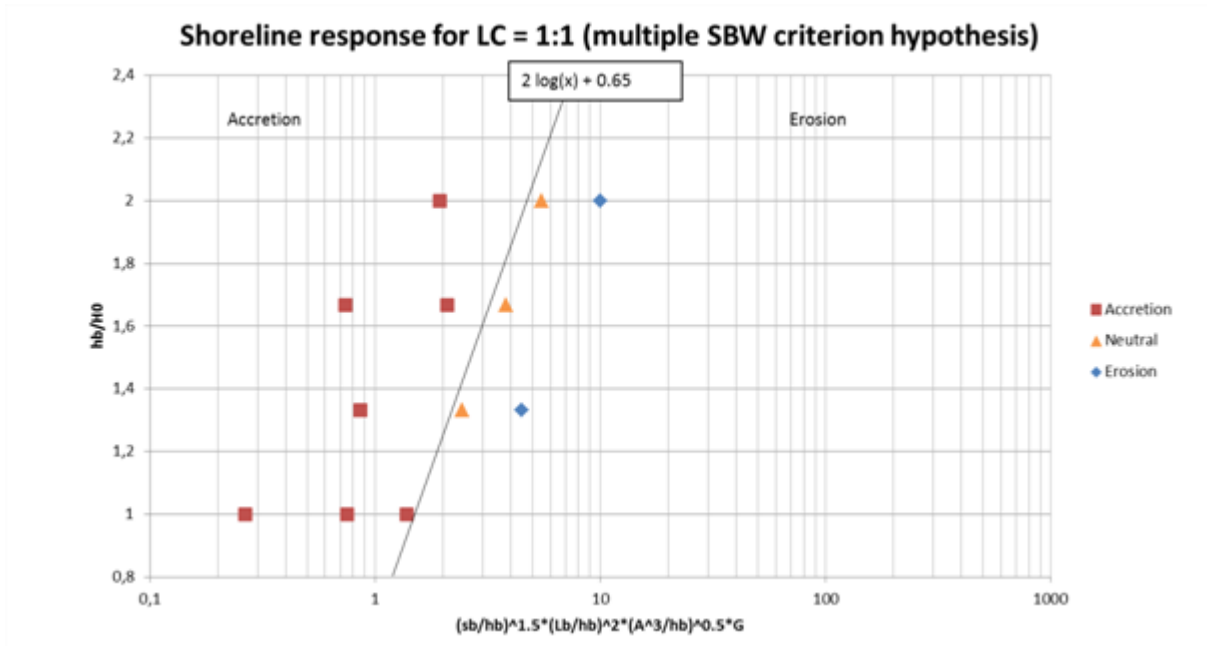


Figure C.8 - Data points for the LC ratio of 1:1 with the added term G

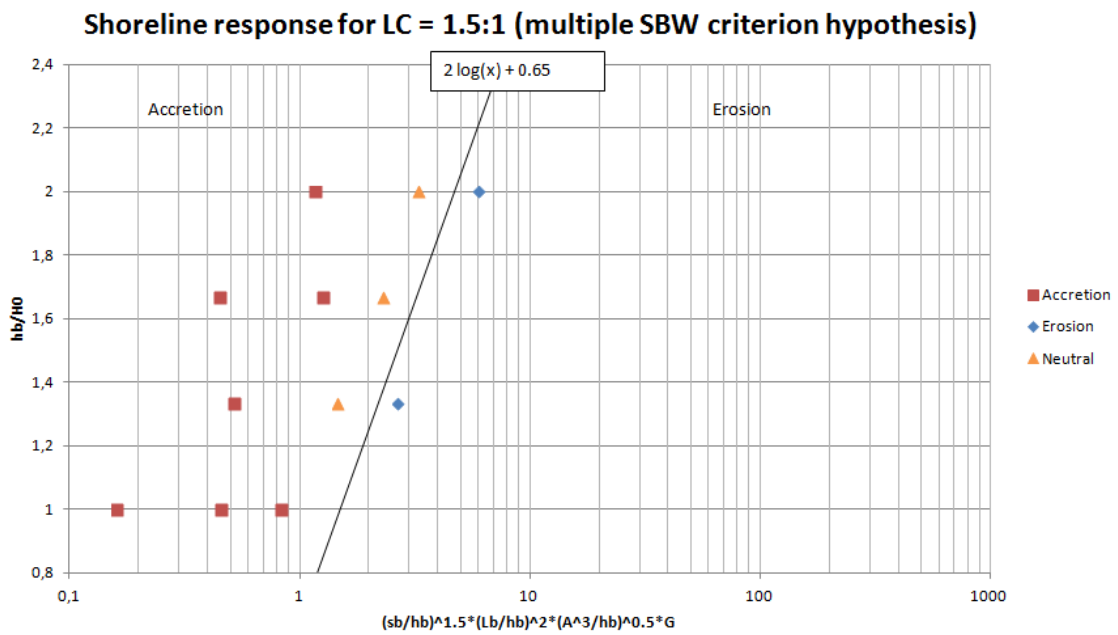


Figure C.9 - Data points for the LC ratio of 1.5:1 with the added term G

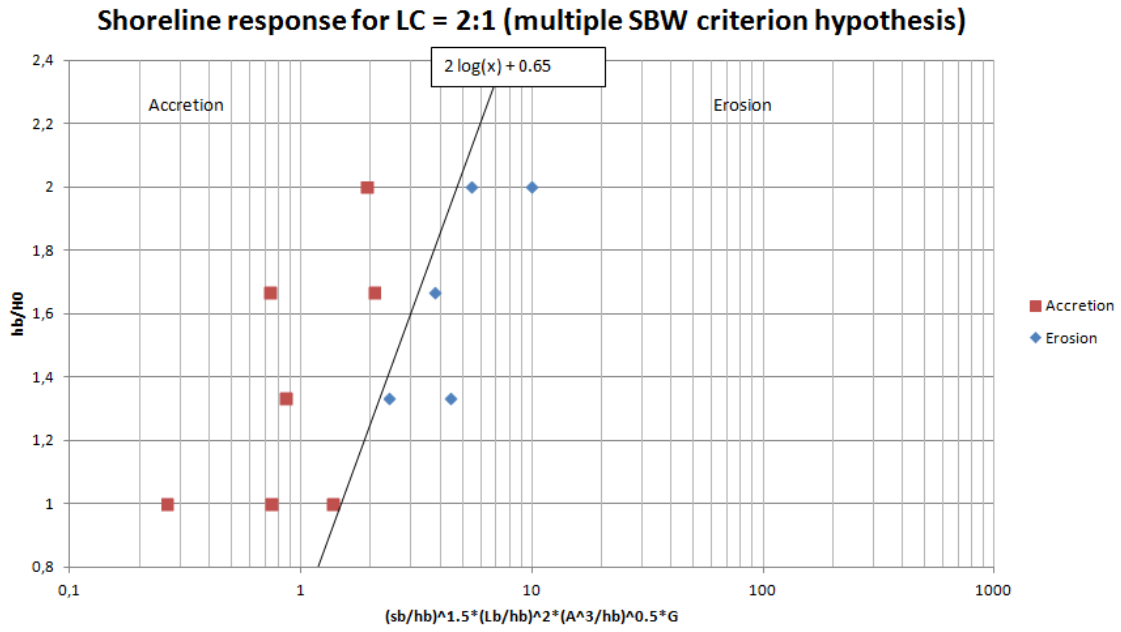


Figure C.10 - Data points for the LC ratio of 2:1 with the added term G

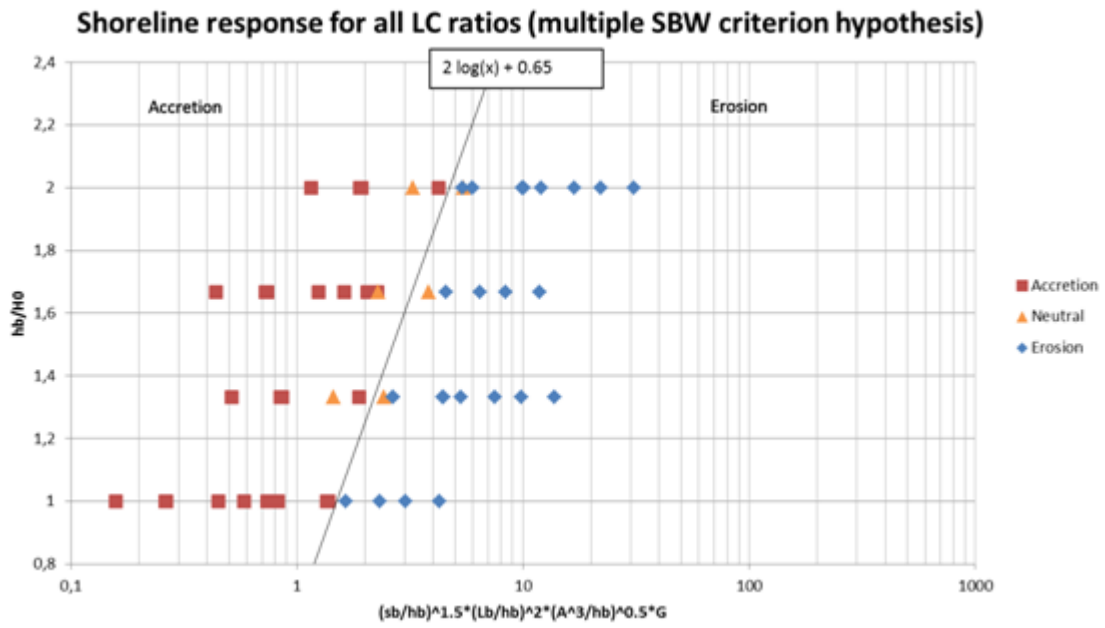


Figure C.11 - Data points of all the LC ratios with the added term G